

R E S E A R C H T R I A N G L E I N S T I T U T E

AFCRL-67-0069

RESEARCH DIRECTED TOWARD THE STUDY OF SEISMICITY
IN THE SOUTHEASTERN UNITED STATES

8

10

41

20

54

60

AD

John W. Minear

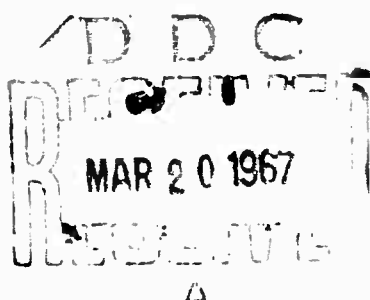
Research Triangle Institute
P. O. Box 12194
Research Triangle Park, North Carolina 27709

Contract No. AF 10(629)-3892

Project No. 8652

Task No. 865207

FINAL REPORT
January 2, 1964 thru December 15, 1966
January 1967



Work sponsored by Advanced Research Projects Agency, Project VELA-UNIFORM
ARPA Order No. 292, Project Code No. 8100 Task 2

Prepared for

U.S. AIR FORCE CAMBRIDGE RESEARCH LABORATORIES
OFFICE OF AEROSPACE RESEARCH
UNITED STATES AIR FORCE
BEDFORD, MASSACHUSETTS

ARCHIVE COPY

R E S E A R C H T R I A N G L E P A R K , N O R T H C A R O L I N A 2 7 7 0 9

F

DISCLAIMER NOTICE

**THIS DOCUMENT IS THE BEST
QUALITY AVAILABLE.**

**COPY FURNISHED CONTAINED
A SIGNIFICANT NUMBER OF
PAGES WHICH DO NOT
REPRODUCE LEGIBLY.**

AFCRL-67-0069

RESEARCH DIRECTED TOWARD THE STUDY OF SEISMICITY
IN THE SOUTHEASTERN UNITED STATES

John W. Minear

Research Triangle Institute
P. O. Box 12194
Research Triangle Park, North Carolina 27709

Contract No. AF 19(628)-3892

Project No. 8652

Task No. 865207

FINAL REPORT

January 2, 1964 thru December 15, 1966

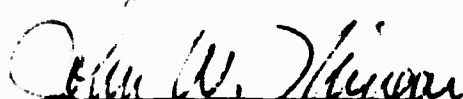
January 1967

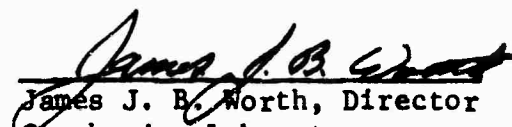
Work sponsored by Advanced Research Projects Agency, Project VELA-UNIFORM
ARPA Order No. 292, Project Code No. 8100 Task 2

Prepared for

AIR FORCE CAMBRIDGE RESEARCH LABORATORIES
OFFICE OF AEROSPACE RESEARCH
UNITED STATES AIR FORCE
BEDFORD, MASSACHUSETTS

Approved by:


John W. Minear
Project Director


James J. B. North, Director
Geophysics Laboratory

Distribution of this document is unlimited.

ABSTRACT

This is the final report covering research directed toward the study of the seismicity of the Southeastern United States. Travel-times determined from local earthquake and refraction data are presented which indicate a crustal structure of $h_1 = 33.0$ km ($a = 5.88$ km/sec), $h_2 = 10.8$ km ($a = 6.58$ km/sec), and an upper mantle velocity of 8.10 km/sec. Fundamental and first higher order Rayleigh group-velocity data determined by digital bandpass filtering are presented for the Southern Appalachian region. The Dunkin modification of the Thomson-Haskell matrix method is used to compute theoretical Rayleigh dispersion curves for comparison with the observed curves. A slight velocity reversal in the upper crust centered at about 15 km, a general increase of crustal velocities and densities with depth below this zone, and an upper mantle low velocity zone beginning at a depth of 70 km are indicated beneath the Southern Appalachians. The Appalachian foreland has crustal structure similar to the Gutenberg-Birch II continental model with a total thickness of 40 km.

A sin x/x analysis of the Bouguer gravity data yields a total crustal thickness of about 50 km beneath the Southern Appalachians.

P-residuals computed at Chapel Hill, North Carolina and McMinnville, Tennessee show a systematic deviation of as much as ± 3 sec.

TABLE OF CONTENTS

1.0	INTRODUCTION	1
2.0	TRAVEL-TIME CURVES FOR THE SOUTHEASTERN UNITED STATES	4
3.0	CRUSTAL THICKNESS FROM GRAVITY DATA	8
4.0	DETERMINATION OF RAYLEIGH GROUP VELOCITY	12
5.0	THEORETICAL RAYLEIGH DISPERSION CURVES	18
5.1	Thomson-Haskell Matrix Method	18
5.2	Numerical Difficulties in the Thomson-Haskell Method	20
5.3	Dunkin Modification of the Haskell Method	25
5.4	Computational Procedure	26
5.5	Variation of Phase Velocity with Layer Parameters	35
6.0	CRUSTAL AND UPPER MANTLE STRUCTURE IN THE SOUTHEASTERN UNITED STATES	40
7.0	CONCLUSIONS	59

ACKNOWLEDGMENTS

REFERENCES

APPENDIX I: Evaluation of the Secular Equation in Computing
Rayleigh Dispersion

APPENDIX II: Modal Shape Computations

APPENDIX III: Fortran Listings of Computer Programs FLATRAY,
STRESS, INTEGRAL, TRAVEL, VARGRAV, and PRESID

APPENDIX IV. Curves of Particle Displacements and Partial
Derivatives of Phase Velocity with respect to Layer
Parameters

1.0 INTRODUCTION

This final report covers the work done on contract AF 19(628)-3892, "Research Directed Toward the Study of the Seismicity of the Southeastern United States". The report is mainly concerned with the work done over the past year; the determination of crustal and upper mantle structure in the Southeastern United States. The First Annual Technical Report [Minear, 1965] covers the development, installation, and calibration of the short-period displacement seismograph at the University of North Carolina and the RTI field refraction system. The Second Annual Technical Report [Minear, 1966] includes the location of local epicenters, the results of the field refraction studies, the results of the computation of P-residuals, the calculations of magnitude, focal depth, and energy release for several local earthquakes, and preliminary crustal structure estimates from gravity data.

Research accomplishments during the performance of the contract are briefly summarized below.

- 1) During the first year of work a short-period displacement seismograph system was designed, constructed, and placed on routine operation at the University of North Carolina seismograph vault at Chapel Hill, North Carolina. Although the system performed well [Minear, 1965], the background noise level at the UNC station was too high to permit recording of local earthquakes located mainly in the Southern Appalachians. At present, a remote vault is currently under construction by the University to provide an up-to-date seismic facility.
- 2) Refraction work was carried out using local quarry blasts as energy sources.

3) Local travel-time curves were developed using several of the major local earthquakes which were well recorded by portable and permanent stations in the region.

4) P-residuals were computed for several hundred epicenters recorded at the Cumberland Plateau Seismological Observatory and Chapel Hill, North Carolina. A systematic deviation of the residuals similar to that noted by other investigators was found. This deviation cannot be explained by crustal velocity variations and must indicate a real error in the Jeffreys-Bullen travel-times.

5) Estimation of focal depth, magnitude, and energy release from previous intensity studies of four Southeastern earthquakes were made.

6) Total thickness of the Southern Appalachian crust was determined using Bouguer gravity anomalies and the $\sin x/x$ method of computing the mass anomaly producing a given gravity anomaly.

7) Crustal and upper mantle structure was determined using fundamental and first higher Rayleigh mode group velocity dispersion.

8) Computer programs were written for bandpass filtering, computation of P-residuals, least squares epicenter location, computation of theoretical travel-times from a given velocity structure, computation of theoretical Rayleigh dispersion curves and modal shape, computation of the variation of phase velocity with layer parameter variations, and the computation of the mass anomaly from a given gravity anomaly profile.

At the start of the project, it was anticipated to do considerable work on phase and amplitude spectra of both seismic signals and background noise. Also, it was hoped that more work could have been done on general seismicity, distribution of epicenters, total depth, and energy release. Failure to

acquire a digital system and the fact that much work had been done on background noise did not make the study of spectra appear worthwhile. The general seismicity study was frustrated by the poor recording station distribution in the region. Therefore, crustal and upper mantle structural studies utilizing refraction, gravity, and surface wave dispersion were concentrated on.

This report specifically covers the local travel-time curves for the Southern Appalachian region (Sec. 2), the determination of crustal thickness from gravity data (Sec. 3), the computation of theoretical dispersion curves (Sec. 4), the determination of Rayleigh group velocities (Sec. 5), and the crustal and upper mantle structure in the Southeastern United States (Sec. 6).

Numerical computational methods, tables, charts, and computer program listings are presented in the Appendices.

2.0 TRAVEL-TIME CURVES FOR THE SOUTHEASTERN UNITED STATES

Travel-time curves were determined by using data from three local earthquakes which were well recorded by Worldwide Standard Seismograph Stations and portable Vela stations operating in the Southeastern United States [Minear, 1966]. Fig. 4 shows the location of the epicenters and recording stations. Travel-time curves drawn from the local earthquake data are shown in Fig. 1. Refraction data obtained from quarry blasts and during the East Coast Onshore Offshore Seismic Experiment and theoretical travel-times computed for a typical linear mountain from the Herglotz-Wiechert equations are also plotted in Fig. 1.

Travel-time curves corresponding to arrivals from the first crustal layer and from the crust mantle boundary are drawn from first arrivals and are estimated accurate to within $\pm .1$ km/sec. Second arrivals were used to define curves corresponding to two major crustal layers. No major third layer in the crust is indicated by the refraction and earthquake data. However, first arrivals from the refraction profiles and second arrivals from 250 to 550 km, indicate that the crustal velocity may increase rather continuously from about 10 km to around 45 km. The local travel-time data yields a crustal model of $h_1 = 33.0$ km ($\alpha = 5.88$ km/sec), $h_2 = 10.8$ km ($\alpha = 6.58$ km/sec), and an upper mantle velocity of 8.10 km/sec. As can be seen from Fig. 4, the epicenters and recording stations are generally located to the west of the core of the Appalachians. Crustal structure determined from the travel-time data thus corresponds to the crust beneath the Appalachian foreland.

Velocity structures of the crust and upper mantle for the Appalachian foreland, the Northern Alps (N), Central Alps (C), and Northern Alpine foreland (F) [Knopoff, et al, 1966], and a linear mountain belt are shown in Fig. 2. Crustal velocities for the Appalachian foreland generally agree

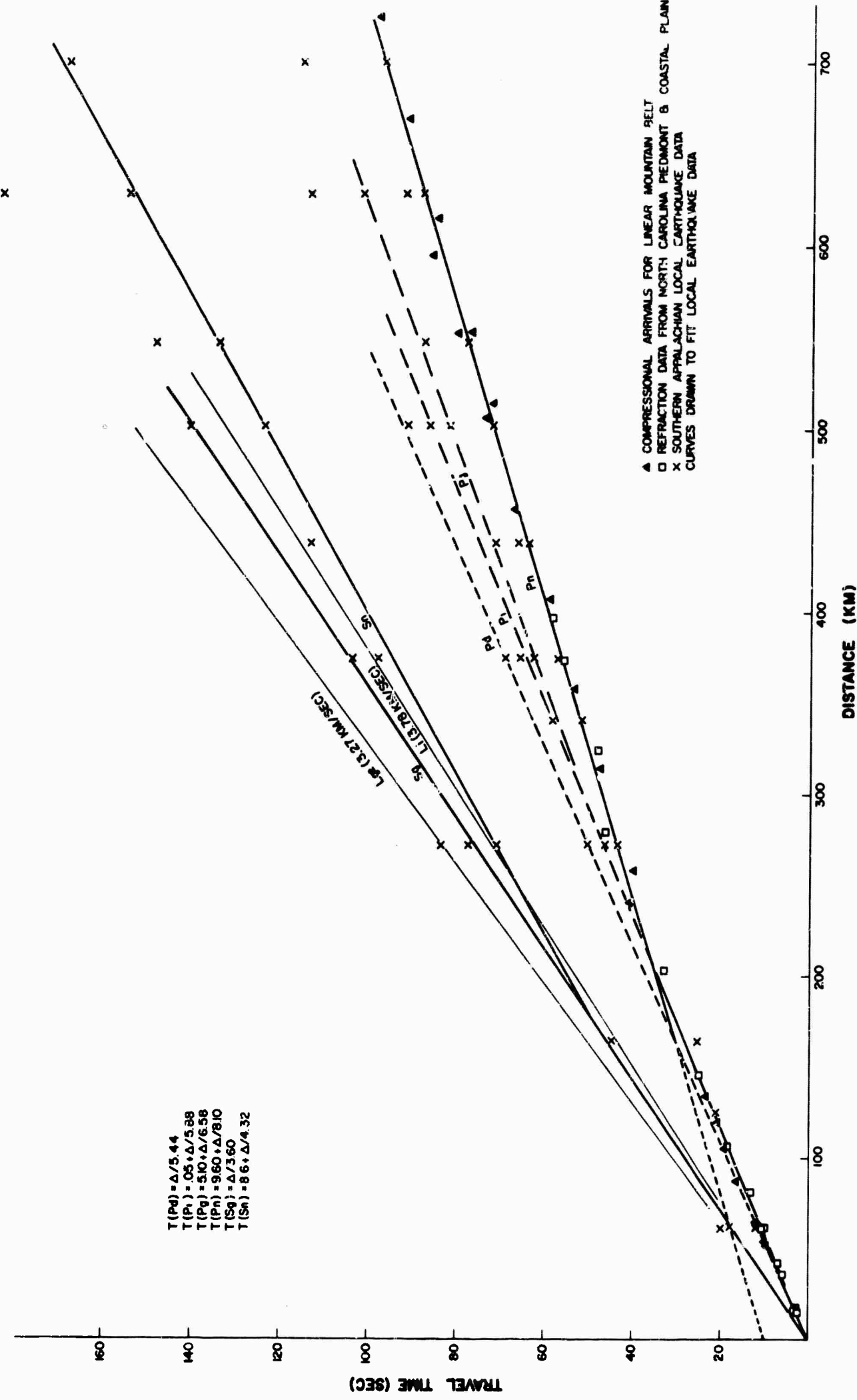


Fig. 1

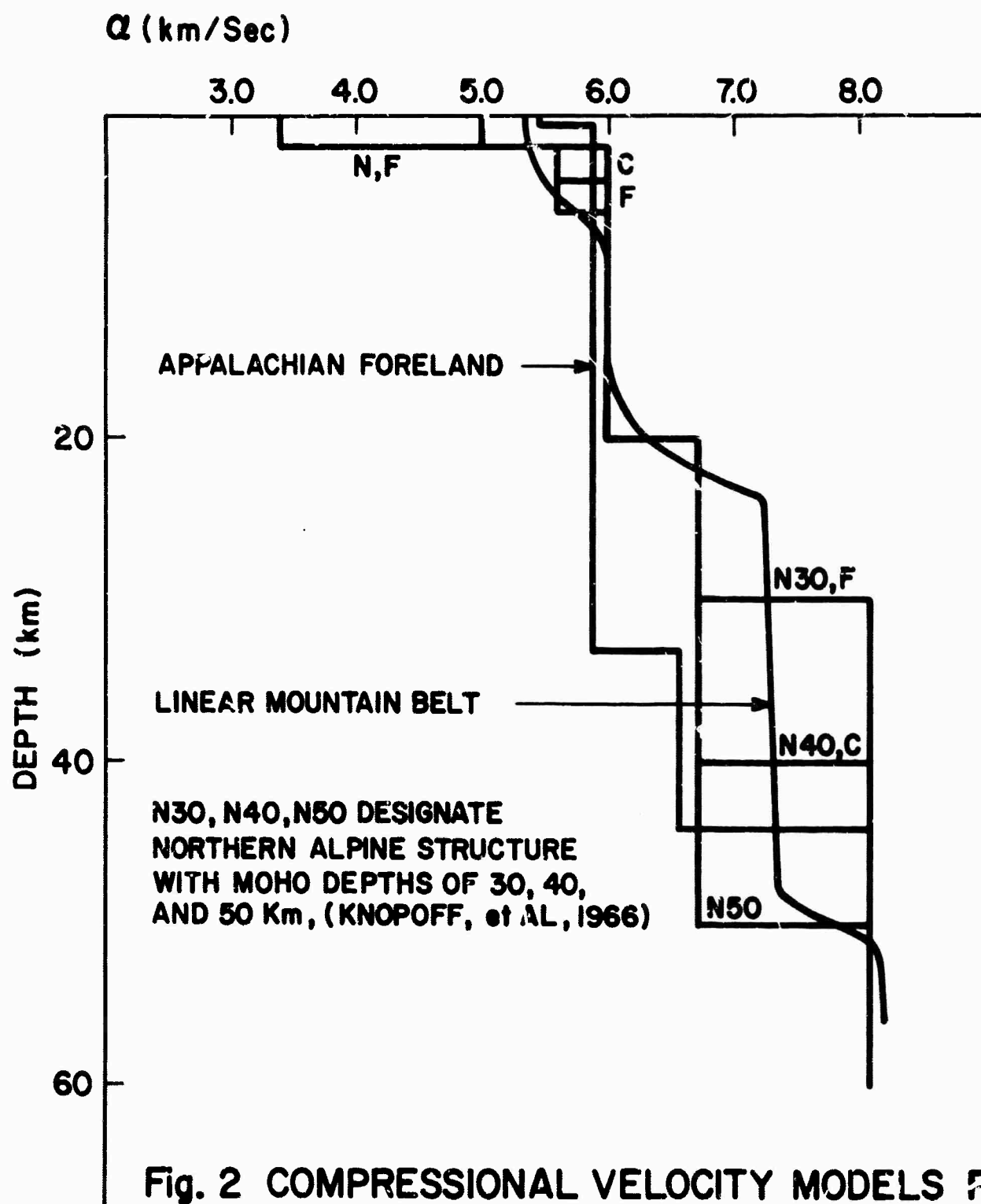


Fig. 2 COMPRESSORIAL VELOCITY MODELS FOR
LINEAR MT. BELT, APPALACHIAN FORELAND,
AND ALPINE STRUCTURE (KNOPOFF, et AL, 1966)

with those for the Northern Alps at depths greater than about 2 km. The disagreement for depths less than 2 km can probably be accounted for by the sedimentary cover present in the Northern Alps. The 5.85 km/sec layer in the Appalachian foreland, extending to a depth of 33 km, is thicker than any of the Alpine structures. However, as mentioned, the Appalachian foreland velocities may increase rather continuously from about 10 to 40 km. Upper mantle depth in the Appalachian foreland is greater than beneath the foreland to the north of the Alps by 14 km and greater than beneath the central Alps by 4 km.

A preliminary summary of seismic refraction work in the vicinity of the Cumberland Plateau Seismological Observatory [Bracherdt et al, 1966] indicates a crustal model of $h_1 = 12$ km ($v_1 = 6.1$ km/sec); $h_2 = 28$ km ($v_2 = 6.7$ km/sec) and an upper mantle velocity of $8.0 +$ km/sec.

3.0 CRUSTAL THICKNESS FROM GRAVITY DATA

Total crustal thickness was computed from Bouguer gravity values along a Northwest-Southeast profile extending from about 460 km off the North Carolina coast (33°N , 73°W) to the Kentucky-Illinois border (38°N , 88°W). The $\sin x/x$ method of Tomoda and Aki [1955] was used to compute the depth to a mass anomaly producing the observed gravity anomalies. Bouguer gravity values were taken from the American Geophysical Union Bouguer Gravity Anomaly Map of the United States. Fig. 3 shows the gravity profile values, the total crustal thickness computed from these anomalies, and regional subsurface geology. The subsurface geological information was obtained from McGuire and Howell [1963] in Kentucky, Hersey, et al [1959] for the North Carolina continental margin, and from the geologic map of North Carolina. Crustal structure to the crust-mantle boundary at location H', and to 2 km at 12-13 is based on refraction profiles of Hersey, et al. The subsurface geology in North Carolina is intended only to indicate possible near surface relations between geology and Bouguer gravity anomalies.

In the $\sin x/x$ method, crustal thickness is computed from

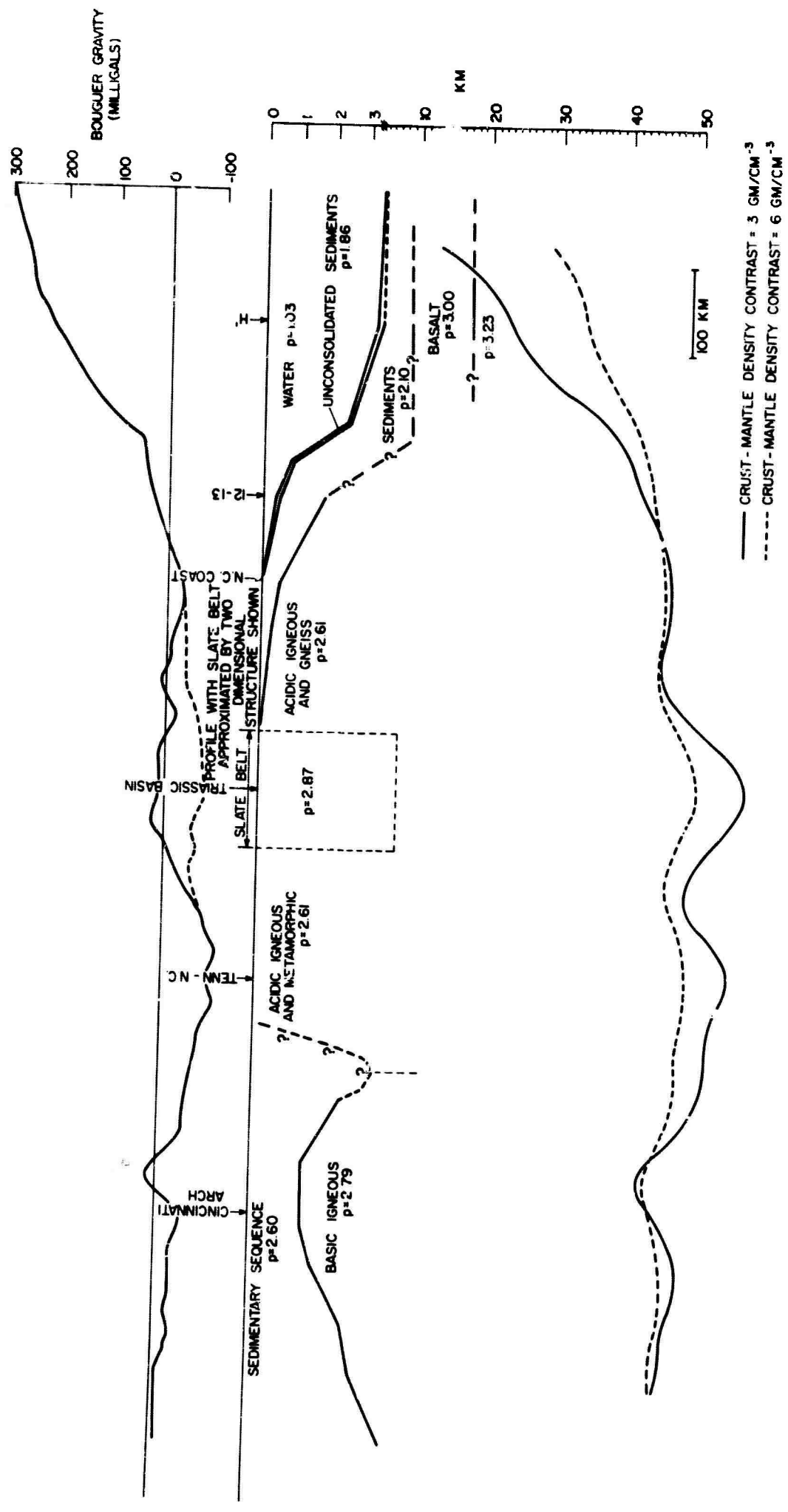
$$d(nx) = d - d'(nx) \quad 3.0-1$$

where d is an assumed thickness and $d'(nx)$ is a correction to this thickness given by

$$d'(nx) = \frac{M(nx)}{\Delta\phi} . \quad 3.0-2$$

$M(nx)$ is the convolution of the observed gravity anomalies $\Delta g(q\Delta x)$ with a symmetric function Φ_n which is a function of assumed crustal thickness and station spacing. Thus,

$$M(nx) = \frac{1}{2\pi^2 k^2} \sum_{q=-m}^{q=m} \Delta g(q\Delta x) \Phi_{n-q} \quad 3.0-3$$



CRUSTAL THICKNESS FROM BOUGUER GRAVITY ANOMALIES

23

Oscillations in the gravity values $\Delta q(q\Delta x)$ due to near surface density irregularities can result in $\Delta q(q\Delta x)$ going positive and negative, such as in the region over the slate belt in Fig. 3. Thus, $M(nx)$ may oscillate between positive and negative values which in turn yields positive and negative oscillations of $d'(nx)$. The ultimate effect is that in the regions of local near surface perturbations, the total crustal thickness, $d(nx)$, may oscillate widely about the assumed thickness, d , as can be seen from 3.0-1. Introduction of a density contrast $\Delta\rho$ which varies with depth will not eliminate these oscillations. One must either choose the station spacing wide enough so that the convolution of the anomalies with the function Φ_n effectively filters out the local perturbations or smooth the total depth function $d(nx)$.

From Fig. 3, it can be seen that the Carolina Slate Belt is associated with a gravity high which effectively introduces a positive perturbation on the regionally decreasing gravity. If the crustal thickness is computed without removing this perturbation, the thickness oscillates about the assumed thickness beneath the belt. As shown in Fig. 3, the local gravity high over the slate belt can be largely accounted for if the belt is approximated by a two-dimensional block with lateral extent equal to the slate belt, an 8 km depth and a density contrast of $.26 \text{ gm/cm}^{-3}$.

Crustal thickness was computed from 3.0-1 using 3.0-2 and 3.0-3 with an assumed crustal thickness of 45 km and a station spacing of 60 km. The thickness values were then smoothed with a three point moving average filter (.25, .50, .25) resulting in the smoothed crustal thickness curves shown in Fig. 3. Two curves are plotted, corresponding to crustal-upper mantle density contrasts of .3 and $.6 \text{ gm/cm}^{-3}$. Since the ocean's crust is denser than the continental crust, the $\Delta\rho = .3$ curve approximates the crustal thickness

better under the continental margin. The agreement with the thickness as determined by refraction work [Hersey, et.al., 1959] at point H' is good. Both curves indicate a crustal thickness of at least 50 km under the Southern Appalachians. Perturbations in the crustal thickness are caused by the Cincinnati Arch and the Carolina Slate Belt. The thinning of the crust necessary to produce the Bouguer anomaly over the Cincinnati arch and the slate belt is about 9 km for the $\Delta p = .6$ curve and about 4.5 km for the $\Delta p = .3$ curve. Due to the magnitude of the crustal thickness changes, it appears that the sources of the local highs over the Cincinnati Arch and the Carolina Slate Belt are relatively near surface.

The crust thus thickens from about 83 km at the North Carolina coast to about 51 km beneath the core of the Appalachians and then thins to about 43 km at the Kentucky-Illinois border.

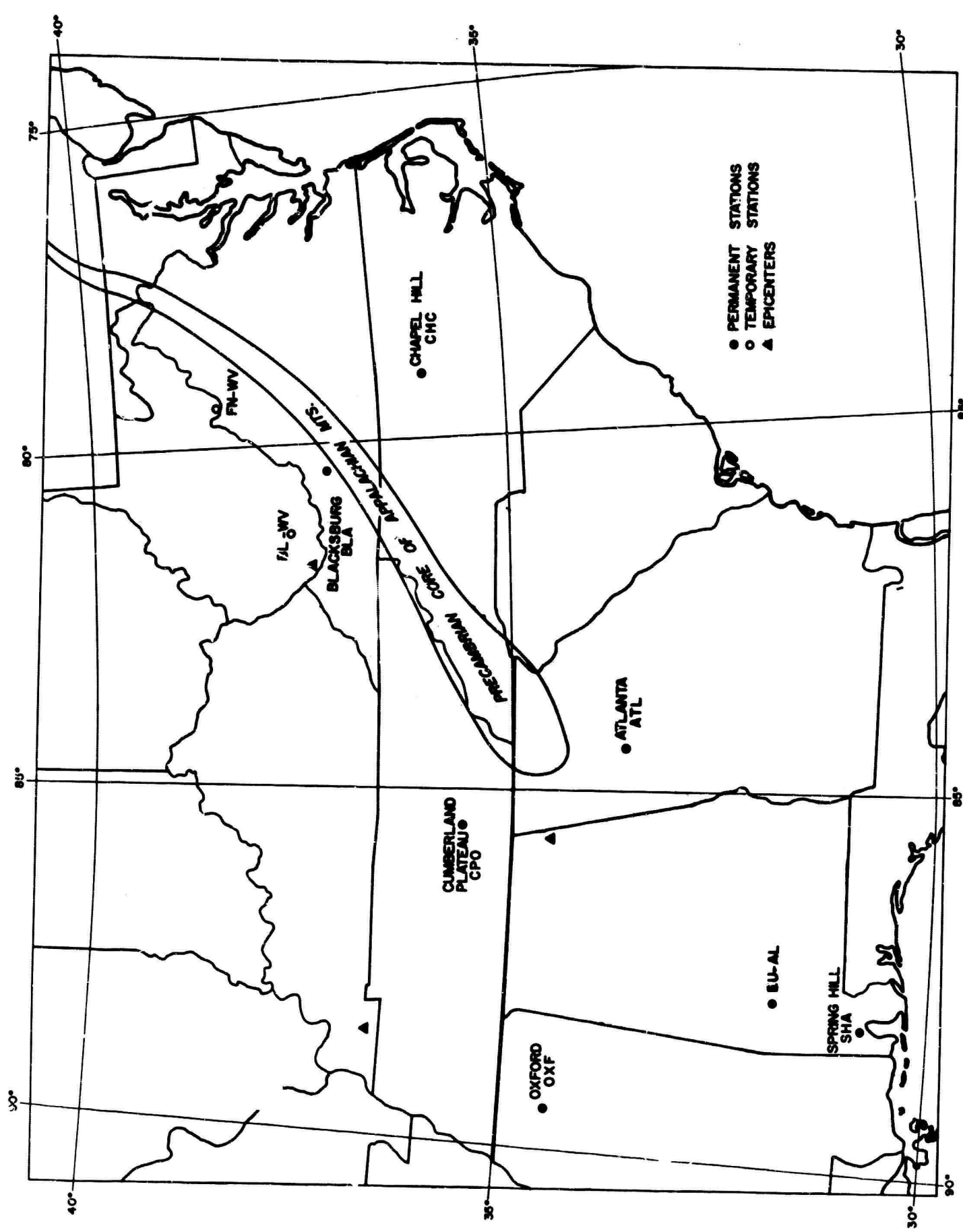
4.0 DETERMINATION OF RAYLEIGH GROUP VELOCITY

The locations of permanent recording stations in the Southeastern United States lie principally along the Appalachian trend (See Fig. 4). Permanent worldwide standard stations capable of recording long-period seismic signals are located at Spring Hill, Alabama (SHA); Atlanta, Georgia (ATL); McMinnville, Tennessee (CPO) ; Blacksburg, Virginia (BLA); and Oxford, Mississippi (OXF). Portable long-period units have been operated by the Geotechnical Corporation under project Vela, but these stations are also located along the Appalachians. Because of the widely space station, it was impossible to calculate phase velocities directly using triangular arrays of stations. Therefore, epicenters were selected to give travel paths parallel or perpendicular to the Appalachian trend. It was hoped that variations in crustal and upper mantle structure between stations located along the Appalachians could be detected by observing the variation of group velocity of a wave train traveling the station sequence SHA -ATL -BLA parallel to the Appalachian trend or by comparing group velocities at BLA and ATL from waves arriving perpendicular to the Appalachian with those of a normal continental structure.

On the basis of epicentral location, signal amplitude, and availability of records, two epicenters were selected for study. Table II gives the information pertinent to these epicenters.

Table II

Epicenter Location (USGS)	Date	Time (USGS)	Magnitude (USGS)	Focal Depth(km) (USGS)	Distance(km) to station
Jalisco, Mex. 17.8N, 105.9W	11 Oct., 1963	10:17:07.6	5.0	33	BLA - 3286.3 OXF - 2467.3 SHA - 2291.0 ATL - 2757.6
S. Alaska 62.7N, 132.0W	29 June, 1964	07:21:32.8	5.6	33	BLA - 5488.0 OXF - 5276.3 SHA - 5110.0 ATL - 5633.9



LOCATION MAP OF PERMANENT AND TEMPORARY SEISMOGRAPH STATIONS USED IN TRAVEL-TIME AND RAYLEIGH WAVE DISPERSION STUDIES

Fig. 4

Records from the standard stations were hand digitized at two second intervals using a plastic grid overlay. This digital data was stored on magnetic tape for processing. Since the azimuths of the epicenters measured from the recording stations did not coincide with either of the horizontal component seismograph orientations, Rayleigh wave motion was contaminated by Love wave motion. In order to separate the Rayleigh and Love wave motions, radial and transverse seismograms were generated from the North-South and East-West components at each station. The relations used in the transformations were

$$\begin{aligned}\text{radial component} &= r = \overline{OE} \cos\theta + \overline{ON} \sin\theta, \text{ and} \\ \text{transverse component} &= t = \overline{OE} \sin\theta - \overline{ON} \cos\theta.\end{aligned}$$

where

θ = azimuth of epicenter from station measured counterclockwise
from east,

\overline{OE} = east-west component amplitude, positive toward east,

\overline{ON} = north-south component amplitude, positive toward north

$r > 0$ => radial motion toward epicenter, and

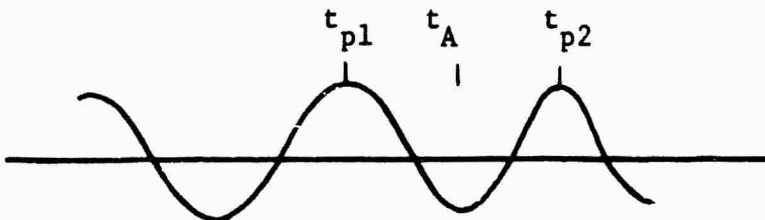
$t > 0$ => transverse motion to right of propagation direction.

Sections of Rayleigh wave motion were then determined from visual inspection of plots of the radial and transverse components. Determination of the particle motion of small amplitude high frequency motion in the presence of large amplitude low frequency motion is difficult. Ideally, the radial and transverse components should be band-pass filtered to separate the frequencies and particle motion then determined for specified frequency intervals. However, due to the computer time involved, this was not feasible for this study. Since only the first higher Rayleigh mode was present on the recordings, the particle motion for the frequencies involved could be fairly well obtained from the unfiltered radial and transverse components.

Vertical component records were convolved with 101 point, digital, band-pass filters described by Minear [1966]. Pass bands of 60-100, 25-62, 16-30, 10-17, and 7-13 sec were used successively. The filtered data was plotted by using a Calcomp plotter. Period was obtained by reading the peak-to-peak period from the Calcomp plots. Arrival time for the period was taken as the time defined by

$$t_A = t_{p1} + \frac{t_{p2} - t_{p1}}{2}$$

with the quantities defined in the following figure.



Group velocity was then obtained by dividing the epicentral distance by the arrival time.

Group velocity vs. period data for the Southern Appalachians is presented in Table III and Figs. 8-11.

TABLE III. RAYLEIGH WAVE GROUP VELOCITIES FOR THE SOUTHERN APPALACHIANS

EPICENTER-N. ALASKA
STATION-ATLANTA, GA.EPICENTER-S. ALASKA
STATION-OXFORD, MISS.

Fundamental Rayleigh		First Higher Rayleigh		Fundamental Rayleigh		Fundamental Rayleigh	
Period(sec)	Group Velocity(km/sec)	Period(sec)	Group Velocity(km/sec)	Period(sec)	Group Velocity(km/sec)	Period(sec)	Group Velocity(km/sec)
59.66	3.72	8.64	3.52	67.04	3.84	12.40	3.01
52.75	3.72	7.85	3.56	54.79	3.67	12.40	2.96
41.13	3.53	7.85	3.55	40.04	3.37	11.78	3.07
36.90	3.62	7.85	3.51	34.54	3.49	11.62	3.05
32.81	3.44	7.07	3.49	31.40	3.41	10.52	2.98
30.62	3.38	7.07	3.47	29.05	3.35	9.89	2.97
26.69	3.29	7.07	3.49	26.85	3.14	9.89	2.92
27.00	3.24	6.28	3.46	24.81	3.29	9.89	2.70
27.00	3.19	6.28	3.45	24.65	3.24	9.73	2.95
24.02	3.14	6.91	3.50	23.71	3.09	9.73	2.88
19.31	3.05	6.12	3.54	23.08	3.05	8.32	2.93
18.68	3.02	6.12	3.47	21.51	2.97	8.16	2.86
18.84	2.96	5.65	3.52	20.25	3.01	8.01	2.89
18.21	2.99	5.34	3.43	19.94	2.94		
18.06	2.86	4.55	2.53	19.94	2.93		
18.06	2.31			18.37	2.91		
17.90	2.91			18.06	2.85		
16.80	2.94			17.74	2.90		
16.17	2.88			17.43	2.88		
15.70	2.81			16.64	2.73		
15.17	3.04			16.17	2.83		
14.13	2.98			16.17	2.76		
13.25	3.02			16.01	2.78		
13.03	3.07			15.86	2.80		
12.09	3.13			14.97	2.88		
12.09	3.00			14.86	2.86		
10.99	3.11			14.70	2.83		
11.99	3.09			13.56	2.81		
9.26	3.01			13.19	3.03		
7.54	3.01			12.87	2.98		
7.54	2.00						
7.22	2.99						
6.59	2.98						

EPICENTER-JALISCO, MEX.
STATION-ATLANTA, GA.EPICENTER-JALISCO, MEX.
STATION-BLACKSBURG, VA.

Fundamental Rayleigh		First Higher Rayleigh		Fundamental Rayleigh		First Higher Rayleigh	
Period(sec)	Group Velocity(km/sec)	Period(sec)	Group Velocity(km/sec)	Period(sec)	Group Velocity(km/sec)	Period(sec)	Group Velocity(km/sec)
55.89	3.76	10.05	3.25	65.16	4.11	18.37	3.76
44.90	3.52	9.89	3.29	62.02	3.81	16.17	3.84
38.78	3.34	9.89	3.22	50.08	3.55	16.01	3.98
33.76	3.20	8.79	3.16	39.41	3.38	14.13	3.32
27.48	3.20	8.32	2.98	32.34	3.16	13.97	3.23
22.45	3.11	8.01	3.13	31.87	3.26	13.82	3.91
19.94	3.03	8.01	3.05	29.67	3.07	13.66	3.59
17.11	2.97	8.01	3.00	26.38	2.99	13.35	3.70
16.80	2.92	7.85	3.08	25.90	2.92	13.35	3.54
12.40	2.89	7.07	3.18	25.40	2.87	13.03	3.49
12.09	2.70	6.28	3.10	19.80	2.77	12.25	3.64
11.93	2.66	5.81	3.03	19.50	2.70	12.09	3.36
11.78	2.85			18.10	2.69	11.93	3.45
11.78	2.82			14.29	2.77	11.93	3.27
11.52	2.78			13.50	2.74	11.78	3.19
10.99	2.69			12.56	2.70	11.46	3.40
10.99	2.66			12.09	2.63	10.68	3.13
10.36	2.75			11.93	2.65	10.05	3.16
10.21	2.75			11.78	2.60	9.73	3.09
10.05	7.72			9.89	2.58	9.26	3.10
10.00	2.69			8.01	2.56	8.16	3.05
9.89	2.73			6.12	2.55	8.01	3.07
8.90	2.62					7.85	3.01
8.80	2.67					5.97	3.03
8.20	2.64						
8.19	2.60						
8.16	2.58						
8.16	2.56						
7.69	2.64						
6.44	2.55						

TABLE III (CONT'D)

EPICENTER-S, ALASKA
STATION-BLACKSBURG, VA.

Fundamental Rayleigh		First Higher Rayleigh	
Period(sec)	Group Velocity(km/sec)	Period(sec)	Group Velocity(km/sec)
66.88	4.06	33.13	4.27
62.64	3.88	32.97	4.16
58.88	3.72	31.09	4.43
49.14	3.73	30.93	4.32
39.41	3.62	30.46	4.54
39.41	3.53	28.73	4.09
31.40	3.45	20.72	4.23
27.00	3.20	20.30	4.35
25.43	3.15	17.11	4.18
25.28	3.10	15.54	4.29
21.82	3.06	15.23	3.94
19.94	3.03	14.44	3.98
19.94	2.97	13.30	4.12
18.68	2.89	13.03	4.20
18.06	3.00	13.03	4.16
18.06	2.94	13.03	4.02
17.58	2.87	12.72	3.90
17.58	2.84	12.72	3.80
16.17	2.89	12.40	3.86
15.86	2.92	12.25	3.83
15.39	2.87	11.93	3.76
13.97	2.84	11.46	3.73
11.62	3.08	11.78	3.70
11.62	3.04	9.89	3.49
11.30	3.06	8.01	3.52
10.21	3.10	7.85	3.46
9.42	3.02	7.69	3.60
9.26	3.00	6.12	3.58
8.32	2.98	6.12	3.54
8.16	2.92	6.12	3.51
8.01	2.93	6.12	3.47
7.85	3.06	5.97	3.55
7.85	2.94	5.65	3.57
7.22	3.00		
7.22	2.99		
7.22	2.97		
6.91	3.07		
6.91	3.04		
6.75	3.05		
6.75	3.03		
6.28	2.96		
6.28	2.90		
6.12	3.02		
5.65	2.91		

5.0 THEORETICAL RAYLEIGH DISPERSION CURVES

The basic Thomson-Haskell matrix method was used to compute phase and group velocity vs. period curves for layered earth models. A computer program was written to compute Rayleigh wave dispersion curves and mode shape using the modified formulation of the Thomson-Haskell method presented by Dunkin [1965]. A program was also written to compute mode shape using the Thomson-Haskell method. A discussion and comparison of the computation methods used is given in this section. Appendix I and II contain detailed descriptions of the actual mechanics of computation and computer programming. Fortran listings of the programs are given in Appendix III.

5.1 Thomson-Haskell Matrix Method

As is well known, the Thomson-Haskell matrix method consists of evaluating the roots of a determinant formed by the repeated multiplication of 4×4 layer matrices which are functions of the layer parameters of density, thickness, compressional velocity, shear velocity, as well as phase velocity and period.

Using Haskell's notation, the displacement-stress matrices at the top and bottom of the m^{th} layer are given by

$$\begin{bmatrix} \frac{\dot{u}_m}{c} \\ \frac{\dot{w}_m}{c} \\ \sigma_m \\ \tau_m \end{bmatrix} = a_m \begin{bmatrix} \frac{\dot{u}_{m-1}}{c} \\ \frac{\dot{w}_{m-1}}{c} \\ \sigma_{m-1} \\ \tau_{m-1} \end{bmatrix} \quad (5.1-1)$$

where $a_m = D_m F_m^{-1}$ is the m^{th} layer matrix. By repeated application of (5.1-1), Haskell shows that, assuming no stresses at the free surface ($\sigma = \tau_o = 0$) and no sources at infinity,

$$\begin{bmatrix} \Delta_n' \\ \Delta_n' \\ \omega_n' \\ \omega_n' \end{bmatrix} = J \begin{bmatrix} \dot{u}_o \\ \dot{w}_o \\ c \\ 0 \\ 0 \end{bmatrix} \quad (5.1-2)$$

where $J = F_n^{-1} a_{n-1} \dots a_1$ is the matrix product of the 4×4 layer matrices a_m , eliminating Δ_n' and ω_n' between the four equations yields

$$\frac{\dot{u}_o}{\dot{w}_o} = \frac{J_{22} - J_{12}}{J_{11} - J_{21}} = \frac{J_{42} - J_{32}}{J_{31} - J_{41}} \quad (5.1-3)$$

Since the J_{ij} , are functions of phase velocity and wave number, (5.1-3) is an implicit relation between c and k and thus the phase velocity dispersion function. The layer matrix elements of a_m are either trigonometric or hyperbolic functions depending on whether the phase velocity is greater than or less than the layer compressional and/or shear velocities. The multiplication of real and imaginary components of matrices on a computer which does not have complex number subroutines would in general add considerable complexity to the problem. However, as shown in Appendix I, the form of the layer matrices leads to a simple solution by which the multiplication of the matrices with real and imaginary elements can be accomplished by the multiplication of certain elements by ± 1 .

5.2 Numerical Difficulties in the Thomson-Haskell Method

In practice, numerical computational difficulties are encountered in the repeated matrix multiplication required to evaluate the roots of (5.1-3). These difficulties are encountered as the product of kH , where k is the wave number, and H is the total thickness of the layered earth model, becomes large. Dorman, Ewing, and Oliver [1960] have used an upper limit of about 30 for kH . When the value of kH reaches about 30, the number of layers can be reduced and the computation continued with a reduced thickness. Little error is introduced by this technique. However, for higher modes and hence, higher frequencies, the product kH may be relatively large even for layered earth models of small total thickness, H .

Dunkin [1965] has shown the numerical difficulties are caused by the computation of large exponentials and a resulting loss of significant figures. Dunkin's development is briefly repeated below in order to show the effect of loss of significance due to the addition of large and small quantities on the Haskell matrix. The argument is applied directly to the Haskell dispersion equation (5.1-3) rather than to the secular equation used by Dunkin.

Let the scalar and vector potential functions for an elastic body have the form

$$\begin{aligned}\phi_n &= \exp(ik(ct-x)) [A_n \exp(ikz\sqrt{c^2/\alpha^2 - 1}) + B_n \exp(-ikz\sqrt{c^2/\alpha^2 - 1})] \\ &= \exp(ik(ct-x)) [\phi_n^+ + \phi_n^-] \\ \psi_n &= \exp(ik(ct-x)) [C_n \exp(ikz\sqrt{c^2/\beta^2 - 1}) + D_n \exp(-ikz\sqrt{c^2/\beta^2 - 1})] \quad (5.2-1) \\ &= \exp(ik(ct-x)) [\psi_n^+ - \psi_n^-]\end{aligned}$$

Using (5.2-1) and the equation

$$\bar{S} (u, v, w) = \nabla \cdot \phi + \nabla \times \psi (\psi_1, \psi_2, \psi_3) \quad (5.2-2)$$

the displacement-stress vector, S_n , can be expressed as

$$S_n (z) = T_n \Phi_n (z) \quad (5.2-3)$$

where

$$\Phi_n (z) = \begin{bmatrix} \phi_n^+ \\ \psi_n^+ \\ \phi_n^- \\ \psi_n^- \end{bmatrix}$$

and T_n is a 4×4 matrix function of c , k , and the layer parameters.

Taking the origin at the z_{n-1} interface (5.2-1) gives

$$\phi_{n-1} = A_n + B_n = \phi_n^+ (z_{n-1}) + \phi_n^- (z_{n-1})$$

$$\psi_{n-1} = C_n + D_n = \psi_n^+ (z_{n-1}) + \psi_n^- (z_{n-1})$$

At the z_n interface

$$\phi_n = A_n \exp ikd_n r_{\alpha n} + B_n \exp -ikd_n r_{\alpha n} = \phi_n^+ (z_n) + \phi_n^- (z_n)$$

$$\psi_n = C_n \exp ikd_n r_{\beta n} + D_n \exp -ikd_n r_{\beta n} = \psi_n^+ (z_n) + \psi_n^- (z_n)$$

The relation between $\phi_n(z_n)$ at the z_n interface and $\phi_n(z_{n-1})$ at the z_{n-1} interface is then

$$\phi_n(z_n) = E_n \phi_n(z_{n-1}) \quad (5.2-4)$$

where

$$E_n = \begin{bmatrix} \exp ikd_n r_{\alpha n} & 0 & 0 & 0 \\ 0 & \exp ikd_n r_{\beta n} & 0 & 0 \\ 0 & 0 & \exp -ikd_n r_{\alpha n} & 0 \\ 0 & 0 & 0 & \exp -ikd_n r_{\beta n} \end{bmatrix} \quad (5.2-5)$$

At the $n-1$ interface

$$S_n(z_{n-1}) = T_n \phi_n(z_{n-1})$$

or

$$\phi_n(z_{n-1}) = T_n^{-1} S_n(z_{n-1}). \quad (5.2-6)$$

Now, by the boundary conditions of the continuity of stress and displacement

$$S_n(z_n) = S_{n+1}(z_n) = T_n \phi_n(z_n) \quad (5.2-7)$$

Substituting (5.2-4) for $\phi_n(z_n)$ and (5.2-6) for $\phi_n(z_{n-1})$ in (5.2-7) gives

$$S_{n+1}(z_n) = T_n E_n T_n^{-1} S_n(z_{n-1}) . \quad (5.2-8)$$

This equation is equivalent to Haskell's equation

$$S_{n+1}(z_n) = a_n S_n(z_{n-1}) , \quad (5.2-9)$$

$$\text{with } a_n = T_n E_n T_n^{-1} .$$

By (5.2-8) the displacement-stress vector is converted into Φ_n , continued through the layer z_n by E_n , and converted back into $S_n(z_n)$ at the interface $n+1$ which is equal to $S_{n+1}(z_n)$. The Haskell layer matrix carries the displacement-stress vector from the n^{th} interface, through the layer, and across the $n+1$ interface in one operation. Eq. (5.2-8) brings into evidence the effect of the "continuing" matrix E_n .

Consider the matrix linking the displacement-stress vectors at the free surface and the last layer of an assumed layered sequence.

$$S_{n-1} = G_{n-1} \dots G_1 S_0 = P S_0 , \quad (5.2-10)$$

where

$$G_n = T_n E_n T_n^{-1}$$

In the Haskell formulation, the matrix from which the dispersion relation is obtained is given by $J = F_n^{-1}P$ and in the Dunkin formulation this matrix is $T_n^{-1}P$. However, considerations of the numerical evaluation of the P matrix will yield results valid to both developments since the T_n^{-1} or F_n^{-1} do not contain exponential powers.

Let P be written as

$$P = A T_m E_m T_m^{-1} B \quad (5.2-11)$$

where

$$A = G_{n-1} \dots G_{m+1}$$

$$B = G_{m-1} \dots G_1$$

Using the definitions of T_m and E_m , it can be shown that the components of P are of the form

$$P_{ij} = B_{ij} \exp(i k d_m r_{\alpha m}) + C_{ij} \exp(i k d_m r_{\beta m}) + D_{ij} \exp(-i k d_m r_{\alpha m}) + E_{ij} \exp(-i k d_m r_{\beta m}) \quad (5.2-12)$$

For the Haskell development, F_n^{-1} is of the form

$$F_n^{-1} = \begin{bmatrix} F_{11} & 0 & F_{23} & 0 \\ 0 & F_{22} & 0 & F_{24} \\ F_{31} & 0 & F_{33} & 0 \\ 0 & F_{42} & 0 & F_{44} \end{bmatrix}$$

which gives for the two components J_{12} and J_{22}

$$J_{12} = F_{11} P_{12} + F_{13} P_{32}, \text{ and} \quad (5.2-13)$$

$$J_{22} = F_{22} P_{22} + F_{24} P_{42}$$

Now suppose that for the m^{th} layer $r_{\alpha m}$ and $r_{\beta m}$ are negative imaginary ($c < \alpha$) so that $\exp ik_m r_{\alpha m}$ and $\exp ik_m r_{\beta m}$ may be large depending on the value of k . If the exponential term is large enough, the effect of the smaller terms in P_{ij} will be neglected in computing the P_{ij} , because of loss of significance. In the evaluation of the roots of (5.1-3) the difference $(J_{12} - J_{22})$ must be taken. Although the P_{ij} are large, their differences may be small. Therefore, terms which were lost because of loss of significance in computing the P_{ij} would be important in the difference of J_{12} and J_{22} . Mode shape is computed from repeated applications of (5.1-1) using the starting values of \dot{u}_o and \dot{w}_o from (5.1-3). Therefore, the same problem with loss of significance is inherent in the Haskell method of computing modal shape.

5.3 Dunkin Modification of the Haskell Method

Dunkin derives the secular or period equation in the form

$$\text{Det } R_{11} = 0 \quad (5.3-1)$$

Where

$$R = \begin{bmatrix} R_{11} & R_{12} \\ R_{21} & R_{22} \end{bmatrix} = T_p^{-1} G_{p-1} \dots G_1 \quad (5.3-2)$$

He shows that $\text{Det } R_{11}$ can be expanded as a product of the second order subdeterminants of T_p^{-1} and G_p yielding

$$\text{Det } R_{11} = t^{p-1} \left| \begin{array}{cc} 12 & g^{p-1} \\ ab & cd \end{array} \right| \dots g^1 \left| \begin{array}{cc} ef \\ 12 \end{array} \right| , \quad (5.3-3)$$

where $g^p |_{kl}^{ij}$ is the second order subdeterminant of G_p involving rows i and j and columns k and ℓ . Dunkin has shown that by using algebraic expressions for the subdeterminants of the G_p , numerical difficulties with loss of significance can be avoided since the products of like exponentials normally occurring in the secular function are excluded at the start. Products of unlike exponentials for a given layer effectively increase the magnitude of $\text{Det } R_{11}$. To prevent machine overflow, the secular function can be divided by the two largest exponents when these exponents become real and the exponential expression becomes hyperbolic. This results in no loss of significance.

Explicit expressions for the g_{kl}^{ij} and the g_{ij} are given in Appendix II for real frequencies and wave numbers. These are slightly different from the definitions of Dunkin, since he assumes complex frequencies.

Mode shapes are computed using the following relation of Dunkin discussed in Appendix II,

$$1) \quad R_n^m(z; a) = r_{11}^{-1} t_{1r}^p g_{rs}^{p-1} \dots g_{vb}^n(z_n - z) g^n(z - z_{n-1}) |_{cd}^{ab} \dots g^1 |_{21}^{ef} \quad (5.3-4)$$

5.4 Computational Procedure

The Dunkin method was programmed in Fortran II for the Bunker-Ramo 340 computer. Equation (5.3-1) was used for the determination of Rayleigh wave dispersion curves. Equation (5.3-4) was used to compute the mode shape once the roots of (5.3-1) were obtained. A double precision program was written in Fortran II for the IBM 360-75 using the Haskell method for computing mode shape. Equation (5.1-1) was used for this computation. Figs. 5 and 6 are flow charts of the computer program FLATRAY used in the computation of Rayleigh dispersion and modal shape. A computer listing of the program is given in Appendix III.

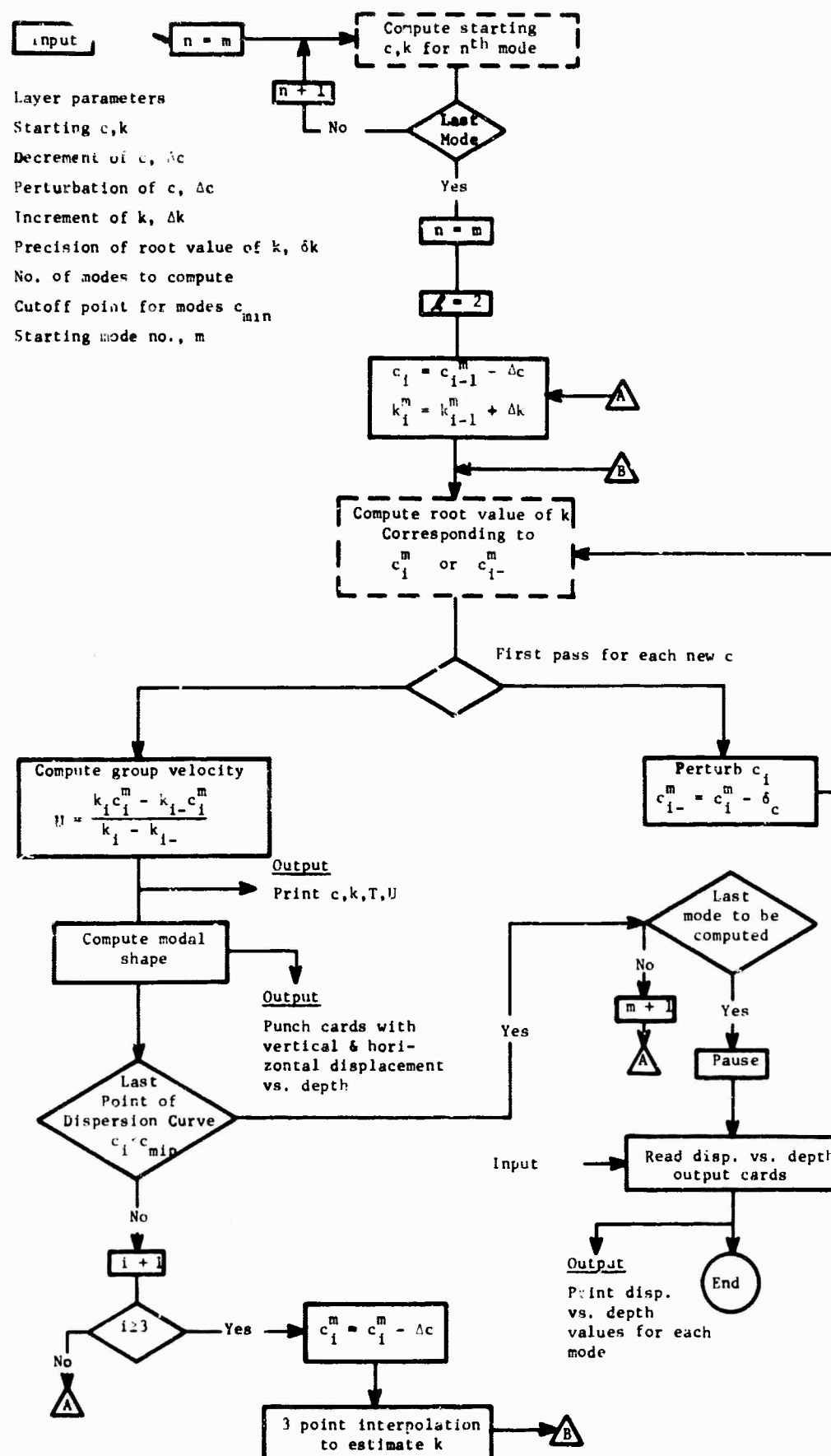


Fig. 5. Flow chart of FLATRAY

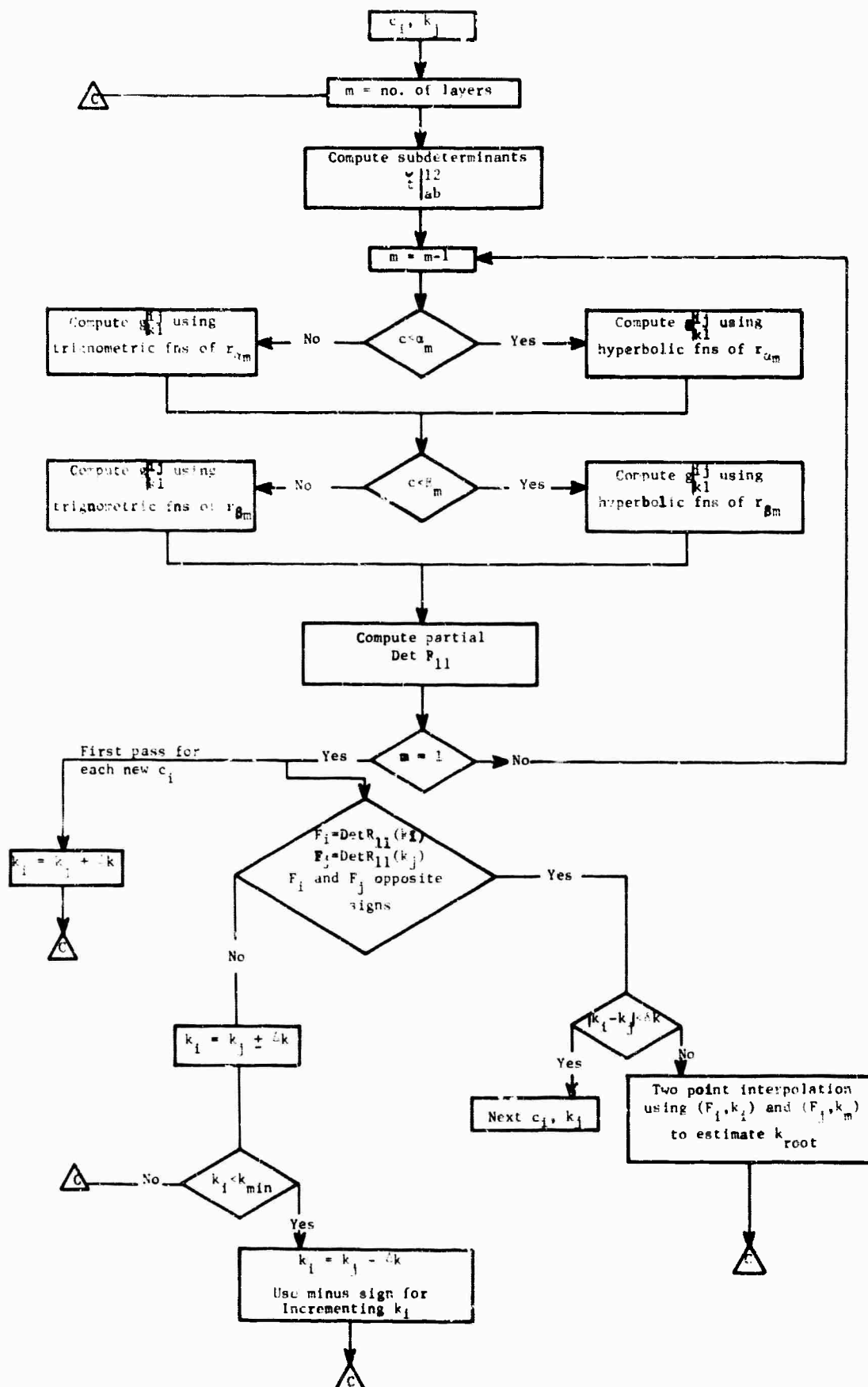


Fig. 6. Flow chart for determining roots of secular function,
Det R₁₁ (Dashed boxes of Fig. 5)

Root Finding Scheme

The technique used for finding the roots of (5.3-1) consists of two steps. In order to determine roots for different modes, a given phase velocity, c_o , and starting wave number, k_{io} , are specified. K_{io} is then incremented using the constant c_o value until a root is bracketed. A two point interpolation scheme is then used until the difference between two values of k which successively bracket the root is less than an input value. If more than one mode is to be investigated, k is incremented from its value at the last root found using the same value of c_o until the next root is found. Thus, the roots along a constant c curve are found which correspond to different modes. In order to define a particular mode, computation begins at c_o and the k_{io} corresponding to the desired mode. C is decremented and k incremented by values specified as input parameters. K is varied at the new $- \Delta c$ until the root is bracketed. Two point interpolation is then used until k is obtained with the desired accuracy. The process of decrementing c and incrementing k is continued until three points on a given modal dispersion curve are found. A three point Gregory-Newton interpolation scheme is then used to estimate the next root on the curve. The process of interpolation and bracketing continues until a dispersion curve is defined to some minimum specified value of c .

Group velocity values are computed by perturbing c a small amount from a value at which a corresponding k was been found. K is found for the perturbed c and a two point difference scheme used to evaluate group velocity, U , according to

$$U = \frac{dw}{dk} = \frac{\frac{2\pi}{T_2} - \frac{2\pi}{T_1}}{k_2 - k_1}$$

From Table VI it can be seen that the group velocity curves computed by the Dunkin method for many layered models agree with those computed for models with reduced thickness to within a few tenths of a per cent. However, the section must be taken thick enough to include the entire depth to which appreciable particle motion extends. This is illustrated by the first higher mode for the Gutenberg-Birch II model. The period value at 5.00 km/sec is 50.0301 sec for the 400 km section, and 46.4060 sec for the 1000 km section. However, reference to the displacement vs. depth curves in Appendix IV shows that the 400 km section does not include the total depth to which vertical particle motion extends at this period.

Although thick sequences can be used to compute shorter period group velocity curves, it is considerably more economical in computer time to use thinner sequences of fewer layers. Displacement depth curves, such as those in Appendix IV, can be used to indicate the necessary total thickness to be used at given periods.

Modal Shape

After a point (c, k) was found on a given dispersion curve, the mode shape for the given (c, k) was computed using (5.3-4). Horizontal and vertical displacements vs. depth values were then punched out on cards to be used in computing the variation of phase velocity due to variation in layer parameters from INTEGRAL. Modal shape was computed using both the Dunkin and Haskell methods. A double precision program was used in computing modal shape by the Haskell Method. Table IV shows the comparative results for the two methods. Values for horizontal and vertical particle amplitudes agree very well ($< .03\%$) for the first four layers in each case considered in Table IV. After this, the differences between the two methods increase rapidly. The rapid increase of particle amplitude with depth in

TABLE IV. Fundamental Rayleigh mode vertical and horizontal
Particle amplitudes computed by Dunkin and Haskell
Methods for the Gutenberg-Birch II model. Displacement
normalized to the vertical displacement at the surface

Period = 25.440
Phase Velocity = 3.8000
7 Layer model

Section Thickness = 140 km

HASKELL METHOD		DUNKIN METHOD	
<u>Vertical</u>	<u>Horizontal</u>	<u>Vertical</u>	<u>Horizontal</u>
1.000000	.695087i	1.000000	-.695087i
.886979	.008458i	.886972	.008445i
.518503	.056959i	.518524	.056825i
.303885	.106318i	.304132	.040085i
.164817	.076121i	.062881	.012639i
.078571	.050969i	.014165	.003463i
.018264	.048431i	.002693	.000995i

Period = 25.1380
Phase Velocity 3.8000
17 Layer model

Section Thickness = 400 km

1.000000	-.695044i	1.000000	-.695044i
.886837	.008611i	.886883	.008583i
.518193	.056916i	.518278	.056948i
.303773	.105662i	.303749	.040119i
.165958	.073450i	.062646	.012667i
.084840	.041298i	.013984	.003497i
.043072	.015424i	.002541	.001030i
.034665	-.021212i	-.000083	.000406i
.087474	-.119106i	-.000634	.000246i
.324986	-.435748i	-.000713	.000199i
1.117859	-1.484503i	-.000685	.000179i
4.078959	-4.927086i	-.000643	.000165i
13.757256	-16.190590i	-.000595	.000153i
45.749210	-53.018184i	-.000553	.000143i
150.983339	-173.243598i	-.000512	.000133i

TABLE IV (Cont'd)

Period = 25.1380 (Cont'd)
 Phase Velocity=3.8000
 17 Layer model

Section Thickness = 400 km

HASSELL METHOD		DUNKIN. METHOD	
Vertical	Horizontal	Vertical	Horizontal
8.176407	-567.580725i	-.000474	.000123i
10070.040164	-11362.129728i	-.001556	.000026i

Period = 106.4400
 Phase Velocity=4.2000
 35 Layer model

Section Thickness = 2898 km

1.000000	-.838062i	1.000000	-.838062i
1.047271	-.599088i	1.047270	-.599012i
1.054375	-.406096i	1.054340	-.405972i
1.048108	-.190905i	1.048030	-.182671i
1.010899	-.052715i	.968018	-.048623i
.954535	.043822i	.883244	.039389i
.886795	.109889i	.793526	.095305i
.812528	.152015i	.703175	.127442i
.735438	.175957i	.615440	.142587i
.658577	.186915i	.532770	.146331i
.583974	.187969i	.456412	.142087i
.513373	.182590i	.387350	.133150i
.447853	.173001i	.325880	.121633i
.387824	.160789i	.271911	.108862i
.333572	.147617i	.225107	.096133i
.284944	.134126i	.184894	.083957i
.184929	.099159i	.115100	.048651i
.14067	.072333i	.055227	.027497i
.024591	.043435i	.008158	.006575i
-.005338	.039627i	-.001498	.004761i
-.034168	.043999i	-.004566	.004231i
-.117644	.086439i	-.011717	.003220i
-.299456	.195575i	-.010744	.002691i

TABLE IV (Cont'd)

Period = 106.4400 (Cont'd)
 Phase Velocity=4.2000
 35 Layer model

Section Thickness = 2898 km			
HASSELL METHOD		DUNKIN METHOD	
Vertical	Horizontal	Vertical	Horizontal
-.734195	.438798i	-.009416	.002297i
-1.730194	.869893i	-.008134	.001934i
-7.174500	-1.427081i	-.023747	.000546i
67.316536	-162.893231i	-.006543	.000141i
2727.220784	-3866.697396i	-.001763	.000036i
58523.227239	-72877.252431i	-.000463	.000009i
.108 x 10 ⁷	-.127 x 10 ⁷ i	-.000119	.000002i
.188 x 10 ⁸	-.214 x 10 ⁸ i	-.000030	.0000001
.319 x 10 ⁹	-.355 x 10 ⁹ i	-.000007	.0000001
.525 x 10 ¹⁰	-.576 x 10 ¹⁰ i	-.000002	.0000001
.855 x 10 ¹¹	-.928 x 10 ¹¹ i	-.000000	.0000001
.329 x 10 ¹²	-.352 x 10 ¹² i	-.000000	.0000001

the Haskell Method results from the repeated multiplication of 4×4 layer matrices and gradual loss of significance in the matrix multiplication. Since the Haskell Method starts at the top layer and works down, and the Dunkin Method starts at the bottom layer and works up, the agreement of the two methods in the near surface layers indicates that the Dunkin Method is yielding correct displacement values over the entire layered sequence. In some cases when relative high frequency points on a dispersion curve were being computed with a many layered model, displacements computed by the Dunkin Method showed some slight perturbations with depth rather than a smooth decrease. Displacement values also tended to change signs as they decreased to very small quantities with depth. This is seen in the vertical displacements for the 35 layer case in Table IV. Horizontal displacement curves generally have one more lobe than the corresponding vertical displacement curves.

Modal shapes for the Gutenberg-Birch model are shown graphically in Appendix IV.

Earth Flattening Approximation

The earth flattening approximation introduced by Alterman, Jarosch, and Pekeris [1961] was used to modify the layer velocities. As has been shown by Kovach & Anderson [1964], the effect of sphericity is not negligible even for higher modes. The linear increase in velocity introduced in the earth flattening approximation is specified by the parameter

$$\xi = \left(\frac{r_m}{a} \right)^2$$

The value of r_m for a layer was taken as the radius to the center of the layer; a is the mean radius of the earth, 6371 km. Layer velocities approximately corrected for sphericity are then given by

$$\alpha'_m = \alpha_m \xi^{-1/2}$$

$$\beta'_m = \beta_m \xi^{-1/2}$$

5.5 Variation of Phase Velocity with Layer Parameters

The energy integrals for elastic wave propagation [Meissner, 1926; Jeffreys, 1934] have been used by several authors, notably Anderson [1964] and Takeuchi and Dorman [1964] to derive explicit relations between the variation of phase velocity and the variation of layer parameters. Necessary data for the evaluation of the partial derivatives of phase velocity with respect to layer parameters are horizontal and vertical particle amplitude vs. depth values.

For Rayleigh waves, the potential and kinetic energy averaged over a cycle are

$$4T = \int \rho \omega^2 (u^2 + w^2) dz$$

$$4V = \int [\lambda(u-w')^2 + \mu(2k^2 u^2 + 2w'^2) + k^2 w^2 + u'^2 + 2ku'w] dz$$

where

u = horizontal displacement

w = vertical displacement

u' = $\frac{\partial u}{\partial z}$, and the integration extends over the entire depth.

Using the fact that the kinetic and potential energy averaged over a period are equal we obtain

$$\omega^2 I_1 = k^2(I_2 + I_5) + k(I_3 + I_6) + (I_4 + I_2), \quad (5.5-1)$$

where

$$\begin{aligned} I_1 &= \int \rho(u^2 + w^2) dz & I_2 &= \int \lambda u^2 dz \\ I_3 &= \int 2\lambda uw' dz & I_4 &= \int \lambda w'^2 dz \\ I_5 &= \int \mu(2u^2 + w^2) dz & I_6 &= - \int \mu u' w dz \\ I_7 &= \int \mu(2w'^2 + u^2) dz \end{aligned} \quad (5.5-2)$$

For a layered sequence of n layers, one can define

$$I_{1m} = \int_{z_m}^{z_{m+1}} \rho(u^2 + w^2) dz \quad (5.5-3)$$

and similarly for the other integrals. Thus,

$$I_i = \sum_{m=1}^n I_{im} \quad (5.5-4)$$

A perturbation of a layer parameter in the m^{th} layer will cause a perturbation in the integral, I_i , for the entire layered sequence of

$$\delta I_i = \delta I_{im} \quad (5.5-5)$$

Differentiating (5.5-1) with respect to the layer parameters, the partial derivatives of c with respect to the layer parameters are obtained. Thus,

$$\left(\frac{\partial c}{\partial \mu_m}\right)_{\rho, \lambda, d, \omega} = (ck^2 \frac{\partial I_{5m}}{\partial \mu} + ck \frac{\partial I_{6m}}{\partial \mu} + c \frac{\partial I_{7m}}{\partial \mu}) / D \quad (5.5-6)$$

where

$$D = k[2k(I_2 + I_5) + I_3 + I_6]$$

with the integration of the integrals in D extending over the entire layered sequence.

$$\left(\frac{\partial c}{\partial \rho_m}\right)_{\lambda, \mu, d, \omega} = -c\omega^2 \frac{\partial I_{1m}}{\partial \rho} / D \quad (5.5-7)$$

$$\left(\frac{\partial c}{\partial \lambda_m}\right)_{\mu, \rho, d, \omega} = (ck^2 \frac{\partial I_{2m}}{\partial \lambda} + ck \frac{\partial I_{3m}}{\partial \lambda} + c \frac{\partial I_{4m}}{\partial \lambda}) / D \quad (5.5-8)$$

$$\left(\frac{\partial c}{\partial \beta_m}\right)_{\rho, \alpha, d, \omega} = 2\rho\beta \left[\left(\frac{\partial c}{\partial \mu_m}\right)_{\rho, \lambda, d, \omega} - 2 \left(\frac{\partial c}{\partial \lambda_m}\right)_{\mu, \rho, d, \omega} \right] \quad (5.5-9)$$

Assuming ρ, α, β as independent and ρ, λ, μ as dependent

$$\left(\frac{\partial c}{\partial \rho_m}\right)_{\alpha, \beta, d, \omega} = \left(\frac{\partial c}{\partial \rho_m}\right)_{\lambda, \mu} + \left(\frac{\partial c}{\partial \lambda_m}\right)_{\rho, \mu} \left(\frac{\partial \lambda_m}{\partial \rho_m}\right)_{\alpha, \beta} + \left(\frac{\partial c}{\partial \mu_m}\right)_{\rho, \lambda} \left(\frac{\partial \mu_m}{\partial \rho_m}\right)_{\alpha, \beta} .$$

Substituting

$$\left(\frac{\partial \lambda_m}{\partial \rho_m}\right)_{\alpha, \beta} = \alpha_m^2 - 2\beta_m^2 \quad \text{and}$$

$$\left(\frac{\partial \mu_m}{\partial \rho_m}\right)_{\alpha, \beta} = \beta_m^2 ,$$

gives

$$\left(\frac{\partial c}{\partial \rho_m}\right)_{\alpha, \beta, d, \omega} = -c\omega^2 \frac{\partial I_{1m}}{\partial \rho} / D + \left(\frac{\partial c}{\partial \lambda_m}\right)_{\mu, \rho, \omega, d} (\alpha_m^2 - 2\beta_m^2) + \beta^2 \left(\frac{\partial c}{\partial \mu_m}\right)_{\rho, \lambda, d, \omega} \quad (5.5-10)$$

$$\left(\frac{\partial c}{\partial \alpha_m}\right)_{\rho, \beta, d, \omega} = 2\rho_m \alpha_m \left(\frac{\partial c}{\partial \lambda_m}\right)_{\rho, \mu, d, \omega} \quad (5.5-11)$$

$$\left(\frac{\partial c}{\partial d}\right)_{\mu, \lambda, \rho, \omega} = [-c\omega^2 \frac{\partial I_1}{\partial d} + ck^2 (\frac{\partial I_2}{\partial d} + \frac{\partial I_5}{\partial d}) + ck (\frac{\partial I_3}{\partial d} + \frac{\partial I_6}{\partial d}) + c(\frac{\partial I_4}{\partial d} + \frac{\partial I_7}{\partial d})] / D$$

The group velocity can be expressed in terms of the integrals I_i by

$$U = \frac{2(I_2 + I_5)k}{\omega} + \frac{(I_3 + I_6)}{ck} \quad (5.5-12)$$

Equations (5.5-6), (5.5-8), (5.5-9), (5.5-10), (5.5-11), (5.5-12), and (5.5-13) with the definitions of (5.5-2) were programmed for the IBM 360-75 computer. The integrals of (5.5-2) were evaluated numerically using polynomial approximations to the particle displacements obtained from the modal shape calculations. A sliding fitting procedure was used in determining the polynomials. In this procedure, a polynomial is fitted to say n points at the depths $z_i, z_{i+1}, \dots, z_{i+n}$; and the integrals and their derivatives evaluated over the interval $z_{i+n} - z_i$. The polynomial fit is then shifted to drop one layer and pick up one layer, i.e., to the points at depths

$z_{i+1}, z_{i+2}, \dots z_{i+1+n}$. By using polynomial approximations, the integrals of the derivatives are simply the integrals of the derivatives of the polynomials. Third degree polynomials were found to give adequate fits to the displacement data.

A Fortran listing of the program, INTEGRAL, for computing the partial derivatives of phase velocity, c , with respect to layer parameters is given in Appendix III. Results of computation of the partial derivatives for the Gutenberg-Birch II continental model are given in Appendix IV.

6.0 CRUSTAL AND UPPER MANTLE STRUCTURE IN THE SOUTHEASTERN UNITED STATES

Gravity, local travel-time, and Rayleigh wave dispersion data were used to determine crustal and upper mantle structure for the Southeastern United States. Results of the Rayleigh dispersion study and a comparison with the gravity and travel-time results are given in this section.

Observed dispersion curves could be constructed only for periods less than about 50 seconds. Therefore, crustal structure was concentrated on and the upper mantle structure below 70 km was assumed to be that of the Gutenberg-Birch II continental model. The Gutenberg-Birch II crustal structure was used as the basic model for estimating the Southern Appalachian structure. Variations of phase velocity with layer parameters computed for the Gutenberg-Birch II model (See Appendix IV) were used to vary this basic model to yield dispersion curves fitting the observed data. Velocity and density structure of the models considered are given in Table V and Fig.

7. Values of the "earth flattening" velocities for the Gutenberg-Birch II are also given to indicate the effective increase of velocity with depth.

Fundamental and first higher Rayleigh mode group velocity vs. period data observed in the Southern Appalachians (Table III) are shown in Figs. 8-11. Rayleigh wave dispersion curves computed as described in Section 5.0 are given in Table VI and Figs. 8-11 for the models Gutenberg-Birch II, 310, 314, 315, and 320 defined in Table V.

Group velocity curves for waves traveling approximately perpendicular (perpendicular waves) to the Appalachians are quite similar (Figs. 8-11). They all have a local minimum of about 2.85 km/sec at a period of 17 sec, and a local maximum of about 3.10 km/sec at around 12 sec. For periods shorter than about 10 seconds the curves flatten out at about 3.0 km/sec. First higher Rayleigh mode curves indicate a broad minimum of 3.5 km/sec

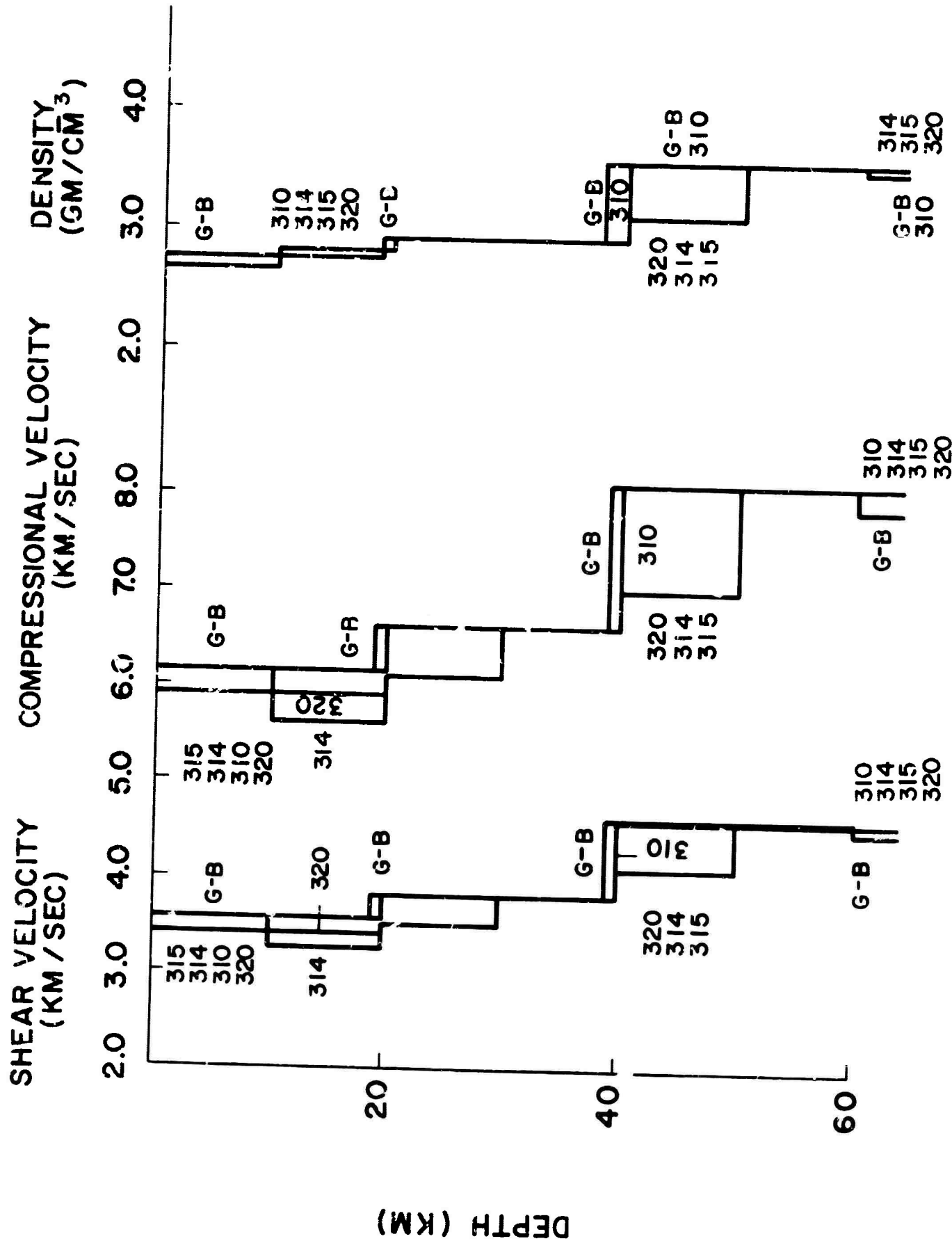
TABLE V. Layer Parameters for Crustal and Upper Mantle Models

GUTENBERG-BIRCH II

FLAT EARTH				EARTH FLATTENING			
α	β	ρ	d	α	β	ρ	d
6.1400	3.5500	2.7500	19.00	6.1486	3.5550	2.7500	19.00
6.5800	3.8000	2.9000	19.00	6.6090	3.8167	2.9000	19.00
8.0800	4.6000	3.5700	22.00	8.1422	4.6354	3.5700	22.00
7.8700	4.5100	3.5100	20.00	7.9574	4.5601	3.5100	20.00
7.8000	4.4500	3.4900	20.00	7.9115	4.5136	3.4900	20.00
7.8300	4.4200	3.5000	20.00	7.9670	4.4974	3.5000	20.00
7.8900	4.4000	3.5100	20.00	8.0541	4.4915	3.5100	20.00
7.9400	4.3900	3.5300	20.00	8.1314	4.4958	3.5300	20.00
8.0000	4.4000	3.5500	20.00	8.2192	4.5206	3.5500	20.00
8.0600	4.4200	3.5600	20.00	8.3074	4.5557	3.5600	20.00
8.1200	4.4500	3.5800	20.00	8.3961	4.6013	3.5800	20.00
8.2000	4.4800	3.6100	20.00	8.5067	4.6476	3.6100	20.00
8.2700	4.5200	3.6300	20.00	8.6074	4.7044	3.6300	20.00
8.3500	4.5700	3.6500	20.00	8.7191	4.7720	3.6500	20.00
8.4300	4.6100	3.6800	20.00	8.8313	4.8294	3.6800	20.00
8.5100	4.6600	3.7000	50.00	8.9670	4.9102	3.7000	50.00
8.7500	4.8100	3.7700	50.00	9.2969	5.1106	3.7700	50.00
9.0000	4.9500	3.8500	100.00	9.6840	5.3262	3.8500	100.00
9.4900	5.2200	4.0000	50.00	10.3422	5.6888	4.0000	50.00
9.7400	5.3600	4.0700	50.00	10.7062	5.8917	4.0700	50.00
9.9900	5.5000	4.1500	100.00	11.1249	6.1248	4.1500	100.00
10.5000	5.7700	4.3000	100.00	11.9007	6.5397	4.3000	100.00
10.9000	6.0400	4.4200	100.00	12.5775	6.9696	4.4200	100.00
11.3000	6.3000	4.5400	100.00	13.2798	7.4038	4.5400	100.00
11.4000	6.3500	4.5700	200.00	13.7780	7.6746	4.5700	200.00
11.8000	6.5000	4.6900	200.00	14.8243	8.1660	4.6900	200.00
12.0500	6.6000	4.7700	200.00	15.7602	8.6321	4.7700	200.00
12.3000	6.7500	4.8500	200.00	16.7759	9.2063	4.8500	200.00
12.5500	6.8500	4.9200	200.00	17.8824	9.7606	4.9200	200.00
12.8000	6.9500	5.0000	200.00	19.0925	10.3666	5.0000	200.00
13.0000	7.0000	5.0600	200.00	20.3437	10.9543	5.0600	200.00
13.2000	7.1000	5.1200	200.00	21.7245	11.6852	5.1200	200.00
13.4500	7.2000	5.1900	200.00	23.3411	12.4949	5.1900	200.00
13.7000	7.2500	5.2700	98.00	24.7819	13.1145	5.2700	98.00
13.6500	7.2000	5.2500	∞	25.0395	13.2077	5.2500	∞

TABLE V. (Cont'd)

MODEL 310				MODEL 314			
α	β	ρ	d	α	β	ρ	d
5.8800	3.3800	2.6700	10.00	5.8800	3.3800	2.6700	10.00
6.1400	3.5500	2.7600	10.00	5.6000	3.2400	2.7600	10.00
6.5800	3.8000	2.9000	10.00	6.1000	3.5000	2.9000	10.00
6.5800	3.8000	2.9000	10.00	6.6000	3.8000	2.9000	10.00
8.0800	4.6000	3.5700	20.00	7.0000	4.1000	3.1000	10.00
				8.0800	4.6000	3.5700	20.00
Same as Gutenberg-Birch II to 400 km				Same as Gutenberg-Birch II to 810 km			
MODEL 315				MODEL 320			
α	β	ρ	d	α	β	ρ	d
5.8800	3.3800	2.6700	10.00	5.8800	3.3800	2.6700	10.00
6.1400	3.5500	2.7600	10.00	5.8800	3.3800	2.7500	10.00
6.5800	3.8000	2.9000	10.00	6.1000	3.5000	2.9000	10.00
6.5800	3.8000	2.9000	10.00	6.6000	3.8000	2.9000	10.00
7.0000	4.1000	3.1000	10.00	7.0000	4.1000	3.1000	10.00
8.0800	4.6000	3.5700	20.00	8.0800	4.6000	3.5700	20.00
Same as Gutenberg-Birch II to 810 km				Same as Gutenberg-Birch II to 810 km			



CRIJSTM AND UPPER MANTLE MODELS

Fig. 7

TABLE VI. Rayleigh wave dispersion curves for Gutenberg-Birch II models,
and models 310, 314, and 315

GUTENBERG-BIRCH II

FUNDAMENTAL RAYLEIGH MODE

Section Thickness 2898.00

c	k	T	U	T
4.5000	.00850	164.2671		
4.4000	.00961	148.5391	3.6990	143.8940
4.3000	.01131	129.1709	3.7695	123.5369
4.1999	.01405	106.4402	3.8361	99.2251
4.0999	.01984	77.2556	3.9112	65.9224
3.9999	.03815	41.1794	3.7346	37.1515
3.8999	.05419	29.7316	3.4039	28.3452
3.7999	.06624	24.9623	3.1759	24.0856
3.6999	.07815	21.7314	3.0493	21.0107
3.5998	.09202	18.9673	2.9510	18.3398
3.4998	.10996	16.3264	3.0336	15.5185
3.3998	.14161	13.0509	3.1084	11.9219

Section Thickness 400.00

4.0000	.03801	41.3293		
3.9000	.05394	29.8693	3.4253	28.4013
3.8000	.06578	25.1380	3.2096	24.1929
3.7000	.07808	21.7493	3.0305	21.0535
3.5999	.09207	18.9572	2.9639	18.3140
3.4999	.11010	16.3054	3.0331	15.4998
3.3999	.14220	12.9958	3.1018	11.9019

Section Thickness 140.00

4.0000	.03730	42.1107		
3.9000	.05409	29.7861	3.4066	28.3880
3.8000	.06576	25.1423	3.1768	24.2579
3.7000	.07762	21.8791	3.0923	21.0892
3.5999	.09150	19.0747	2.9947	18.3862
3.4999	.11001	16.3184	3.0426	15.4971
3.3999	.14249	12.9695	3.0988	11.8907

FIRST HIGHER RAYLEIGH MODE

Section Thickness 2898.00

c	k	T	U	T
6.0000	.01020	102.6767		
5.9000	.01091	97.6155	4.5030	96.2532
5.8000	.01174	92.2541	4.4644	90.8938
5.6999	.01269	86.8711	4.4340	85.5044
5.5999	.01377	81.4673	4.4137	80.0789
5.4999	.01503	75.9839	4.3971	74.5686
5.3999	.01653	70.4033	4.3821	68.9585
5.2999	.01832	64.7021	4.3720	63.2178

TABLE VI. (Cont'd)

FIRST HIGHER RAYLEIGH MODE (Cont'd)

Section Thickness 2898.00 (Continued)

c	k	T	U	T
5.1998	.02053	59.578	4.3631	57.3296
5.0998	.02331	52.5603	4.3539	51.2881
4.9999	.02690	46.7207	4.3448	45.1023
4.8999	.03172	40.4258	4.3363	38.7565
4.7999	.03854	33.9652	4.3316	32.2275
4.6998	.04900	27.2834	4.3340	25.4277
4.5998	.06780	20.1477	4.3586	17.9272

Section Thickness 1000.00

5.4000	.01661	70.0684		
5.3000	.01837	64.5405	4.4587	62.8706
5.2000	.02062	58.5864	4.3608	57.0707
5.0999	.02345	52.5303	4.3509	50.9751
4.9999	.02708	46.4060	4.2904	44.9442
4.8999	.03199	40.0905	4.3225	38.4821
4.7999	.03879	33.7500	4.3062	32.1265
4.6998	.04933	27.1034	4.3338	25.2612

Section Thickness 400.00

5.0000	.02512	50.0301		
4.9000	.03111	41.2115	4.4079	39.2169
4.8000	.03846	34.0337	4.3302	32.2991
4.6999	.04883	27.3780	4.3458	25.4449
4.5999	.06819	20.0320	4.3531	17.8824
4.4999	.11357	12.2945	4.1959	11.2612
4.4000	.15149	9.4265		
4.3000	.17634	8.2863	3.5422	8.0520
4.2000	.20128	7.4324	3.3111	7.2619
4.0999	.22937	6.6814	3.3545	6.4906
3.9999	.25763	5.8694	3.4094	5.6467
3.8999	.32599	4.9423	3.4869	4.6556
3.7999	.43139	3.8330	3.4694	3.5446
3.6999	.61350	2.7681	3.4616	2.4623

Section Thickness 140.00

3.9000	.32410	4.9709	3.9114	8.4005
3.8000	.43142	3.8327	3.4763	3.5371
3.7000	.61704	2.7521	3.4545	2.4586

TABLE VI. (Cont'd)

SECOND HIGHER RAYLEIGH MODE

Section Thickness 400.00

C	k	T	U	T
4.9000	.05537	23.1581	4.2866	22.2932
4.8000	.06549	19.9891	4.2627	19.1184
4.6999	.08015	16.6789	4.2938	15.6739
4.5999	.10807	12.6396	4.3836	11.0562
4.5000	.25165	5.5484	3.9105	5.3337
4.3999	.29310	4.8721	4.4642	6.2623
4.2999	.32739	4.4632	3.2661	4.3787
4.1999	.36497	4.0990	3.1949	4.0190
4.0999	.40722	3.7634	3.4253	3.6417
3.9999	.47463	3.3096	3.4644	3.1683
3.8999	.59153	2.7237	3.5669	2.5201
3.7998	.84393	1.9593	3.4754	1.8086

Section Thickness 140.00

4.6000	.09402	14.5273		
4.5000	.25218	5.5369	3.8832	5.3339
4.3999	.29289	4.8756	3.5369	4.7581
4.2999	.32734	4.4640	3.3107	4.3744
4.1999	.36532	4.0951	3.3051	4.0019
4.0999	.40970	3.7406	3.3130	3.6409
3.9999	.47503	3.3069	3.4600	3.1671
3.8999	.58812	2.7395	3.5842	2.5214
3.7998	.84289	1.9617	3.4812	1.8076

TABLE VI. (Cont'd)

MODEL 314

FUNDAMENTAL RAYLEIGH MODE

Section Thickness 810 km

c	k	T	U	T
4.5000	.00800	174.4980	3.6546	152.3970
4.4000	.00910	156.9458	3.6739	133.7163
4.3000	.01054	138.6728	3.7362	111.4856
4.1999	.01273	117.4773	3.8025	84.3855
4.0999	.01661	92.2917		

Section Thickness 310 km

c	k	T	U	T
4.0000	.02547	61.6759	3.4695	39.4730
3.9000	.03856	41.7795	3.1635	33.1033
3.8000	.04824	34.2777	2.9694	29.2182
3.7000	.05646	30.0793	2.3125	26.2169
3.5999	.06486	26.9112	2.7168	23.4925
3.4999	.07445	24.1143	2.7635	20.7638
3.3999	.08602	21.4831	2.8034	17.8086
3.2999	.10206	18.6555	2.8919	13.9951
3.1999	.12901	15.2204		

FIRST HIGHER RAYLEIGH MODE

Section Thickness 310 km

c	k	T	U	T
5.0000	.02685	46.8048	4.4483	36.2523
4.9000	.02886	44.4386	4.3098	27.9880
4.8000	.03353	39.0360	4.2401	21.5914
4.6999	.04475	29.8741	4.1392	16.2429
4.5999	.05888	23.1967	3.8165	13.1554
4.4999	.08004	17.4449	3.5115	11.5744
4.3999	.10431	13.6899	3.3171	10.4853
4.2999	.12285	11.8943	3.2139	9.5683
4.1998	.13938	10.7339	3.1330	8.6651
4.0993	.15650	9.7925	3.1344	7.7859
3.9999	.17704	8.8727	3.1097	6.8751
3.8999	.20128	8.0045	3.1614	5.9217
3.7999	.23306	7.0948		
3.6999	.27476	6.1807		

TABLE VI. (Cont'd)

MODEL 315

FUNDAMENTAL RAYLEIGH MODE

Section Thickness 810 km

c	k	T	U	T
4.5000	.00820	170.2393		
4.4000	.00930	153.5283	3.6992	148.7251
4.3000	.01086	134.5723	3.7313	129.1714
4.1999	.01334	112.1333	3.8018	105.2905
4.0999	.01812	84.5767	3.8692	74.8110

Section Thickness 310 km

c	k	T	U	T
4.0000	.03053	51.4482		
3.9000	.04399	36.6250	3.4296	34.8049
3.8000	.05404	30.5995	3.2226	29.4172
3.7000	.06472	26.2377	3.0726	25.3270
3.5999	.07614	22.9218	3.0533	21.9835
3.4999	.09221	19.4693	3.0333	18.5069
3.3999	.11718	15.7708	3.0416	14.7044
3.2999	.16256	11.7130	3.0354	10.5790
3.1999	.25847	7.5969	3.0323	6.3232

FIRST HIGHER RAYLEIGH MODE

Section Thickness 310 km

c	k	T	U	T
5.0000	.02700	46.5387		
4.9000	.02898	44.2546		
4.8000	.03375	38.7906	4.4580	35.9338
4.6999	.04593	29.1047	4.3170	27.2273
4.5999	.06249	21.8596	4.3459	19.5919
4.4999	.09907	14.0942	4.1502	13.0875
4.3999	.12798	11.1578	3.7883	10.7461
4.2999	.14814	9.8638	3.4936	9.6058
4.1998	.16823	8.8928	3.4019	8.6584
4.0998	.19220	7.9737	3.4011	7.7268
3.9999	.22623	6.9435		
3.8999	.27637	5.8296	3.4963	5.4822
3.7999	.36302	4.5549	3.4527	4.2315
3.6999	.49743	3.4140	3.3824	3.1453
3.5998	.72066	2.4220	3.3589	2.1583
3.4998	1.18182	1.5191	3.3175	1.2885
3.3998	3.20689	.5763		

TABLE VI. (Cont'd)

MODEL 310

FUNDAMENTAL RAYLEIGH MODE

Section Thickness 400 km

c	k	T	U	T
4.0000	.02439	64.4070		
3.9000	.04255	37.8649	3.5912	34.7723
3.8000	.05805	28.4813	3.2801	27.2310
3.7000	.07023	24.1816	3.1144	23.2675
3.5999	.08334	20.9422	2.9759	20.2145
3.4999	.09981	17.9868	2.9384	17.2780
3.3999	.12365	14.9456	2.9835	14.1014
3.2999	.16535	11.5152	3.0190	10.4775

FIRST HIGHER RAYLEIGH MODE

Section Thickness 140 km

c	k	T	U	T
4.4000	.12476	11.4457		
4.3000	.16172	9.0352	3.6088	8.7490
4.2000	.18471	8.0990	3.3507	7.9020
4.0999	.21052	7.2797	3.2917	7.0921
3.9999	.24138	6.5077	3.4153	6.2579
3.8999	.29117	5.5333	3.4070	5.2734
3.7999	.36986	4.4707	3.4199	4.1854
3.6999	.49765	3.4125	3.3786	3.1475

MODEL 320

FUNDAMENTAL RAYLEIGH MODE

Section Thickness 310 km

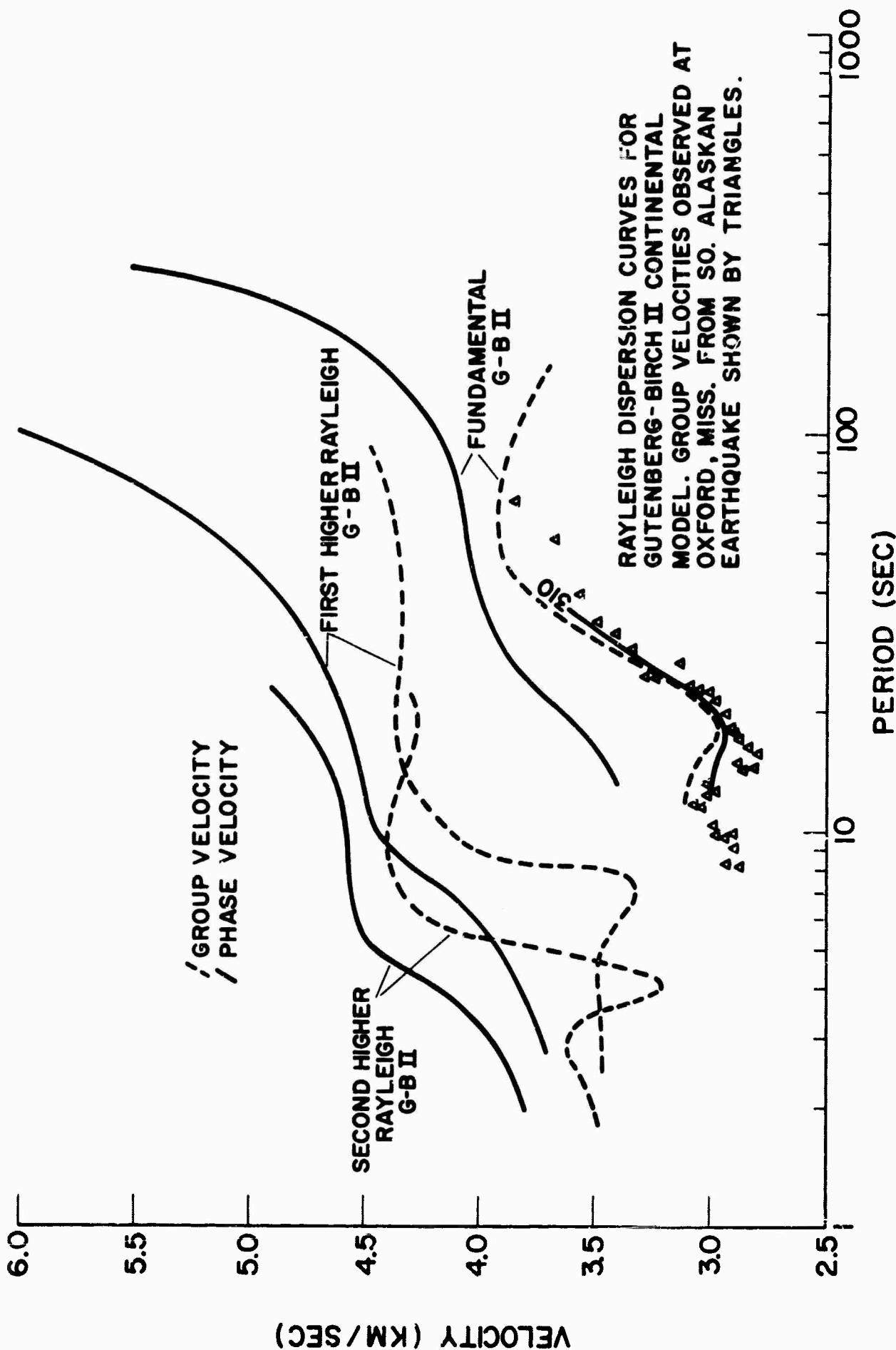
c	k	T	U	T
4.0000	.02676	58.6913		
3.9000	.03996	40.3191	3.4514	38.1989
3.8000	.04957	33.3568	3.1758	32.1857
3.7000	.05820	29.1794	2.9781	28.3310
3.5999	.06716	25.9897	2.8662	25.2547
3.4999	.07764	23.1217	2.7526	22.4878
3.3999	.09056	20.4061	2.8481	19.5889
3.2999	.11217	16.9749	2.8878	16.0079
3.1999	.15391	12.7579	3.0158	10.8511

TABLE VI. (Cont'd)

FIRST HIGHER RAYLEIGH MODE

Section Thickness 310 km

C	K	T	U	T
5.0000	.02694	46.6523		
4.9000	.02888	44.4016		
4.8000	.03358	38.9835	4.4617	36.0753
4.6999	.04490	29.7720	4.2997	27.9473
4.5999	.05957	22.9299	4.2645	21.2086
4.5000	.08333	16.7565		
4.4000	.11006	12.9742	3.8455	12.4357
4.3000	.12959	11.2758	3.5636	10.9456
4.1999	.14771	10.1280	3.3148	9.8943
4.0999	.16573	9.2470	3.2854	9.0110
3.9999	.18724	8.3893	3.1800	8.1781
3.8999	.21377	7.5367	3.1997	7.3062
3.7999	.24984	6.6182	3.2181	6.3649
3.6999	.30270	5.6103	3.2358	5.3289



8

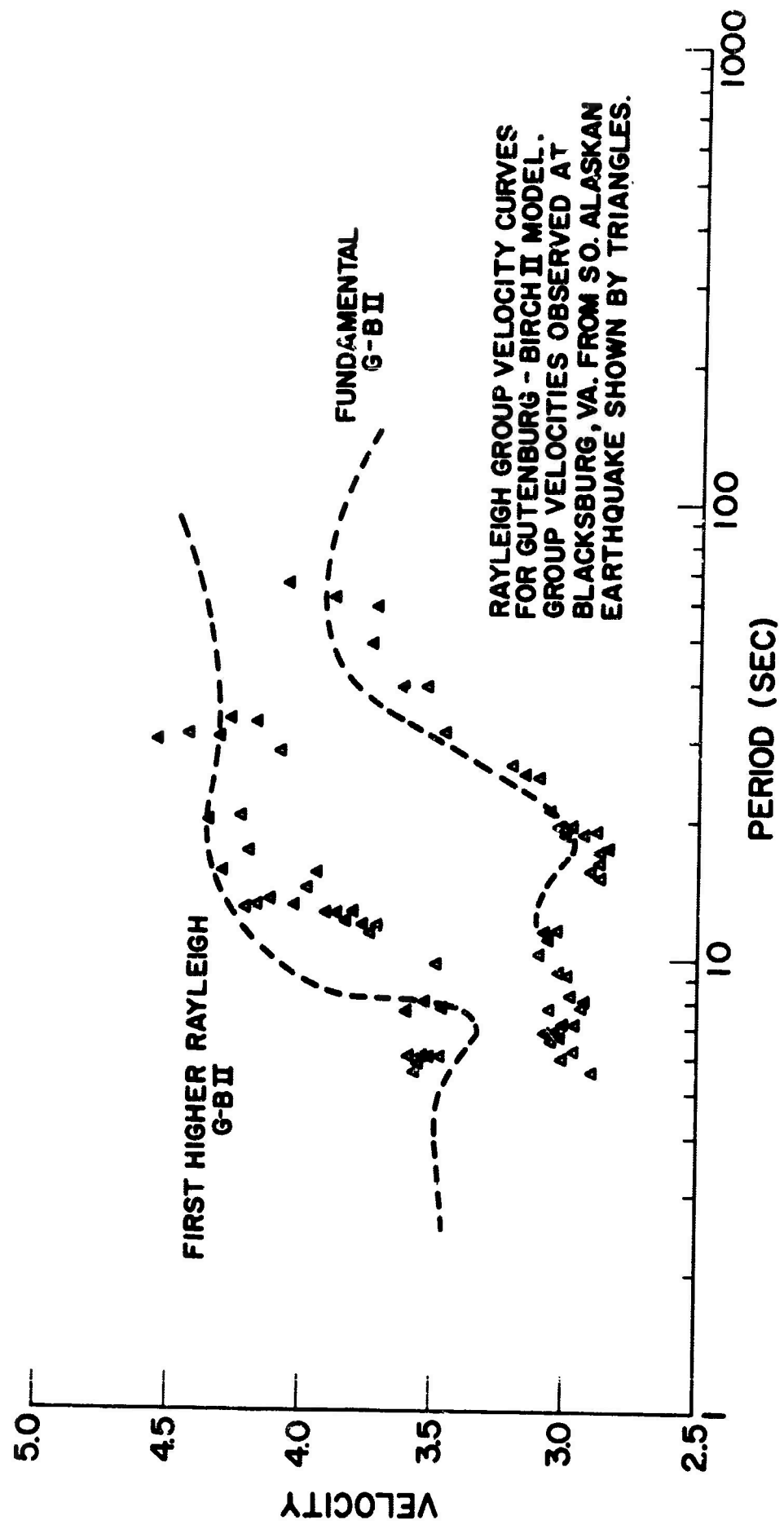


Fig. 9

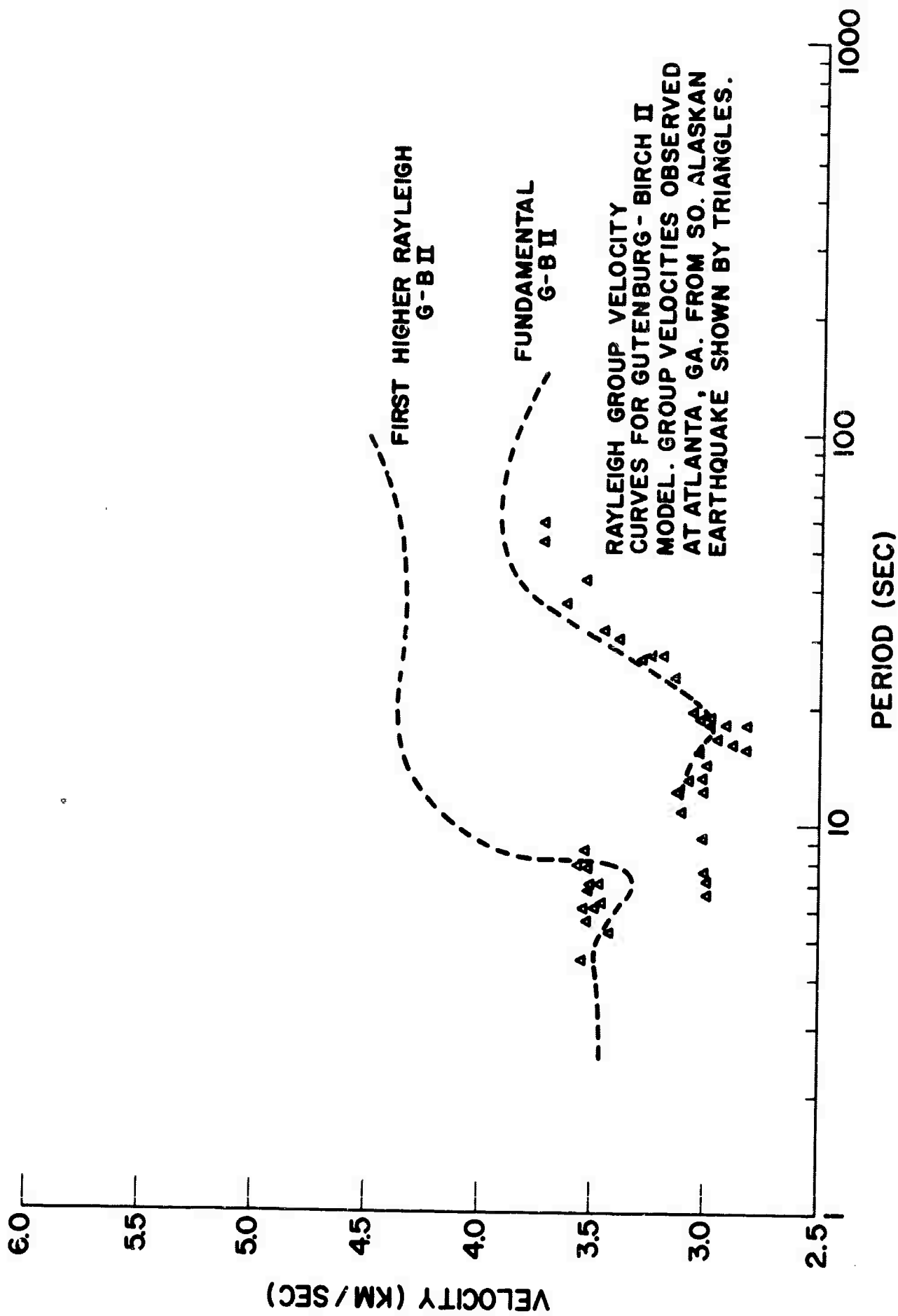


Fig. 10

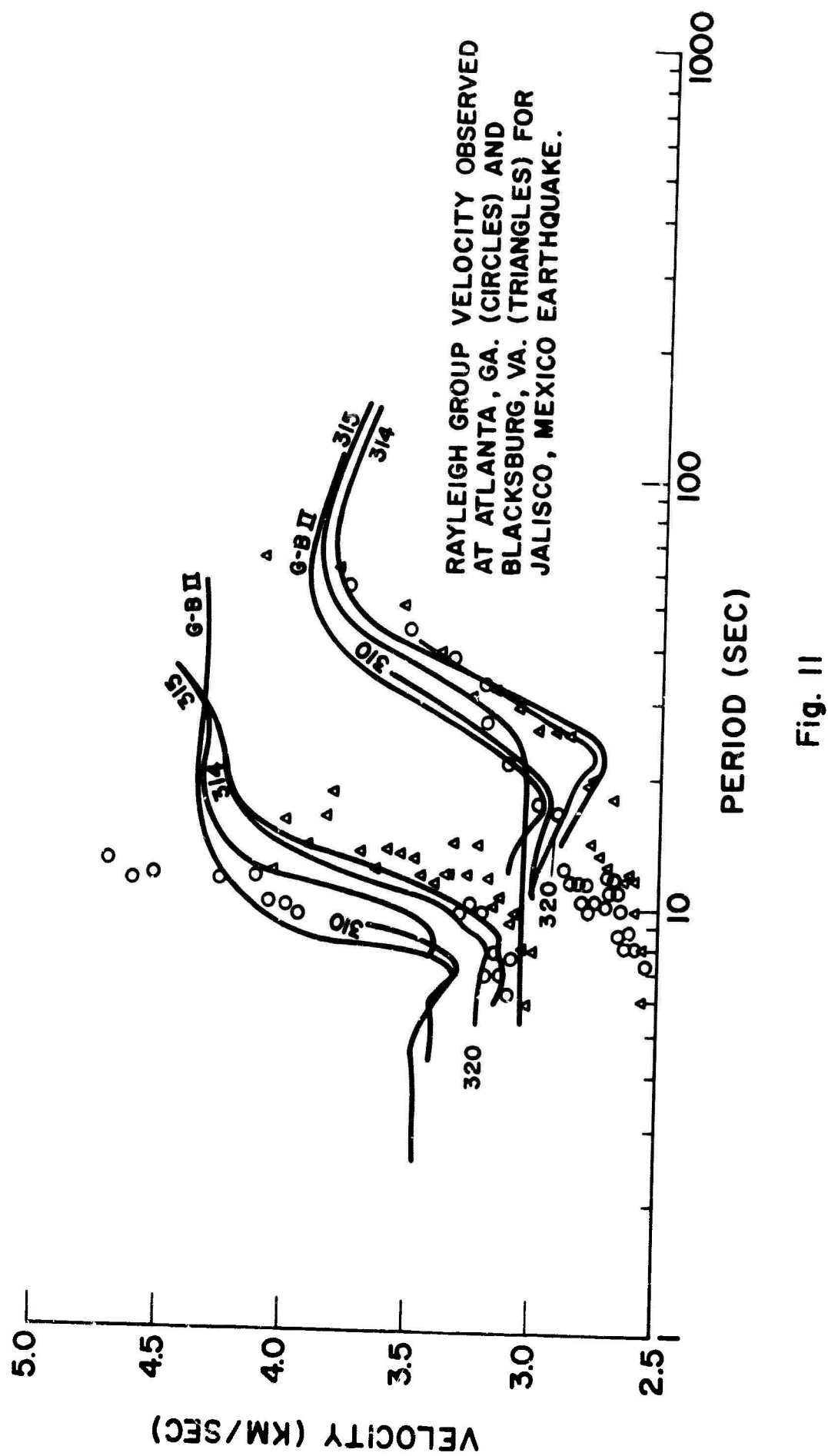


Fig. II

from 6-10 sec. Group velocities recorded at Oxford indicate a slightly shorter period for the minimum and a gradual decrease in velocity for periods shorter than 12 sec. However, in general the curves are quite similar to those for Atlanta and Blacksburg. Waves arriving at Atlanta from Jalisco, Mexico, (parallel waves) have both fundamental and first higher Rayleigh mode group velocities considerably lower than do the perpendicular wave trains for periods less than about 20 sec. The rapidly "tailing-off" of group velocities below 15 sec is probably due to a thick sedimentary sequence (approximately 400 km of the travel path for these waves lie across the Gulf Coastal Plain).

The most significant difference is between the Blacksburg and Atlanta group velocities for parallel wave trains. A minimum of 2.75 km/sec occurs at a period of 22 sec and a maximum of 2.80 km/sec occurs at a period of 16 sec for the Blacksburg velocities. Group velocities at periods greater than 30 sec trend toward those for the perpendicular waves. First higher mode Rayleigh group velocities for Blacksburg are lower by about .1 km/sec than those for Atlanta.

Several models were constructed using the variation of phase velocity with layer parameter curves for the Gutenberg-Birch II model. Basic differences in the models are:

- 1) 314, 315, and 320 have a crustal thickness of 50 km, while 310 and G-B (Gutenberg-Birch II) have a crustal thickness of 40 km;
- 2) 314 has a low velocity zone centered at 15 km in the upper crust. Except for this low velocity zone, 320 is identical to 314;
- 3) G-B and 310 have a low velocity zone in the upper mantle beginning at 60 km while the low velocity begins at 70 km for 314, 315, and 320.
- 4) Velocities in the first 10 km of G-B are slightly higher than those in the other models.

For waves traveling perpendicular to the Appalachians, the group velocity data agree well with model 310 or G-B values for the fundamental Rayleigh mode at periods less than 30 sec. At longer periods, the values fall below those for 310 and approach those for 314 and 315. First higher Rayleigh mode values observed at Blacksburg lie between those for 314 and 315 for periods greater than 10 sec. Thus, it appears that waves arriving at Atlanta, Oxford, and Blacksburg from the Southern Alaska epicenter are just beginning to "feel" the Appalachian structure. The length of the "Appalachian path" is about 240 km in the Appalachian foreland in each case, assuming that the Appalachian structure extends beneath the Mississippi Embayment (Oxford station).

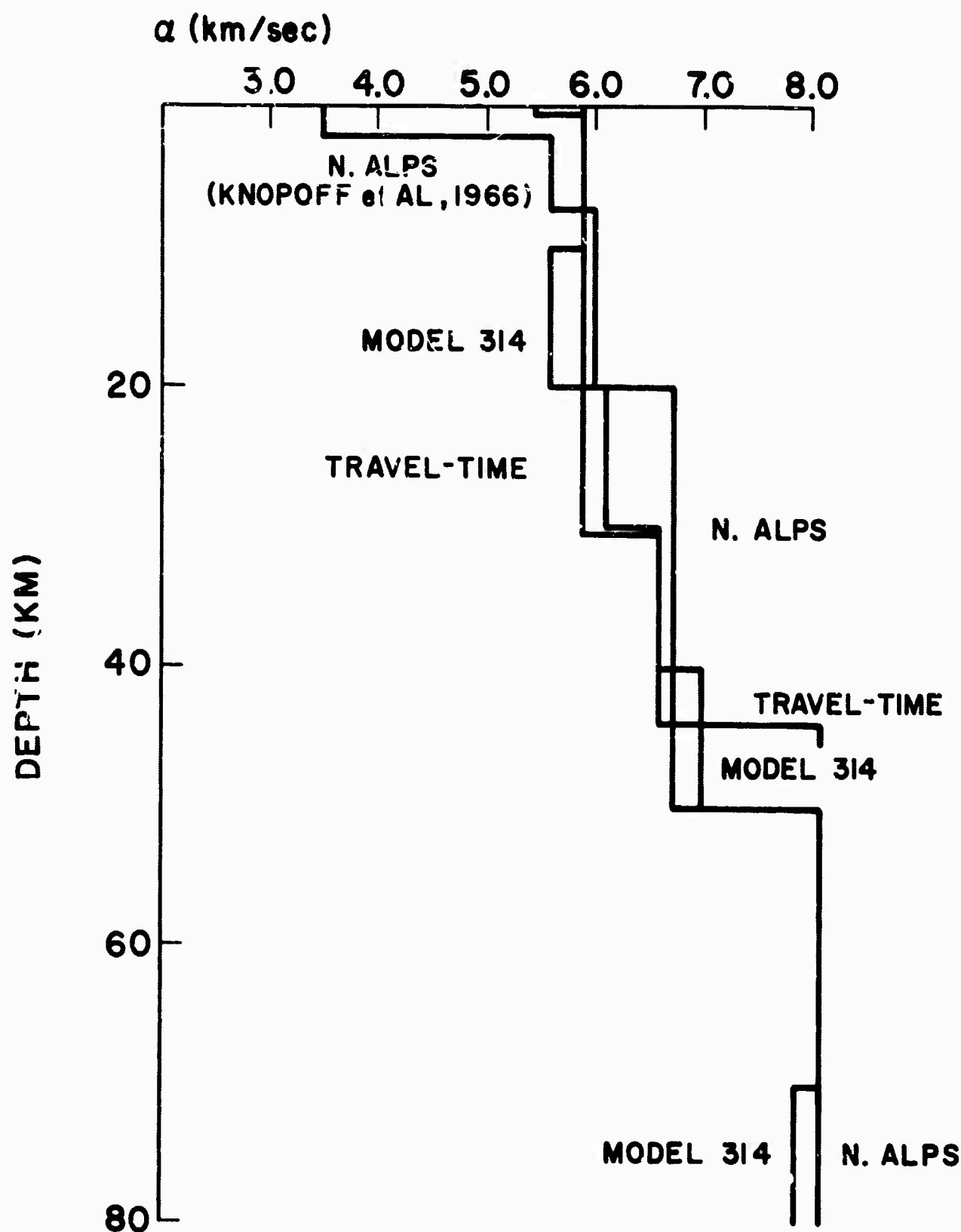
Waves arriving at Atlanta from Jalisco, Mexico yield group velocities considerably below those of G-B for periods less than 20 sec (See Fig. 11). Fundamental mode group velocities at Blacksburg show fair agreement with the theoretical curves for either models 314 or 320 being considerably below curves for G-B, 315, and 310 at all periods. On the basis of fundamental mode group velocities it is impossible to determine which of models 314 or 320 most closely approximate the crustal structure. However, first higher Rayleigh mode group velocities from model 314 give a considerably better fit to the observed data than do those from model 320 in the period range from 6 to 15 sec. In this period range, the group velocity curve for 314 lies between that for 320 and the observed group velocities. Thus, a slight velocity reversal in the crust is indicated by the first higher mode group velocities.

An alternative to the low velocity zone is to lower the velocities and/or densities in the first 10 km of the crust. However, refraction data give a compressional velocity of 5.88 km/sec for the upper crust which has

been used in models 314 and 320. The shear velocity value of 3.88 km/sec in models 314 and 320 corresponds to a Poisson ratio of .25.

Group velocities for periods greater than about 30 sec indicate a mantle low velocity zone beginning at about 70 km.

Compressional velocity crustal and upper mantle structure to the west of the Southern Appalachians determined from the travel times of local earthquakes and for the Southern Appalachian structure as determined from Rayleigh wave dispersion are shown in Fig. 12. Gravity and Rayleigh wave dispersion data indicate a total crustal thickness of about 50 km beneath the Southern Appalachians. Travel-time and dispersion data indicate an upper mantle velocity of 8.10 km/sec. Dispersion data indicate a slight low velocity zone in the upper crust and a general increase of velocity and density with depth below this zone. With the exception of the higher crustal velocity in the first 2 km, the Southern Appalachian structure approximated by model 314 is similar to the Northern Alpine structure with a 50 km crust reported by Knopoff et al [1966].



COMPRESSORIAL VELOCITY STRUCTURE FOR THE SOUTHEASTERN UNITED STATES AND THE NORTHERN ALPS.

Fig. 12

7.0 CONCLUSIONS

The conclusions which have been drawn from this study are:

- 1) Focal depths of local earthquakes in the Southeastern United States are shallow ranging from about 7 to 18 km.
- 2) Systematic deviations in P-residuals observed at Chapel Hill, North Carolina, and McMinnville, Tennessee, have magnitudes from + 3 to -3 sec. The deviations indicate systematic errors in the Jeffreys-Bullen travel-times.
- 3) Travel-time curves constructed from local earthquakes and refraction data indicate a crustal structure for the Appalachian foreland of $h_1 = 33.0$ km ($a = 5.88$ km/sec), $h_2 = 10.8$ km ($a = 6.58$ km/sec), and an upper mantle velocity of 8.10 km/sec.
- 4) Rayleigh wave dispersion data indicate a crustal low velocity zone centered at about 15 km, an upper mantle low velocity zone beginning at 70 km, and a total crustal thickness of 50 km beneath the core of the Southern Appalachians.
- 5) Gravity data indicate a total crustal thickness beneath the Southern Appalachians of at least 50 km which is in agreement with the Rayleigh dispersion data. Gravity data indicate a crustal thickness of about 45 km in central Kentucky thickening eastward to about 50 km beneath the core of the Appalachian and thinning to 23 km beneath the North Carolina continental margin at about the 2400 fathom contour.
- 6) Higher Rayleigh modes can be observed using digital filtering techniques. Care must be taken to isolate Rayleigh type motion and to remove interference effects. This is particularly true for higher modes than the first.
- 7) It should be possible to use higher modes than the first to delineate fine detail in the crust.

ACKNOWLEDGEMENTS

I wish to particularly express my
gratitude and thanks to the Superior Stone
Company of Raleigh, North Carolina, and
to the many local quarry managers who made
possible the refraction program of this
research.

REFERENCES

Anderson, D. L. Universal dispersion tables, I, Love waves across oceans and continents on a spherical earth, Bull. Seismol. Soc. Am., 54, 681-726, 1964.

Alterman, Z., H. Jarosch, and C. L. Pekeris, Propagation of Rayleigh waves in the earth, Geophys. J., 4, 219-241, 1961.

Borcherdt, R. D., and John C. Roller. A preliminary summary of a seismic-refraction survey in the vicinity of the Cumberland Plateau Observatory, Tennessee, USGS Technical Letter, Crustal Studies-43, February, 1966.

Dorman, James, Maurice Ewing, and Jack Oliver. Study of shear-velocity distribution in the upper mantle by mantle Rayleigh waves. Bull. Seismol. Soc. Am., 50, d7-115, 1960.

Dunkin, John W. Computations of modal solutions in layered, elastic media at high frequencies, Bull. Seismol. Soc. Am., 55, 335-358, 1965.

Gutenberg, B., and C. F. Richter. Earthquake magnitude, intensity, energy, and acceleration, Bull. Seismol. Soc. Am., 32, 18-191, 1942.

Haskell, N. A. The dispersion of surface waves on multilayered media, Bull. Seismol. Soc. Am., 43, 37-34, 1953.

Hersey, J. B., Elizabeth T. Bunce, R. F. Wyrick, and F. T. Dietz. Geophysical investigation of the continental margin between Cape Henry, Virginia, and Jacksonville, Florida, Bull. Geol. Soc. Am., 70, 437-466, 1959.

Jeffreys, H. The surface waves of earthquakes, MNRAS, Geophys. Supp., 3, 253-261, 1934.

Knopoff, L., S. Mueller, and W. L. Pilant. Structure of the crust and upper mantle in the Alps from the phase velocity of Rayleigh waves, Bull. Seismol. Soc. Am., 56, 1009-1044, 1966.

Kovach, R. L., and D. L. Anderson. Higher mode surface waves and their bearing on the structure of the earth's mantle, Bull. Seis. Soc. Am., 54, 161-182, 1964.

MacCarthy, G. R., and E. Z. Sinha. North Carolina earthquakes, 1957, J. Elisha Mitchell Soc., 117-274, November, 1957.

MacCarthy, G. R., and J. D. Waskom. The Virginia-North Carolina Blue Ridge earthquake of October 28, 1963, J. Elisha Mitchell Soc., 82-84, December, 1964.

McGuire, W. H., and Paul Howell. Oil and gas possibilities in the Cambrian and Lower Ordovician in Kentucky, Spindletop Research Center Report, 1963.

Meissner, E. Elastische Oberflächen Querwellen Verhandl., Intern., Kongr. Tech. Mech., 2nd, Zuric, 3-11, 1926.

Minear, John W. Quarterly Report No. 9, Seismicity of the Southeastern United States, AFCRL Project CRL-46116, 1966.

_____. Research directed toward the study of seismicity in the Southeastern United States, Annual Technical Report #2, Air Force Cambridge Research Lab, Project CRL-46116, January, 1966.

_____. Semi-Annual Technical Report, Seismicity of the Southeastern United States, Project CRL-46116, January 1965.

Takeuchi, H., and J. Dorman. Partial derivatives of surface wave phase velocity with respect to physical parameter changes within the earth, J. Geophys. Research, 69, 3429-3441, 1964.

Tomoda, Y., and K. Aki. Use of the function $\sin x/x$ in gravity problems, Bull. Earthquake Res. Inst., Tokyo, 443-448.

APPENDIX I

EVALUATION OF THE SECULAR EQUATION IN COMPUTING RAYLEIGH DISPERSION

In the Dunkin Method, the Rayleigh dispersion equation is the secular equation

$$\text{Det } R_{11} = r \left| \begin{smallmatrix} 12 \\ 12 \end{smallmatrix} \right| - t^p \left| \begin{smallmatrix} 12 \\ ab \end{smallmatrix} \right| g^{p-1} \left| \begin{smallmatrix} ab \\ cd \end{smallmatrix} \right| \dots g^1 \left| \begin{smallmatrix} mn \\ 12 \end{smallmatrix} \right| \quad (I-1)$$

Writing out (I-1) explicitly yields

$$\begin{aligned} \text{Det } R_{11} = & \cancel{t} \left| \begin{smallmatrix} 12 \\ 12 \end{smallmatrix} \right| g^{p-1} \left| \begin{smallmatrix} 12 \\ cd \end{smallmatrix} \right| \dots \\ & + \cancel{t} \left| \begin{smallmatrix} 12 \\ 13 \end{smallmatrix} \right| g^{p-1} \left| \begin{smallmatrix} 13 \\ cd \end{smallmatrix} \right| \dots \\ & + \cancel{t} \left| \begin{smallmatrix} 12 \\ 14 \end{smallmatrix} \right| g^{p-1} \left| \begin{smallmatrix} 14 \\ cd \end{smallmatrix} \right| \dots \quad (I-2) \\ & + \cancel{t} \left| \begin{smallmatrix} 12 \\ 23 \end{smallmatrix} \right| g^{p-1} \left| \begin{smallmatrix} 23 \\ cd \end{smallmatrix} \right| \dots \\ & + \cancel{t} \left| \begin{smallmatrix} 12 \\ 24 \end{smallmatrix} \right| g^{p-1} \left| \begin{smallmatrix} 24 \\ cd \end{smallmatrix} \right| \dots \\ & + \cancel{t} \left| \begin{smallmatrix} 12 \\ 34 \end{smallmatrix} \right| g^{p-1} \left| \begin{smallmatrix} 34 \\ cd \end{smallmatrix} \right| \dots \end{aligned}$$

where the ... signifies multiplication of the form $g^{p-2} \left| \begin{smallmatrix} cd \\ ef \end{smallmatrix} \right| \dots g^1 \left| \begin{smallmatrix} mn \\ 12 \end{smallmatrix} \right|$.

Continuing the process

$$\begin{aligned} \text{Det } R_{11} = & a_1 g^{p-1} \left| \begin{smallmatrix} 12 \\ 12 \end{smallmatrix} \right| g^{p-2} \left| \begin{smallmatrix} 12 \\ ef \end{smallmatrix} \right| \dots + a_1 g^{p-1} \left| \begin{smallmatrix} 12 \\ 13 \end{smallmatrix} \right| g^{p-2} \left| \begin{smallmatrix} 13 \\ ef \end{smallmatrix} \right| \dots + \\ & + 4 \text{ more similar terms with } a_1 \text{ as a factor} \\ & + 5 \text{ more expressions with } a_2, a_3, a_4, a_5, \text{ and } a_6 \\ & \text{replacing } a_1 \end{aligned}$$

where

$$a_1 = \check{t} \begin{vmatrix} 12 \\ 12 \end{vmatrix} \quad (I-3)$$
$$a_2 = \check{t} \begin{vmatrix} 12 \\ 13 \end{vmatrix}, \text{ etc.}$$

Collecting terms with like coefficients $g^{p-1} \begin{vmatrix} 12 \\ ef \end{vmatrix}$, $g^{p-1} \begin{vmatrix} 13 \\ ef \end{vmatrix}$, etc., gives

$$\text{Det } R_{11} = A_1 g^{p-2} \begin{vmatrix} 12 \\ ef \end{vmatrix} \dots + A_2 g^{p-2} \begin{vmatrix} 13 \\ ef \end{vmatrix} \dots + A_3 g^{p-2} \begin{vmatrix} 14 \\ ef \end{vmatrix} \dots \quad (I-4)$$
$$+ A_4 g^{p-2} \begin{vmatrix} 23 \\ ef \end{vmatrix} \dots + A_5 g^{p-2} \begin{vmatrix} 24 \\ ef \end{vmatrix} \dots + A_6 g^{p-2} \begin{vmatrix} 34 \\ ef \end{vmatrix} \dots$$

where

$$A_1 = (a_1 b_{11} + a_2 b_{21} + a_3 b_{31} + a_4 b_{41} + a_5 b_{51} + a_6 b_{61}) ,$$

$$b_{11} = g^n \begin{vmatrix} 12 \\ 12 \end{vmatrix} ,$$

$$b_{21} = g \begin{vmatrix} 13 \\ 12 \end{vmatrix} ,$$

$$b_{31} = g \begin{vmatrix} 14 \\ 12 \end{vmatrix} , \text{ etc.}$$

(I-4) is of the form (I-2); the sum of six terms which are each products of the second order subdeterminants. The process of evaluating the second order subdeterminants of a given layer, multiplying by six previously determined coefficients, a_i , and summing to obtain six new coefficients, A_i , is repeated until the entire layered sequence has been traversed from bottom to top. This can be quickly and easily adapted to computer processing

as is indicated in the following considerations of the real and imaginary structure of t_{ab}^{12} and $g^p t_{ab}^{12}$. t_{ab}^{12} is of the form of a 6×1 row matrix

$$\begin{bmatrix} R & R & I & I & R & R \end{bmatrix} \quad I = \text{pure imaginary quantity} \quad (I-5)$$

$R = \text{pure real quantity}$

The real and imaginary structure of the g_{cd}^{ab} is of the form of a 6×6 matrix

$$g_{cd}^{ab} = \begin{bmatrix} R & R & I & I & R & R \\ R & R & I & I & R & R \\ -I & -I & R & R & -I & -I \\ -I & -I & R & R & -I & -I \\ R & R & I & I & R & R \\ R & R & I & I & R & R \end{bmatrix} \quad (I-6)$$

The ab indices have been taken as the row indices and the cd indices the column indices with 1=12, 2=13, 3=14, 4=23, 5=24, and 6=34; $g_{34}^{12} = g_{16}$, etc. Multiplication of t_{ab}^{12} by the $g^{p-1}_{ef}^{ab}$ in (I-2) yields a matrix of the form

$$\begin{bmatrix} R & R & I & I & R & R \\ R & R & I & I & R & R \\ R & R & I & I & R & R \\ R & R & I & I & R & R \\ R & R & I & I & R & R \\ R & R & I & I & R & R \end{bmatrix} \quad (I-7)$$

Elements of this matrix correspond to the terms $a_1 b_{11}$, $a_2 b_{21}$, etc. in (I-4). Thus, the six new coefficients A_1 are simply the sum of the elements in a column of (I-7). The six new coefficients can then be considered as just another 6×1 row matrix of the form of (I-5), minus ones have been inserted in (I-6) to account for the multiplication of two like-signed imaginary quantities.

APPENDIX II

MODAL SHAPE COMPUTATIONS

In the Dunkin Method, mode shape is computed from the relation

$$R_n^m(z;a) = r_{11}^{-1} t_{1r}^p g_{rs}^{p-1} \dots g_{vb}^n (z_n - z) g^n(z - z_{n-1}) \left| \begin{matrix} ab \\ cd \end{matrix} \dots g^1 \right|_{21}^{ef} \quad (II-1)$$

where a denotes the component of displacement. $R_n^m(z;a)$ is the a^{th} component of the displacement-stress vector, at the depth z , normalized to the vertical displacement at the free surface. Note that r_{11}^{-1} is simply a constant multiplier for all of the displacement-stress components. Thus, it may be dropped and the $R_n^m(z;a)$ at different depths divided by the vertical displacement at the surface to normalize the displacements. The equation actually used for the determination of mode shape was

$$R_n^m(z;a) = t_{1r}^p g_{rs}^{p-1} \dots g_{vb}^n (z_n - z) g^n(z - z_{n-1}) \left| \begin{matrix} ab \\ cd \end{matrix} \dots g^1 \right|_{21}^{ef} \quad (II-2)$$

Writing (II-2) explicitly

$$\begin{aligned} R_n^m(z;a) &= t_{11}^p g_{1s}^{p-1} g_{st}^{p-2} \dots \\ &+ t_{12}^p g_{2s}^{p-1} g_{st}^{p-2} \dots \quad (II-3) \\ &+ t_{13}^p g_{3s}^{p-1} g_{st}^{p-2} \dots \\ &+ t_{14}^p g_{4s}^{p-1} g_{st}^{p-2} \dots \end{aligned}$$

When the dots denote the product of g_{ij}^n post multiplying g_{st}^{p-2} .

$$\begin{array}{c}
 \text{Sum over } s \longrightarrow \\
 R_n^m(z; a) = a_1 g_{11}^{p-1} g_{1t}^{p-2} \dots + a_1 g_{12}^{p-1} g_{2t}^{p-2} \dots + a_1 g_{13}^{p-1} g_{3t}^{p-2} \dots + a_1 g_{14}^{p-1} g_{4t}^{p-2} \dots \\
 \\
 \text{Sum over } r \left| a_2 g_{21}^{p-1} g_{1t}^{p-2} \dots + a_2 g_{22}^{p-1} g_{2t}^{p-2} \dots + \dots \right. \\
 \downarrow a_4 g_{41}^{p-1} g_{1t}^{p-2} \dots + \dots
 \end{array} \quad (\text{II-4})$$

where

$$a_1 = t_{11}^p, \quad a_2 = t_{12}^p, \quad a_3 = t_{13}^p, \quad \text{and} \quad a_4 = t_{14}^p.$$

$R_n^m(z; a)$ has been expanded into 16 terms of the form $a_i g_{ij}^{p-1} g_{jt}^{p-2} \dots$. Now the g^{p-1} which have explicit subscripts can be included in the constant factor a_i . Collecting terms with common factors of g_{ij}^{p-2} yields

$$\begin{aligned}
 R_n^m(z; a) &= (a'_1 + a'_2 + a'_3 + a'_4) g_{1t}^{p-2} \dots + (a'_1 + a'_2 + a'_3 + a'_4) g_{2t}^{p-2} \dots \\
 &\quad + \dots + (a'_1 + a'_2 + a'_3 + a'_4) g_{4t}^{p-2} \dots
 \end{aligned} \quad (\text{II-5})$$

$$a'_i = a_i g_{ik}^{p-1}, \text{ etc.}$$

which is of the form of (II-3).

Continuing this process yields

$$\begin{aligned}
 R_n^m(z; a) &= a_1 g^n(z - z_{n-1}) \left| \begin{matrix} a_1 & & & \\ & \ddots & & \\ & & g^1 & \text{ef} \\ & & & |_{12} \end{matrix} \right. \dots \\
 &\quad + a_2 g^n(z - z_{n-1}) \left| \begin{matrix} a_2 & & & \\ & \ddots & & \\ & & g^1 & \text{ef} \\ & & & |_{12} \end{matrix} \right. \dots \\
 &\quad + a_3 g^n(z - z_{n-1}) \left| \begin{matrix} a_3 & & & \\ & \ddots & & \\ & & g^1 & \text{ef} \\ & & & |_{12} \end{matrix} \right. \dots \\
 &\quad + a_4 g^n(z - z_{n-1}) \left| \begin{matrix} a_4 & & & \\ & \ddots & & \\ & & g^1 & \text{ef} \\ & & & |_{12} \end{matrix} \right. \dots
 \end{aligned} \quad (\text{II-6})$$

The horizontal component, u , of displacement corresponds to $a=1$ and the vertical component, w , to $a=2$, so that

$$u = a_2 g^n \left|_{cd}^{12} \dots + a_3 g^n \left|_{cd}^{13} \dots + a_4 g^n \left|_{cd}^{14} \dots \text{ and} \quad (\text{II-7})\right.\right.$$

$$w = a_1 g^n \left|_{cd}^{21} \dots + a_3 g^n \left|_{cd}^{23} \dots + a_4 g^n \left|_{cd}^{24} \dots \quad (\text{II-8})\right.\right.$$

Note that $\zeta^n \left|_{kl}^{ij} = 0$, if $i=j$ or $k=l$.

Writing (II-7) explicitly

$$\begin{aligned} u = & a_2 g^n \left|_{12}^{12} g^{n-1} \left|_{ef}^1 \dots + a_2 g^n \left|_{13}^{12} g^{n-1} \left|_{ef}^{13} \dots + a_2 g^n \left|_{14}^{12} g^{n-1} \left|_{ef}^{14} \dots \right.\right.\right. \\ & + a_2 g^n \left|_{23}^{12} g^{n-1} \left|_{ef}^{23} \dots + a_2 g^n \left|_{24}^{12} g^{n-1} \left|_{ef}^{24} \dots + a_2 g^n \left|_{34}^{12} g^{n-1} \left|_{ef}^{34} \dots \right.\right.\right. \\ & + a_3 g^n \left|_{12}^{13} g^{n-1} \left|_{ef}^{12} \dots + 5 \text{ more terms in } a_3 \quad (\text{II-9})\right.\right. \\ & + a_4 g^n \left|_{12}^{14} g^{n-1} \left|_{ef}^{12} \dots + 5 \text{ more terms in } a_4 \right.\right. \end{aligned}$$

u is expressed in terms of the sum of 18 terms of the form $a_m g^n \left|_{kl}^{ij} g^{n-1} \left|_{ef}^{kl} \dots$
 Collecting terms with common $g^{n-1} \left|_{ef}^{kl}$ gives u as the sum of six terms of
 the form $a_m g^{n-1} \left|_{ef}^{ij} \dots$

$$\begin{aligned} u = & a'_1 g^{n-1} \left|_{ef}^{12} \dots + a'_2 g^{n-1} \left|_{ef}^{13} \dots + a'_3 g^{n-1} \left|_{ef}^{14} \dots + \right.\right. \\ & a'_4 g^{n-1} \left|_{ef}^{23} \dots + a'_5 g^{n-1} \left|_{ef}^{24} \dots + a'_6 g^{n-1} \left|_{ef}^{34} \dots , \quad (\text{II-10})\right.\right. \end{aligned}$$

where

$$a_1' = a_2 g_{12}^{12} + a_3 g_{12}^{13} + a_4 g_{12}^{14}, \text{ etc.}$$

The process of evaluating the displacements u and w now proceeds exactly as for the evaluation of $\text{Det } R_{11}$ described in Appendix I.

Let us consider the real and imaginary forms of the factors appearing in (II-4), (II-6), and (II-10). From the definition of T_p^{-1} given by Dunkin, t_{1r} is of the form

$$t_{1r} = [I \ R \ R \ I], \quad I = \text{pure imaginary quantity} \quad (II-11)$$

$$R = \text{pure real quantity}$$

The layer matrices G_n are of the form

$$G_n = \begin{bmatrix} R & I & I & R \\ I & R & R & I \\ I & R & R & I \\ R & I & I & R \end{bmatrix} \quad (II-12)$$

$$\text{Thus } t_{1r} g_{rs}^{p-1} = [I \ R \ R \ I] \quad (II-13)$$

Each successive multiplication by a layer matrix G_n yields a row matrix of the form $[I \ R \ R \ I]$ until the first multiplication by a second order subdeterminant is encountered. In order to account for the multiplication of two imaginaries in the evaluation of column 2 and 3 in (II-13) minus ones are inserted in (II-12) to give

$$G_n = \begin{bmatrix} R & -I & -I & R \\ I & R & R & I \\ I & R & R & I \\ R & -I & -I & R \end{bmatrix} \quad (II-14)$$

By (II-9) and the definitions of g_{kl}^{nij} , the form of the matrix by which a_2 , a_3 , and a_4 of (II-7) are multiplied is

$$\begin{bmatrix} R & R & I & I & R & R \\ R & R & I & I & R & R \\ I & I & R & R & I & I \end{bmatrix} \quad (II-15)$$

and for a_1 , a_3 , a_4 in the case of the vertical component

$$\begin{bmatrix} R & R & I & I & R & R \\ I & I & R & R & I & I \\ R & R & I & I & R & R \end{bmatrix} \quad (II-16)$$

For the u component

$$[RRI] \cdot \begin{bmatrix} R & R & I & I & R & R \\ R & R & I & I & R & R \\ -I & -I & R & R & -I & -I \end{bmatrix} = [RRIIRR] \quad (II-17)$$

and for the w component

$$[IRI] \cdot \begin{bmatrix} R & R & -I & -I & R & R \\ I & I & R & R & I & I \\ R & R & -I & -I & R & R \end{bmatrix} = [IIRRRI] \quad (II-18)$$

Minus ones have been inserted to account for multiplication of two imaginaries.

To continue the process to the surface, the form of the matrices composed of the second order subdeterminant elements is

$$\begin{bmatrix} R & R & I & I & R & R \\ R & R & I & I & R & R \\ -I & -I & R & R & -I & -I \\ -I & -I & R & R & -I & -I \\ R & R & I & I & R & R \\ R & R & I & I & R & R \end{bmatrix}$$

(II-19)

for the u component and

$$\begin{bmatrix} R & R & -I & -I & R & R \\ R & R & -I & -I & R & R \\ I & I & R & R & I & I \\ I & I & R & R & I & I \\ R & R & -I & -I & R & R \\ R & R & -I & -I & R & R \end{bmatrix}$$

(II-20)

and for the w component. Minus ones have been inserted in the appropriate elements to account for the multiplication of two pure imaginary quantities. Since the lower subscripts in (II-1) for the surface layer matrix are 21, the layer matrix of the surface layer is a 6 x 1 column matrix. The final multiplications are then of the forms:

u component

$$[R \ R \ I \ I \ R \ R] \cdot \begin{bmatrix} R \\ R \\ -I \\ -I \\ R \\ R \end{bmatrix} = [R \ R \ R \ R \ R \ R]$$

w component

$$[I \ I \ R \ R \ I \ I] \cdot \begin{bmatrix} R \\ R \\ I \\ I \\ R \\ R \end{bmatrix} = [I \ I \ I \ I \ I]$$

EXPLICIT FORMS OF LAYER MATRIX COMPONENTS g_{ij}

$$g_{11} = g_{44} = \frac{2\beta^2}{c^2} \cosh P - \frac{p\beta^2}{k^2 c^2} \cosh Q$$

$$g_{12} = g_{34} = \frac{i\beta p}{r_\alpha c^2 k^2} \sinh P + \frac{2ir_\beta \beta^2}{c^2} \sinh Q$$

$$g_{13} = g_{24} = \frac{i\beta^2}{\mu kc^2} \cosh P - \frac{i\beta^2}{k\mu c^2} \cosh Q$$

$$g_{14} = \frac{\beta^2}{kr_\alpha c^2 \mu} \sinh P + \frac{p\beta^2 r_\beta}{\mu kc^2} \sinh Q$$

$$g_{21} = g_{43} = -\frac{2ir_\alpha \beta^2}{c^2} \sinh P - \frac{ip\beta^2}{k^2 r_\beta c^2} \sinh Q$$

$$g_{22} = g_{33} = -\frac{p\beta^2}{k^2 c^2} \cosh P + \frac{2\beta^2}{c^2} \cosh Q$$

$$g_{23} = \frac{r_\alpha \beta^2}{\mu kc^2} \sinh P + \frac{\beta^2}{\mu r_\beta c^2 k} \sinh Q$$

$$g_{31} = g_{42} = \frac{2i\mu \beta^2 p}{kc^2} \cosh P - \frac{2ip\mu \beta^2}{kc^2} \cosh Q$$

$$g_{32} = -\frac{\mu p^2 \beta^2}{k^3 c^2 r_\alpha} \sinh P - \frac{4\mu kr_\beta \beta^2}{c^2} \sinh Q$$

$$g_{41} = -\frac{4\mu kr_\alpha \beta^2}{c^2} \sinh P - \frac{\mu p^2 \beta^2}{r_\beta c^2 k^3} \sinh Q$$

SUMMARY OF EXPLICIT FORMS OF SECOND ORDER SUBDETERMINANTS $g \begin{vmatrix} ij \\ kl \end{vmatrix}$

$$g \begin{vmatrix} 12 \\ 12 \end{vmatrix} = g \begin{vmatrix} 34 \\ 34 \end{vmatrix} = -2\gamma(\gamma - 1) + (2\gamma^2 - \gamma + 1)\overline{CP} \overline{CQ} - [\frac{(\gamma-1)^2}{r_\alpha r_\beta} + \gamma^2 r_\alpha r_\beta] \overline{SQ} \overline{SP}$$

$$g \begin{vmatrix} 12 \\ 13 \end{vmatrix} = g \begin{vmatrix} 24 \\ 34 \end{vmatrix} = + (\rho \lambda^2 k)^{-1} [\frac{\overline{SQ} \overline{CP}}{r_\beta} + r_\alpha \overline{SP} \overline{CQ}]$$

$$g \begin{vmatrix} 12 \\ 14 \end{vmatrix} = g \begin{vmatrix} 12 \\ 23 \end{vmatrix} = g \begin{vmatrix} 14 \\ 34 \end{vmatrix} = g \begin{vmatrix} 23 \\ 34 \end{vmatrix} = i(\rho \lambda^2 k)^{-1} \left\{ (2\gamma-1)(1-\overline{CP} \overline{CQ}) + [\frac{(\gamma-1)}{r_\alpha r_\beta} + \gamma r_\alpha r_\beta] \overline{SP} \overline{SQ} \right\}$$

$$g \begin{vmatrix} 12 \\ 24 \end{vmatrix} = g \begin{vmatrix} 13 \\ 34 \end{vmatrix} = - (\rho \lambda^2 k)^{-1} [r_\beta \overline{CP} \overline{SQ} + \frac{1}{r_\alpha} \overline{SP} \overline{CQ}]$$

$$g \begin{vmatrix} 12 \\ 34 \end{vmatrix} = - (\rho \lambda^2 k)^{-2} [2(1-\overline{CP} \overline{CQ}) + (\frac{1}{r_\alpha r_\beta} + r_\alpha r_\beta) \overline{SQ} \overline{SP}]$$

$$g \begin{vmatrix} 13 \\ 12 \end{vmatrix} = g \begin{vmatrix} 34 \\ 24 \end{vmatrix} = - (\rho \lambda^2 k) [\gamma^2 r_\beta \overline{CP} \overline{SQ} + \frac{(\gamma-1)^2}{r_\alpha} \overline{SP} \overline{CQ}]$$

$$g \begin{vmatrix} 13 \\ 13 \end{vmatrix} = g \begin{vmatrix} 24 \\ 24 \end{vmatrix} = \overline{CQ} \overline{CP}$$

$$g \begin{vmatrix} 13 \\ 14 \end{vmatrix} = g \begin{vmatrix} 13 \\ 23 \end{vmatrix} = g \begin{vmatrix} 14 \\ 24 \end{vmatrix} = g \begin{vmatrix} 23 \\ 24 \end{vmatrix} = i(\gamma r_\beta \overline{CP} \overline{SQ} + \frac{(\gamma-1)}{r_\alpha} \overline{SP} \overline{CQ})$$

$$g \begin{vmatrix} 13 \\ 24 \end{vmatrix} = + \frac{r_\beta}{r_\alpha} \overline{SQ} \overline{SP}$$

$$g \begin{vmatrix} 14 \\ 12 \end{vmatrix} = g \begin{vmatrix} 23 \\ 12 \end{vmatrix} = g \begin{vmatrix} 34 \\ 14 \end{vmatrix} = g \begin{vmatrix} 34 \\ 23 \end{vmatrix} = i(\rho k \lambda^2) \left\{ \gamma(\gamma-1)(2\gamma-1)(1-\bar{CQ}\bar{CP}) + \left[\frac{(\gamma-1)^3}{r_\alpha r_\beta} + r_\alpha r_\beta \gamma^3 \right] \bar{SQ} \bar{SP} \right\}$$

$$g \begin{vmatrix} 14 \\ 13 \end{vmatrix} = g \begin{vmatrix} 23 \\ 13 \end{vmatrix} = g \begin{vmatrix} 24 \\ 14 \end{vmatrix} = g \begin{vmatrix} 24 \\ 23 \end{vmatrix} = -i \left(\frac{(\gamma-1)}{r_\beta} \bar{CP} \bar{SQ} + r_\alpha \gamma \bar{CQ} \bar{SP} \right)$$

$$g \begin{vmatrix} 14 \\ 14 \end{vmatrix} = g \begin{vmatrix} 23 \\ 23 \end{vmatrix} = 1 + 2\gamma(\gamma-1)(1-\bar{CQ}\bar{CP}) + \left(\frac{(\gamma-1)^2}{r_\alpha r_\beta} + \gamma^2 r_\alpha r_\beta \right) \bar{SP} \bar{SQ}$$

$$g \begin{vmatrix} 14 \\ 23 \end{vmatrix} = g \begin{vmatrix} 23 \\ 14 \end{vmatrix} = g \begin{vmatrix} 14 \\ 14 \end{vmatrix} = 1$$

$$g \begin{vmatrix} 24 \\ 12 \end{vmatrix} = g \begin{vmatrix} 34 \\ 13 \end{vmatrix} = + (\rho \lambda^2 k) \left[\frac{(\gamma-1)^2}{r_\beta} \bar{CP} \bar{SQ} + r_\alpha \gamma^2 \bar{SP} \bar{CQ} \right]$$

$$g \begin{vmatrix} 24 \\ 13 \end{vmatrix} = + \frac{r_\alpha}{r_\beta} \bar{SP} \bar{SQ}$$

$$g \begin{vmatrix} 34 \\ 12 \end{vmatrix} = (\rho \lambda^2 k)^2 [2\gamma^2(\gamma-1)^2 (\bar{CP} \bar{CQ} - 1) - \frac{(\gamma-1)^4}{r_\alpha r_\beta} + \gamma^4 r_\alpha r_\beta] \bar{SP} \bar{SQ}$$

EXPLICIT FORMS OF $\tau \Big|_{ab}^{12}$

$$\tau \Big|_{12}^{12} = -\frac{\beta^2 \mu}{2\omega} (4k^4 r_\alpha r_\beta + p^2)$$

$$\tau \Big|_{13}^{12} = -\frac{r_\alpha}{r_\beta} \quad \tau \Big|_{24}^{12} = \frac{i\beta^2}{2\omega} r_\alpha k (2k^2 - p)$$

$$\tau \Big|_{14}^{12} = \tau \Big|_{23}^{12} = \frac{i\beta^2 k}{2\omega} (2k^2 r_\alpha r_\beta + p)$$

$$\tau \Big|_{34}^{12} = -\frac{\beta^2 k^2}{2\mu\omega} (r_\alpha r_\beta + 1)$$

$$P = kdr_c \quad Q = kdr_\beta$$

$$\gamma = \frac{2\beta^2}{c^2} \quad p = 2k^2 - \frac{\omega^2}{\beta^2}$$

$$r_c = \sqrt{\frac{c^2}{\alpha^2} - 1}$$

$$SP = \sin P \quad c > \alpha$$

$$CP = \cos P$$

$$r_\beta = \sqrt{\frac{c^2}{\beta^2} - 1} \quad c \geq \beta$$

$$SQ = \sin Q$$

$$CQ = \cos Q$$

$$r_\alpha = -i \sqrt{1 - \frac{c^2}{\xi^2}}$$

SP = sinh P

c < α

CP = cosh P

$$r_\beta = -i \sqrt{1 - \frac{c^2}{\beta^2}}$$

SQ = sinh Q

c < β

CP = cosh Q

The g_{ij} expressions are written for the hyperbolic functions ($c < \alpha, c < \beta$).

For $c > \alpha, c > \beta$, the hyperbolic functions transform according to

cosh P	→	cos P	$c > \alpha$
cosh Q	→	cos Q	$c > \beta$
sinh P	→	-i sin P	$c > \alpha$
sinh Q	→	-i sin Q	$c > \beta$

APPENDIX III

**FORTRAN LISTINGS OF COMPUTER PROGRAMS
FLATRAY, STRESS, INTEGRAL, TRAVEL, VARGRAV, AND PRESID**

INPUT DATA AND FORMAT FOR FLATRAY

<u>CARD</u>	<u>FORMAT</u>	<u>DATA DESCRIPTION</u>
1	I4	Model identification no.
	I4	No. of layers <41
	I4	No. of modes to be computed <11
	F10.4	Precision of root values of k
	F10.4	Cutoff k value to automatically stop computation
2	8F10.6	Layer parameters stored in sequence α, β, ρ, d ; two layers to a card
3	F10.6	Starting c value
	F10.6	Minimum c value
	F10.6	Decrement of c
	F10.6	Starting k value
	F10.6	k increment for individual modes
	F10.6	k increment to find starting points of different modes
	F10.6	c perturbation
	F10.6	k perturbation
4	20I4	Mode no. to be found stored sequentially

```

      DIMENSION ALPHA(40),BETTA(40),MHO(40),THICK(40),ROOTS(15,40),MODE
1(14),PEM10D(15,40),H(6),E(8),G(6,6),A(6),UDISP(40),WUDISP(40)
1,-(14)
      COMMUN UDISP,WDIS=,H
      MEAU 150,MODEL,NLAYER,NODE,XMIN ,XMAX
150 FORMAT(3I4,2F10.4)
      HEAD 200,(ALPHA(I),BETTA(I),RHU(I),THICK(I),I=1,NLAYER)
200 FORMAT(8F10.6)
      PRINI 900,MODEL
900 FORMAT(31+LAYER PARAMETERS FOR MODEL RTI 14 // 6H LAYER,5X,6H AL
1P4,A,7X,6H BETTA,7X,4H MHO,5X,14H THICKNESS(KM),3X, 6H H(KM) /)
1THICK#0,
      U3 902 I=1,NLAYER
1THICK=TTICK +THICK(I)
      PRINI 902,I,ALPHA(I),BETTA(I),MHO(I),THICK(I),TTICK
902 FORMAT(1A,(3,3X,F10.4,X,F8.4,X,F8.4,X,F8.2,X,F8.2)
1)ALE TTICK
      HEAD 200, CMAX,CMIN,DEL0,AK,DELK,DE,K1,PTRBC,PTRB K
      HEAD 350, (NODE(I),I=1,NODE)
350 FORMAT(20I4)
1P04=0
      NEMUD = 1
      CMAX1 =CMAX
      NUD = 10
      INUDE(1)
      ISH1 =10
      IAB NLAYEM-1
      IY=1
      AK=NU01S(IH,IN)=AK
      IPINR =1
      C = CMAX
      JUMP1=1
500  IDISP= 1
      JUMP=1
      ICPI=1
      US=XR
      SJN= 1.
      I3RAU = 10
      IVOXZ=1
10J  I=1A
      UMEGA=XK=C
      HALPH = SQRT(ABS((C/ALPHA(|X+1|))**2-1.))
      M3ET=SUMT(ABS((C/BETTA(|X+1|))**2-1.))
      A_2,*AK**2-OMEGA**2/(BETTA(|X+1|)**2)
      H2*AC= BETTA(|X+1|)**2/(2.*OMEGA**2)
      AMU=BETTA(|X+1|)**2*MHO(|X+1|)
      H(1)=T1=-REFAC*AMU*(-4.*AK**4*RALPH**4*MBET+AL**2)
      H(2)=T12=dEFAC*RALPH*XK*(2.*XK**2-A_2)
      H(3)=T13=dEFAC*XK*(-2.*XK**2*RALPH**4*MBET+AL)
      H(4)=T14=T13
      H(5)=T15=-R3ET*T12/RALPH
      H(6)=T16=-B3EFAC*XK**2*(-RALPH*R3ET+1.)/AMU
      D1=AM2,* BETTA(|X|)**2/C**2
      U[V$S].
      H4C=R4U(|X|)*C**2*XK
      HALPH=SUMT(ABS((C/ALPHA(|X|))**2-1.))
      M3ET =SQRT(ABS((C/BETTA(|X|))**2-1.))
      XK=RALPH*THICK(|X|)
      XK=R3ET*TICK(|X|)
      IC=ALPHA(|X|)1,2,2
      PAU=1.
      U3=COS(P)
      S3=SIN(P)
      GO TO 3
      PAU=-1.
      U3=COS(P)
      S3=SIN(P)
      GO TO 6
      PAU=1.
      U3=(EXP(IQ)+EXP(-IQ))/2.
      S3=(EXP(IQ)-EXP(-IQ))/2.
      U[V$C]C
      G(1,1)=(GAM-1.)*+2*(HALPH+R3ET)*GAM**2*HALPH*R3ET*FACB+FACB
      G(1,1)+-G(1,1)*S0*SP-2.*GAM*(GAM-1.)*(2.*GAM**2-2.*GAM+1.)*CP*CU
      G(1,2)+(S0*CP/R3ET+HALPH*SP*CD*FACB)/RHOC
      G(1,3)+((GAM-1.)/(HALPH*R3ET)+GAM*HALPH*R3ET*FACB+FACB)*SP*S0+(2.*GAM-1.)*(-CP*CD)
      G(1,3)+G(1,3)/MHOC
      G(1,4)+G(1,3)
      G(1,5)+-(R3ET*CP*S0*FACB+SP*CD/RALPH)/RHOC
      G(1,6)+-(2.0*(1.-CP*CU)+(1.0/(HALPH*R3ET)+RALPH*R3ET*FACB+FACB)*SU+S
      1M)/MHUCE**2)
      G(2,1)=R4OC=(GAM**2*R3ET*FACB*CP+3J*(GAM-1.)*+2*SP*CD/RALPH)
      G(2,2)=C0*CP
      G(2,3)=GAM*R3ET*FACB*CP+S0*(GAM-1.)*SP*CD/RALPH
      G(2,4)=G(2,3)
      G(2,5)=R3ET*S0*SP*FACB/RALPH
      G(2,6)=G(1,5)
      G(3,1)=((GAM-1.)*+3/(HALPH*R3ET)*RA_PHR3ET*GAM**3*FACB+FACB)*SU
1*SP
      G(3,1)+-4H**2*(GAM*(GAM-1.)*(2.*GAM-1.)*(1.-CD*CP) +G(3,1))
      G(3,2)+ ((LA4-1.)*CP+S0/R3ET+HALPH*GAM*FACB*CD*SP)
      G(3,3)+1.+2.*GAM*(GAM-1.)*(1.-CP*CU)+(GAM-1.)*+2/(RALPH*R3ET)*GAM
1*CD*HALPH*R3ET*FACB+FACB)*SP*S0
      G(3,4)+G(3,3)-1.
      G(3,5)+-G(2,3)
      G(3,6)+-G(1,3)
      G(4,1)+G(3,1)
      G(4,2)+G(3,2)
      G(4,3)+G(3,3)-1.
      G(4,4)+G(3,3)

```

```

      U(4,5)=G(2,3)
      U(4,6)=G(1,3)
      U(5,1)=(GAM-1.)+2*CP*SQ/HBEI+HALF*GAM=GAM=SP*CO*FACA)*HHUC
      U(5,2)=RALPH*SP*SU*FACA/HBET
      U(5,3)=G(3,2)
      U(5,4)=G(3,2)
      U(5,5)=G(2,2)
      U(5,6)=G(1,2)
      U(6,1)=(GAM-1.)*C/(HALPH*HBEI)+GA4*4*RALPH*HBET*FACA*FACH)=SP*S
10
      U(6,2)=U(5,1)
      U(6,3)=G(3,1)
      U(6,4)=G(3,1)
      U(6,5)=G(2,1)
      U(6,6)=G(1,1)
      IF(101SF-1)62,62,8012
62 IF(1-1)402,402,101
101 D3 30 J=1,6
      SUM=0,
      U3 40 K=1,6
      SUM=SUM+B(K)*G(I,K,J)
40 CONTINUE
      A1J)ESUM
30 CONTINUE
      D3 8 J=1,6
      B(J)=A(J)/DIVS
8 CONTINUE
      I=1-1
      G3 TU 51
402 F=di1)*G(1,1)+B(2)*G(2,1)+B(3)*G(3,1)+B(4)*G(4,1)+B(5)*G(5,1)+B(6)
1*3(6,1)
      F=F/UVS
      IF(15HT-1) 605,301,603
C ** COMPUTE FIRST ROOT OF EACH MODE
603 IF(INDX2-1)605,604,605
604 14DXZ=0
      X<1=X4
      F1=F
      XEL XK+DELK1
      U3 TU 100
605 AF =XBS(F)
      AF1=XBS(F1)
      IF(AF-AF1) 606,607,607
607 IF(XBS(F1-F)=AF) 608,609,609
608 IF(XBS(F1-F)-AF1) 608,609,609
609 IF(XBS(XK-XK)-XKMIN) 308,308,610
610 U3 TU (703,704),JUMP
703 F2=F
      JJMPZ=2
      X<2=XK
      X<= XdS((XK+F1-XK+F2)/(F1-F2))
      13HAL=1
      U3 TU (1100,60),JUMP1
706 13HAL=0
      F1=F2
      X<1=X<2
704 13HAL=0
      IF(XK-XK1) 614,613,613
614 X<=XK+XKMIN
      F2=F
      X<=XK
      U3 TU (1100,60),JUMP1
513 F2=F
      X<=XK
      X<=XK-XKMIN
      U3 TU (1100,60),JUMP1
606 IF(15RAC-1)308,706,707
707 IF(VN00-1)617,618,617
617 IF(AF-AF1) 619,619,620
620 X<= XK-2.*0ELK1
      SIGN=-1.
      IF(XK-Q,)1014,1014,100
1014 X<=XK+0ELK1
      NUUDZ=1
      U3 TU 500
619 X<1=X<
      F1=F
      X<=XK +SIGN*0ELK1
      IF(XK-Q,)1014,1014,100
305 IF(15HT-1)3000,508,3000
3000 IF(15RAC-10) 300,708,708
708 F2=F1
      X<=X<1
300 F1=F
      X<= XdS((XK2+F1-XK+F2)/IF1-, -)
      M00=SIH,IN)=XK
      M=100(M,IN)= (2,*3,1416)/IXX*C
      IF(15HT-1) 950,901,950
950 14Z|M=1
      IF(M-MODE(MODE)) 615,615,616
616 F1=F
      X<1=X<
      X<=XK+0ELK1
      U3 TU 100
617 X<=X<2.*XKMIN
      UEL<1= ROOTS(M-1,1)
      XMIN= .01*0ELK1
      1514=10
      NUUDZ=1
      U3 TU 500
618 1514=1
      JJMPZ=1
      1400=1
      14 MODE(MODE)

```

```

10)SM=10
JUMP=2
X=XHOUTS(M ,1)
J=1
X=MINE .01*XK
JMP=1
IVS1
d000 ISLIX
A_>2.*XX*XX-(XX*C)**2/(BETTA(IA+1))**2
A_>3=AL*AL
HALPH=SQRT(ABS((C/ALPHA(IX+1))**2-1.))
AMU=BETTA(IX+1)**2*RHU(IX+1)
B(1)=BETTA(IX+1)**2/(AK*C**2)
B(2)=+AL*BETTA(IX+1)**2/(2.*AK**3*C*C*RALPH)
B(3)=-BETTA(IX+1)**2/(2.*AMU*(AK*C)**2)
B(4)=BETTA(IX+1)**2/(2.*AMU*HALPH*(C*XX)**2)
8001 IF(I=L) 8010.8010,8009
8009 Be(SU*BETTA(I))**2
AMU=BETTA(I)**2*RHU(I)
HALPH=SQRT(ABS((C/ALPHA(I))**2-1.))
MRET=SQRT(ABS((C/BETTA(I))**2-1.))
P=4*HALPH*THICK()
UXX=RRET*THICK()
J=(C-ALPHA(I)) 8002,8003,8005
8003 FACA=1.
C=CUS(P)
SPSIN(P)
GO TU 8030
8004 FAUB=1.
C=(EXP(P)+EXP(-P))/2.
SP=(EXP(P)-EXP(-P))/2.
8030 IF(C=dETT(I)) 8004,8005,8005
8005 FAUD=1,
LJCUST(U)
SP=SIN(Q)
GO TU 8006
8006 FAUC=-1.
Cj=(EXP(Q)+EXP(-Q))/2.
Sj=(EXP(Q)-EXP(-Q))/2.
8006 BIG = BETTA(I)**2/(XX*C*C)
A_>2.*XX*AK-(XX*C)**2/BETTA(I)**2
U(1,1)=2.*BTSU*CP/(C*C)-AL*BIG*CO/AK
U(1,2)=(AL*BIG*SP/(RALPH*XX))+2.*BIG*RRET*SO*FACB*AK
U(1,3)=BIG*(CP-CO)/AMU
U(1,4)=BIG*SP/(AMU* HALPH)+BIG*SU*MRET*FACB/AMU
U(2,1)=-2.*BIG*RALPH*SP*FACA*XX-AL*3IG*SO/(XX*RRET)
U(2,2)=AL*BIG*CP/XX+2.*BIG*CO*XX
U(2,3)=HALPH*BIG*SP*FACA/AMU+JG*SU/(RRET*AMU)
U(2,4)=G(1,3)
U(3,1)=2.*AMU*AL*BIG*(CP-CO)
U(3,2)=+AMU*AL*AL*BIG*SP/(RALPH*XX)-4.*AMU*RRET*SU*FACB*BIG*AK
1X4
U(3,3)=G(2,2)
U(3,4)=-G(1,2)
U(4,1)=-4.*AMU*AK*AK*RALPH*BIG*SP*FACA-AMU*AL*AL*BIG*SO/
1(X+AK*RRET)
G(4,2)=-G(3,1)
G(4,3)=-G(2,1)
G(4,4)=U(1,1)
UJ 8007 J=1.4
SP=U,
UJ 8008 K=1.4
SP=SUM*G(K,J)
8009 CNTINUE
A(J)=SUM
8010 CNTINUE
UJ 8011 J=1.4
E(J)= B(J)
M(J)=B(J)*A(J)
8011 CNTINUE
IF((L-1)89.83,84
83 I=-1
GO TU 8001
8012 E(1)=B(1)
E(0)=g(2)
E(/)=g(j)
E(0)=B(4)
)=-(-1)81.81.82
81 MOL=THICK()
I4ICK(I)=0,
I_>10
I_>1
GO TU 8009
84 )-(L-1) 85.85.86
85 I4ICK(I)=MOL
DIVS=1,
GO TU 51
8014 I=(L-1)90.87.88
87 U0ISM(2) =-A(2)*G(1,1)-A(3)*G(2,1)-A(4)*G(3,1)
=0ISM(2) =A(1)*G(1,1)+A(3)*G(4,1)-A(4)*G(5,1)
U0ISM(2)= U0ISM(2)/DIVS
M0ISM(2)= M0ISM(2)/DIVS
)_,10
E(1)=E(1)
E(2)=E(2)
E(3)=E(3)
E(4)=E(4)
GO TU 8009
88 I4ICK(I)=0,
DIVS=1,
GO TU 51
89 U0ISM(1) =-A(2)*G(1,1)-A(3)*G(2,1)-A(4)*G(3,1)
=0ISM(1) =A(1)*G(1,1)+A(3)*G(4,1)-A(4)*G(5,1)
U0ISM(1)= U0ISM(1)/DIVS
M0ISM(1)= M0ISM(1)/DIVS

```

```

101SP=1
14ICK(1)=HOLD
L=IX+1
PJNCH 2701,MODEL,IM,L,TOTAL,C,PENIUD(IM,IN)
PJNCH 1032,(UDISP(J),WDISP(J),J=1,L)
UJ=WDISP(1)
UJ 1001 J=1,IX+1
UDISP(J)=UDISP(J)/DIV
WDISP(J)=WDISP(J)/DIV
1001 CONTINUE
1PUN=IPUN+2
PJNCH 2701,MODEL,IM,L,TOTAL,C,PENIUD(IM,IN)
PJNCH 1032,(UDISP(J),WDISP(J),J=1,L)
2701 FDNAT(S14,SP9,3)
1032 FDNAT(6E13,6)
UJ TU (8025,901,8026),IJMP
82 MLO=THICK()
14ICK(1)=U,
L=0
UJ TU 8009
89 14ICK(1)=HOLD
L=IU
M=1
UIVS=1,
UJ TU 51
90 UJ TU(92,91,93,96),M
92 UJ 8014 K=1,6
SJMU,
UJ 8015 J=2,4
SJMSUM=B(J)*G(J-1,K)
8015 CONTINUE
A(K)=SUM
8014 CONTINUE
UJ 8031 J=1,6
B(J)=A(J)/DIVS
8031 CONTINUE
J=-1
M=2
UJ TU 51
91 IFL(-1) 94,94,95
92 UJ 8016 J=1,6
SJMU,
UJ 8017 K=1,6
SJMSUM=B(K)*G(K,J)
8017 CONTINUE
A(J)=SUM
8016 CONTINUE
UJ 8018 J=1,6
B(J)=A(J)/DIVS
8018 CONTINUE
I=1-1
UJ TU 51
94 UDISPL(+1)=-A(1)*G(1,1)-A(2)*G(2,1)-A(3)*G(3,1)-A(4)*G(4,1)
-A(5)*G(5,1)-A(6)*G(6,1)
UDISPL(+1)=UDISP(L+1)/DIVS
B(1)=H(1)
B(2)=H(2)
B(3)=H(3)
B(4)=H(4)
I=1
M=3
UIVS=1,
UJ TU 51
95 A(1)=-B(1)*G(1,1)-B(3)*G(4,1)+B(4)*G(5,1)
A(2)=-B(1)*G(1,2)-B(3)*G(4,2)+B(4)*G(5,2)
A(3)=-B(1)*G(1,3)-B(3)*G(4,3)-B(4)*G(5,3)
A(4)=-B(1)*G(1,4)+B(3)*G(4,4)-B(4)*G(5,4)
A(5)=-B(1)*G(1,5)-B(3)*G(4,5)+B(4)*G(5,5)
A(6)=-B(1)*G(1,6)-B(3)*G(4,6)+B(4)*G(5,6)
UJ 8019 J=1,6
B(J)=A(J)
8019 CONTINUE
M=4
I=1-1
UJ TU 51
96 IFL(-1) 97,97,98
95 U(1,J)=G(1,1)
U(1,4)=G(1,4)
U(2,3)=G(2,3)
U(2,4)=G(2,4)
U(3,1)=G(3,1)
U(3,2)=G(3,2)
U(3,5)=G(3,5)
U(3,6)=G(3,6)
U(4,1)=G(4,1)
U(4,2)=G(4,2)
U(4,5)=G(4,5)
U(4,6)=G(4,6)
U(5,3)=G(5,3)
U(5,4)=G(5,4)
U(6,3)=G(6,3)
U(6,4)=G(6,4)
UJ 8020 J=1,6
SJMU,
UJ 8021 K=1,6
SJMSUM=B(K)*G(K,J)
8021 UJ /I4UE
A(J)=SUM
8020 CONTINUE
UJ 8022 J=1,6
H(J)=A(J)/DIVS
8022 CONTINUE
I=-1
UJ TU 51
97 WDISP(L+1)=-A(1)*U(1,1)-A(2)*U(2,1)+A(3)*U(3,1)+A(4)*U(4,1)

```

```

1=A(5)*G(5,1)-A(6)*G(6,1)
W0ISPL(L+1)= W0ISP(L+1)/DIVS
B(1)=E(5)
B(2)=E(6)
B(3)=E(7)
B(4)=E(8)
L=L
L=L-1
L_=L
GO TO 8001
8025 X<=RUDTS(M, 1)+DELK
I=N2
I=N2
I=N2
I=N2
C= CMAX-DELC
2000 PRINT 1030,M,TOTAL
1030 FORMAT(6H-MODE I3 /19H SECTION THICKNESS F8.2 //11X, 15H PHASE VEL
1031 1U,1T,4X,2H K, 8X,10H PERIOD(S),4X,15H GROUP VELOCITY,8X,10H PERIOD
1U(S))
Y(I,N) 1031,CMAX,RDOTS(M,1),PERIOD(M,1)
1031 FFORMAT(12X,F10.4,3X,F10.5,4X,F10.4)
GO TO 500
301 IF(|NDX2-1|) 502,501,502
501 I=NUX2 = 10
X<1XX
F1=F
XK =XK + DELK
GO TO 100
502 AF=ABS(F)
AF=ABS(F1)
IF(AF-AF1) 504,503,503
503 I=ABS(F1-F) -AF) 507,506,506
504 I=ABS(F1-F)-AF1)507,506,506
505 I=ABS(XK1-XK)-XMIN)508,508,610
507 I=|BRAC-1| 508,706,513
513 I=(AF-AF1) 510,510,511
511 I=(UP-1) 2004,2004,510
2004 I=(UP1-1) 2006,2006,2005
2005 X<1XX
F1=F
GO TO 2006
2005 I=N4=-1,
X<=XK-2,+ DELK
I=N1=10
I=|XK-RDOTS(M,N-1)) 2002,2002,60
2002 X<=RUDTS(M,N-1)
I=N1=10
I=N1=1,
GO TO 500
510 X<1XX
F1=F
XK=XK+DELK+SIGN
I=(XK-RDOTS(M,N-1)) 2002,2002,60
60 I=(XK-XKMAX) 100,100,520
504 I=|BRAC-10| 709,710,710
710 F2=F1
X<2XX
707 F1=F
XK= ABS((XK2+F1-XK+F2)/(F1+F2))
I=(PTNB-1)530,529,530
529 RDOTS(M,N)=XK
PERIOD(M,N)=(2.*3.1416)/(XK*C)
I0ISM=10
IJMP=2
I_=1
GO TO 8000
901 I=(PTNB -1)531,528,531
528 C=C-PTRC
I=(C-CMIN)520,520,546
546 I=(N-3)532,533,533
534 X<= RDOTS(M,N)
I=N1=10
I=N1=1
I=|XK-XKMAX) 500,500,61
533 X<1= RDOTS(M,N-2)
X<3=RDOTS(M,N)
A<2=RDOTS(M,N-1)
C1= CMAX1-C
D1= -(XK3-XK1)/(2.*DELC)
D2=(A<3 -2.*XK2 +XK1)/DELC**2
X< A1=D1+C1 +(D2*C1*(C1-DELC))/2,
I=N1=10
I=N1=1
I=|XK-XKMAX) 500,500,61
531 C=C-DELC
I=N1=1
I=(C-CMIN)520,521,521
521 I=(N-3) 522,523,523
522 X<=RUDTS(M,N)+.5*(RDOTS(M,N)-RDOTS(M,N-1))
I=N1=N+1
I=N1=1
I=|XK-XKMAX)500,500,520
523 X<1=RDOTS(M,N-2)
X<2=RDOTS(M,N-1)
X<3=RDOTS(M,N)
C1=CMAX1-C
CMAX1 =CMAX1-DELC
D1= -(XK3-XK1)/(2.*DELC)
D2= (XK3 -2.*XK2 +XK1)/ DELC **2
I=N1=N+1
X< A1=D1+C1 +(D2*C1*(C1-DELC))/2,
I=N1=1
I=|XK-XKMAX)500,500,520
520 I=(M-MODE(NMODE))524,525,525
524 I=OD=I*OD+1
NEWRUD = 1

```

```

14=MUD (IMUD)
A<#MUD>S(IM,1)
A<MINx,.01*XX
A<MAX=10.*ROOTS(IM,1)
I>IRH=1
CMAX=CMAX
C=CMAX
ID:SP=10
IL=1
IJHP=3
IV=1
IX=NAYER-1
IDIAL=THICK
GO TU 0000
8026 C=CMAX-DELC
IV=2
IX=NAYER-1
ID=1
GO TU 2000
530 W1=RUDTS(IM,IN)*(C+PTRBC)
W2=YR=C
U< RUDTS(IM,IN) -XK
Nz=(N2-N1)/DK
C=C+PTRBC
I3HR=2,+3.1416/((N2-N1)/2.+N1)
I>IRH=1
X<MAX=RUDTS(IM,IN)+10.,*(RUDTS(IM,IN)-RUDTS(IH,IN-1))
X<INx,.01*RUDTS(IM,IN)
PRIN/ 1020,C,RUDTS(IM,IN),PERIOD(IM,IN),R,TGR
1020 FOMMAT(12X,F10.4,3X,F10.5,4X,F10.4,6X,F10.4,12X,F10.4)
GO TU 531
61 C=C+PTRBC
PRINI 1031,C,RUDTS(IM,IN),PERIOD(IM,IN)
GO TU 520
529 MJNCM 2701,IPUN
PAUSE 7
HEAD 350,IPUN
UD 556 I=1,IPUN
HEAD 2701,MODEL,IM,L,TOTAL,C,PERIOD(1,1)
HEAD 1032,(UDISP(J),WDISP(J),J=1,L)
PRINI 557,MODEL,IM,C,PERIOD(1,1),TOTAL
557 FOMMAT(104-MODEL RTI 14 /, 5H MODE 14/, 15H PHASE VELDCITY F8.3 /,
1 7H PERIOD F9.3/, .22H SECTION )WICKNESS(KH) F9.3 // )
PRINI 2703
2703 FOMMAT ( 52H DISPLACEMENTS AT LAYER INTERFACES NORMALIZED TO THE
151M VERTICAL DISPLACEMENT AT THE SURFACE (INTERFACE 0) / )
PRINI 2704
2704 FOMMAT(104 INTERFACE ,5X,13H HORIZ. DISP.,5X,12H VERT. DISP.)
UD 556 J=0,L-1
PRINI 556 ,J,UDISP(J+1),WDISP(J+1)
556 FOMMAT (5X,13,11X,E13.6,9X,E13.6)
PRINI 1024
1024 FOMMAT (19H END OF COMPUTATION )
PAUSE
END

```

INPUT DATA AND FORMAT FOR STRESS

<u>CARD</u>	<u>FORMA.</u>	<u>DATA DESCRIPTION</u>
1	I5	No. of layers in model
	I5	No. of (c,k) pairs for which modal shape is to be computed
2	8F10.4	Layer parameters stored in sequence, α, β, ρ, d ; two layers to a card
3	E13.6	c
	E13.6	k
	E13.6	Horizontal to vertical surface dis- placement ratio, $\frac{u_o}{w_o}$

Repeat card 3 for each set of c,k, $\frac{u_o}{w_o}$.

```

      C PROGRAM STRESS.          J.W.DUNN   GU-163
  5.0001  DIMENSION ALFA$50<,BETA$50<,D$50).HH0450<,LAMBDAM$0<,AN$4,4<,
  1 MU$50)
  5.0002  REAL LAMBDA,MU
  5.0003  DOUBLE PRECISION AN,WATIO,SINQ,UDOT,WDOT,X,Y,PW,QW,HALFAN
  5.0004  ICOSH,COSQH,SINPH,SIQPH,UDOT,WDOT,WDTN,X,Y,PW,QW,HALFAN
  5.0005  DOUBLE PRECISION DXIPP,DXIPP,DXPQW,DXCIPQ,DXCIPQ,HBET1N,ON1,HNC2,ALPA
  5.0006  DOUBLE PRECISION RHO,NON,PERIOD
  5.0007  DOUBLE E PRECISION C,ALPHA,BETA,K,D,DM,OAENAM,TESTER,C$QARE
  5.0008  DOUBLE PRECISION MMHAT44<, OLDPAT44<
  5.0009  1966 CONTINUE
  5.0009  READ(1,1) LAYENS,NCASES
  C NCASES IS THE NUMBER OF CASES OF C,K,RATIO FOR A GIVEN SET OF
  C LAYER PARAMETERS, ALPHA, BETA, RHO, D.
  5.0010  561 HEAD$1,1<(ALPA$4<,BETA$4<,RHO(I),D(I) , Y = 1, LAYENS)
  5.0011  WRITE(3,1) (ALPA(I),BETA(I),RHO(I),D(I),I=1,LAYENS)
  5.0012  1 FORMAT(1P10.4)
  5.0013  1 FORMAT(2T5)
  5.0014  KWHITE = LAYERS - 1
  5.0015  DO 200 LD=1,NCASES
  5.0016  HEAD$1,2<K,NATIO
  5.0017  C$QARE = C$C
  5.0018  PERIOD = 6.2811963072/4K$C
  5.0019  UDOT=MMAT
  5.0020  WDOT=0.0
  5.0021  OLDMAT = 0< UDOT
  5.0022  OLDMAT = 0< WDOT
  5.0023  2 FORMAT(4I13.6C
  5.0024  WRITE(3,9<C,PERIOD
  5.0025  3 FORMAT(4I11,5I,15PHASE-VELOCITY$,E20.12,/,5X,7HPERIOD$,5X,E20.12,
  1//,10X,4HINTERPACE,1X,10X,12HMORIZ.DISP.,8I,10X,11HVENT.DISP.,/C
  5.0026  380
  5.0027  487TP 43,10$M,DDOT,WDOT
  5.0028  10 704TP410X,2X,15,7X,1X,6X,E20.12,6X,E20.12<
  5.0029  DO 100 491,LAYERS
  5.0030  491K$C$BPF$4NC **2 + RHO$NC
  5.0031  LAMBDA$4< RHO$NC * HALPA$4<**2-2.0*HBETAN$**2<
  5.0032  100 CONTINUE
  5.0033  1201 SIG$0$0.
  5.0034  1202 TAU$0$0.
  5.0035  1201 OLDMAT = 0< SIGU
  5.0036  1204 OLDMAT = 0< TAUH
  5.0037  1205 DO 200 N = 1, KWHITE
  5.0038  200 N1 = N + 1
  5.0039  1207 ALPA = HALPA$NC
  5.0040  1208 BON = RHO$NC
  5.0041  1209 BATEA = BETA$NC
  5.0042  1210 DM = D$NC
  5.0043  1211 X=DABS((C/ALPA)**2-1.)
  5.0044  1212 Y = DABS((C/BATEA)**2-1.)
  5.0045  1213 RALFAN = DSQRT(X)
  5.0046  1214 HBETAN = DSQRT(Y)
  5.0047  1215 GAMMAN = 2.*$BATEA/CC**2

  5.0048  1216 PW = K * RALFAN * DM
  5.0049  1217 QJ = K * R$BETA$4 * DM
  5.0050  1218 TESTER = C-ALPHA
  5.0051  1219 TP = (C-ALPHA) 225,220,220
  5.0052  220 COSPM = DCOS(TP)
  5.0053  221 S$MPM = DSIN(TP)
  5.0054  222 APASYN=1.0
  5.0055  GO TO 230
  5.0056  225 DXIPP = DEXP$PM
  5.0057  RECIPP = 1.0/DEXPPM
  5.0058  COSPM = $DEXPPM * RECIPP/2.0
  5.0059  SINPM = $DEXPPM-RECIPP/2.0
  5.0060  APASIN=1.0
  5.0061  230 CONTINUE
  5.0062  TESTER = C - BATEA
  5.0063  IP (C-BALPA) 231,237,237
  5.0064  231 DEXPON$DZEF$4NC
  5.0065  RECIP0 = 1.0/DEXPON
  5.0066  COSPM = $DEXPON * RECIP0/2.0
  5.0067  SINPM = $DEXPON-RECIP0/2.0
  5.0068  APASIN=1.0
  5.0069  GO TO 239
  5.0070  232 SINOM = DSIN$PM
  5.0071  COSOM = DCOS(TP)
  5.0072  233 CONTINUE
  5.0073  GR1 = GAMMAN-1.
  5.0074  PM$2 = RHO(M)*CSQARE
  5.0075  1111 AN$1,1C = GAMMAN COSPM-GH1*COSOM
  5.0076  1112 AN$1,2C = SINPM/RALFAN & GAMMAN * HBETAN + SINOM*BETASYNC
  5.0077  1113 AN$1,3C = -COSPM - COSOM / HNC2
  5.0078  1114 AN$1,4C = -T$INPM/RALFAN & HBETAN + SINOM*BETASYNC / HNC2
  5.0079  1115 AN$2,1C = -GAMMAN + RALFAN + SINPM * APASYN & GH1 / HBETAN * SINOM
  5.0080  1116 AN$2,2C = -GH1*COSPM + GAMMAN * COSOM
  5.0081  1117 AN$2,3C = RALFAN + SINPM * APASIN & SINPM / HBETAN / HNC2
  5.0082  1118 AN$2,4C = AN$1,3C
  5.0083  1119 AN$2,1C = PM$2 * GAMMAN + GH1 * SCOSPM - COSOM
  5.0084  1120 A = 1,2C = PM$2 * GH1 * SINPM / RALFAN & GAMMAN **2 + HBETAN
  1*HNC2
  5.0085  1121 AN$3,1C = AN$2,2C
  5.0086  1122 AN$3,2C = AN$1,2C
  5.0087  1123 AN$3,4C = AN$1,2C
  5.0088  1124 AN$4,1C = AN$1,1C
  5.0089  WRITE(1,1030)
  5.0090  1030 FORMAT(' MATRIX OF A-B.    ')
  5.0091  DO 101 M=1,4
  5.0092  1011 WRITE(1,1111) (AN(M$1,L),L=1,4)
  5.0093  1111 FORMAT(5X,E20.12)
  5.0094  DO 102 N=1,4
  5.0095  1021 WRITE(1,1111) (AN(M$1,L),L=1,4)
  5.0096  1111 FORMAT(5X,E20.12)
  5.0097  DO 103 M=1,4
  5.0098  1031 WRITE(1,1111) (AN(M$1,L),L=1,4)
  5.0099  1111 FORMAT(5X,E20.12)
  5.0100  1041 M$1=M+1
  5.0101  1042 M$1=M+1
  5.0102  1043 M$1=M+1
  5.0103  1044 M$1=M+1
  5.0104  1045 M$1=M+1
  5.0105  1046 M$1=M+1
  5.0106  1047 M$1=M+1
  5.0107  1048 M$1=M+1
  5.0108  1049 M$1=M+1
  5.0109  1050 M$1=M+1
  5.0110  1051 M$1=M+1
  5.0111  1052 M$1=M+1
  5.0112  1053 M$1=M+1
  5.0113  1054 M$1=M+1
  5.0114  1055 M$1=M+1
  5.0115  1056 M$1=M+1
  5.0116  1057 M$1=M+1
  5.0117  1058 M$1=M+1
  5.0118  1059 M$1=M+1
  5.0119  1060 M$1=M+1
  5.0120  1061 M$1=M+1
  5.0121  1062 M$1=M+1
  5.0122  1063 M$1=M+1
  5.0123  1064 M$1=M+1
  5.0124  1065 M$1=M+1
  5.0125  1066 M$1=M+1
  5.0126  1067 M$1=M+1
  5.0127  1068 M$1=M+1
  5.0128  1069 M$1=M+1
  5.0129  1070 M$1=M+1
  5.0130  1071 M$1=M+1
  5.0131  1072 M$1=M+1
  5.0132  1073 M$1=M+1
  5.0133  1074 M$1=M+1
  5.0134  1075 M$1=M+1
  5.0135  1076 M$1=M+1
  5.0136  1077 M$1=M+1
  5.0137  1078 M$1=M+1
  5.0138  1079 M$1=M+1
  5.0139  1080 M$1=M+1
  5.0140  1081 M$1=M+1
  5.0141  1082 M$1=M+1
  5.0142  1083 M$1=M+1
  5.0143  1084 M$1=M+1
  5.0144  1085 M$1=M+1
  5.0145  1086 M$1=M+1
  5.0146  1087 M$1=M+1
  5.0147  1088 M$1=M+1
  5.0148  1089 M$1=M+1
  5.0149  1090 M$1=M+1
  5.0150  1091 M$1=M+1
  5.0151  1092 M$1=M+1
  5.0152  1093 M$1=M+1
  5.0153  1094 M$1=M+1
  5.0154  1095 M$1=M+1
  5.0155  1096 M$1=M+1
  5.0156  1097 M$1=M+1
  5.0157  1098 M$1=M+1
  5.0158  1099 M$1=M+1
  5.0159  1100 M$1=M+1
  5.0160  1101 M$1=M+1
  5.0161  1102 M$1=M+1
  5.0162  1103 M$1=M+1
  5.0163  1104 M$1=M+1
  5.0164  1105 M$1=M+1
  5.0165  1106 M$1=M+1
  5.0166  1107 M$1=M+1
  5.0167  1108 M$1=M+1
  5.0168  1109 M$1=M+1
  5.0169  1110 M$1=M+1
  5.0170  1111 M$1=M+1
  5.0171  1112 M$1=M+1
  5.0172  1113 M$1=M+1
  5.0173  1114 M$1=M+1
  5.0174  1115 M$1=M+1
  5.0175  1116 M$1=M+1
  5.0176  1117 M$1=M+1
  5.0177  1118 M$1=M+1
  5.0178  1119 M$1=M+1
  5.0179  1120 M$1=M+1
  5.0180  1121 M$1=M+1
  5.0181  1122 M$1=M+1
  5.0182  1123 M$1=M+1
  5.0183  1124 M$1=M+1
  5.0184  1125 M$1=M+1
  5.0185  1126 M$1=M+1
  5.0186  1127 M$1=M+1
  5.0187  1128 M$1=M+1
  5.0188  1129 M$1=M+1
  5.0189  1130 M$1=M+1
  5.0190  1131 M$1=M+1
  5.0191  1132 M$1=M+1
  5.0192  1133 M$1=M+1
  5.0193  1134 M$1=M+1
  5.0194  1135 M$1=M+1
  5.0195  1136 M$1=M+1
  5.0196  1137 M$1=M+1
  5.0197  1138 M$1=M+1
  5.0198  1139 M$1=M+1
  5.0199  1140 M$1=M+1
  5.0200  1141 M$1=M+1
  5.0201  1142 M$1=M+1
  5.0202  1143 M$1=M+1
  5.0203  1144 M$1=M+1
  5.0204  1145 M$1=M+1
  5.0205  1146 M$1=M+1
  5.0206  1147 M$1=M+1
  5.0207  1148 M$1=M+1
  5.0208  1149 M$1=M+1
  5.0209  1150 M$1=M+1
  5.0210  1151 M$1=M+1
  5.0211  1152 M$1=M+1
  5.0212  1153 M$1=M+1
  5.0213  1154 M$1=M+1
  5.0214  1155 M$1=M+1
  5.0215  1156 M$1=M+1
  5.0216  1157 M$1=M+1
  5.0217  1158 M$1=M+1
  5.0218  1159 M$1=M+1
  5.0219  1160 M$1=M+1
  5.0220  1161 M$1=M+1
  5.0221  1162 M$1=M+1
  5.0222  1163 M$1=M+1
  5.0223  1164 M$1=M+1
  5.0224  1165 M$1=M+1
  5.0225  1166 M$1=M+1
  5.0226  1167 M$1=M+1
  5.0227  1168 M$1=M+1
  5.0228  1169 M$1=M+1
  5.0229  1170 M$1=M+1
  5.0230  1171 M$1=M+1
  5.0231  1172 M$1=M+1
  5.0232  1173 M$1=M+1
  5.0233  1174 M$1=M+1
  5.0234  1175 M$1=M+1
  5.0235  1176 M$1=M+1
  5.0236  1177 M$1=M+1
  5.0237  1178 M$1=M+1
  5.0238  1179 M$1=M+1
  5.0239  1180 M$1=M+1
  5.0240  1181 M$1=M+1
  5.0241  1182 M$1=M+1
  5.0242  1183 M$1=M+1
  5.0243  1184 M$1=M+1
  5.0244  1185 M$1=M+1
  5.0245  1186 M$1=M+1
  5.0246  1187 M$1=M+1
  5.0247  1188 M$1=M+1
  5.0248  1189 M$1=M+1
  5.0249  1190 M$1=M+1
  5.0250  1191 M$1=M+1
  5.0251  1192 M$1=M+1
  5.0252  1193 M$1=M+1
  5.0253  1194 M$1=M+1
  5.0254  1195 M$1=M+1
  5.0255  1196 M$1=M+1
  5.0256  1197 M$1=M+1
  5.0257  1198 M$1=M+1
  5.0258  1199 M$1=M+1
  5.0259  1200 M$1=M+1
  5.0260  1201 M$1=M+1
  5.0261  1202 M$1=M+1
  5.0262  1203 M$1=M+1
  5.0263  1204 M$1=M+1
  5.0264  1205 M$1=M+1
  5.0265  1206 M$1=M+1
  5.0266  1207 M$1=M+1
  5.0267  1208 M$1=M+1
  5.0268  1209 M$1=M+1
  5.0269  1210 M$1=M+1
  5.0270  1211 M$1=M+1
  5.0271  1212 M$1=M+1
  5.0272  1213 M$1=M+1
  5.0273  1214 M$1=M+1
  5.0274  1215 M$1=M+1
  5.0275  1216 M$1=M+1
  5.0276  1217 M$1=M+1
  5.0277  1218 M$1=M+1
  5.0278  1219 M$1=M+1
  5.0279  1220 M$1=M+1
  5.0280  1221 M$1=M+1
  5.0281  1222 M$1=M+1
  5.0282  1223 M$1=M+1
  5.0283  1224 M$1=M+1
  5.0284  1225 M$1=M+1
  5.0285  1226 M$1=M+1
  5.0286  1227 M$1=M+1
  5.0287  1228 M$1=M+1
  5.0288  1229 M$1=M+1
  5.0289  1230 M$1=M+1
  5.0290  1231 M$1=M+1
  5.0291  1232 M$1=M+1
  5.0292  1233 M$1=M+1
  5.0293  1234 M$1=M+1
  5.0294  1235 M$1=M+1
  5.0295  1236 M$1=M+1
  5.0296  1237 M$1=M+1
  5.0297  1238 M$1=M+1
  5.0298  1239 M$1=M+1
  5.0299  1240 M$1=M+1
  5.0300  1241 M$1=M+1
  5.0301  1242 M$1=M+1
  5.0302  1243 M$1=M+1
  5.0303  1244 M$1=M+1
  5.0304  1245 M$1=M+1
  5.0305  1246 M$1=M+1
  5.0306  1247 M$1=M+1
  5.0307  1248 M$1=M+1
  5.0308  1249 M$1=M+1
  5.0309  1250 M$1=M+1
  5.0310  1251 M$1=M+1
  5.0311  1252 M$1=M+1
  5.0312  1253 M$1=M+1
  5.0313  1254 M$1=M+1
  5.0314  1255 M$1=M+1
  5.0315  1256 M$1=M+1
  5.0316  1257 M$1=M+1
  5.0317  1258 M$1=M+1
  5.0318  1259 M$1=M+1
  5.0319  1260 M$1=M+1
  5.0320  1261 M$1=M+1
  5.0321  1262 M$1=M+1
  5.0322  1263 M$1=M+1
  5.0323  1264 M$1=M+1
  5.0324  1265 M$1=M+1
  5.0325  1266 M$1=M+1
  5.0326  1267 M$1=M+1
  5.0327  1268 M$1=M+1
  5.0328  1269 M$1=M+1
  5.0329  1270 M$1=M+1
  5.0330  1271 M$1=M+1
  5.0331  1272 M$1=M+1
  5.0332  1273 M$1=M+1
  5.0333  1274 M$1=M+1
  5.0334  1275 M$1=M+1
  5.0335  1276 M$1=M+1
  5.0336  1277 M$1=M+1
  5.0337  1278 M$1=M+1
  5.0338  1279 M$1=M+1
  5.0339  1280 M$1=M+1
  5.0340  1281 M$1=M+1
  5.0341  1282 M$1=M+1
  5.0342  1283 M$1=M+1
  5.0343  1284 M$1=M+1
  5.0344  1285 M$1=M+1
  5.0345  1286 M$1=M+1
  5.0346  1287 M$1=M+1
  5.0347  1288 M$1=M+1
  5.0348  1289 M$1=M+1
  5.0349  1290 M$1=M+1
  5.0350  1291 M$1=M+1
  5.0351  1292 M$1=M+1
  5.0352  1293 M$1=M+1
  5.0353  1294 M$1=M+1
  5.0354  1295 M$1=M+1
  5.0355  1296 M$1=M+1
  5.0356  1297 M$1=M+1
  5.0357  1298 M$1=M+1
  5.0358  1299 M$1=M+1
  5.0359  1300 M$1=M+1
  5.0360  1301 M$1=M+1
  5.0361  1302 M$1=M+1
  5.0362  1303 M$1=M+1
  5.0363  1304 M$1=M+1
  5.0364  1305 M$1=M+1
  5.0365  1306 M$1=M+1
  5.0366  1307 M$1=M+1
  5.0367  1308 M$1=M+1
  5.0368  1309 M$1=M+1
  5.0369  1310 M$1=M+1
  5.0370  1311 M$1=M+1
  5.0371  1312 M$1=M+1
  5.0372  1313 M$1=M+1
  5.0373  1314 M$1=M+1
  5.0374  1315 M$1=M+1
  5.0375  1316 M$1=M+1
  5.0376  1317 M$1=M+1
  5.0377  1318 M$1=M+1
  5.0378  1319 M$1=M+1
  5.0379  1320 M$1=M+1
  5.0380  1321 M$1=M+1
  5.0381  1322 M$1=M+1
  5.0382  1323 M$1=M+1
  5.0383  1324 M$1=M+1
  5.0384  1325 M$1=M+1
  5.0385  1326 M$1=M+1
  5.0386  1327 M$1=M+1
  5.0387  1328 M$1=M+1
  5.0388  1329 M$1=M+1
  5.0389  1330 M$1=M+1
  5.0390  1331 M$1=M+1
  5.0391  1332 M$1=M+1
  5.0392  1333 M$1=M+1
  5.0393  1334 M$1=M+1
  5.0394  1335 M$1=M+1
  5.0395  1336 M$1=M+1
  5.0396  1337 M$1=M+1
  5.0397  1338 M$1=M+1
  5.0398  1339 M$1=M+1
  5.0399  1340 M$1=M+1
  5.0400  1341 M$1=M+1
  5.0401  1342 M$1=M+1
  5.0402  1343 M$1=M+1
  5.0403  1344 M$1=M+1
  5.0404  1345 M$1=M+1
  5.0405  1346 M$1=M+1
  5.0406  1347 M$1=M+1
  5.0407  1348 M$1=M+1
  5.0408  1349 M$1=M+1
  5.0409  1350 M$1=M+1
  5.0410  1351 M$1=M+1
  5.0411  1352 M$1=M+1
  5.0412  1353 M$1=M+1
  5.0413  1354 M$1=M+1
  5.0414  1355 M$1=M+1
  5.0415  1356 M$1=M+1
  5.0416  1357 M$1=M+1
  5.0417  1358 M$1=M+1
  5.0418  1359 M$1=M+1
  5.0419  1360 M$1=M+1
  5.0420  1361 M$1=M+1
  5.0421  1362 M$1=M+1
  5.0422  1363 M$1=M+1
  5.0423  1364 M$1=M+1
  5.0424  1365 M$1=M+1
  5.0425  1366 M$1=M+1
  5.0426  1367 M$1=M+1
  5.0427  1368 M$1=M+1
  5.0428  1369 M$1=M+1
  5.0429  1370 M$1=M+1
  5.0430  1371 M$1=M+1
  5.0431  1372 M$1=M+1
  5.0432  1373 M$1=M+1
  5.0433  1374 M$1=M+1
  5.0434  1375 M$1=M+1
  5.0435  1376 M$1=M+1
  5.0436  1377 M$1=M+1
  5.0437  1378 M$1=M+1
  5.0438  1379 M$1=M+1
  5.0439  1380 M$1=M+1
  5.0440  1381 M$1=M+1
  5.0441  1382 M$1=M+1
  5.0442  1383 M$1=M+1
  5.0443  1384 M$1=M+1
  5.0444  1385 M$1=M+1
  5.0445  1386 M$1=M+1
  5.0446  1387 M$1=M+1
  5.0447  1388 M$1=M+1
  5.0448  1389 M$1=M+1
  5.0449  1390 M$1=M+1
  5.0450  1391 M$1=M+1
  5.0451
```

```

S.0101      DD 8889 KXY # 1,4
S.0102      MODKXY # MODKXY,2C
S.0103      NFEXP # NTMP1#MODKXY
S.0104      NFAC # 3-1<**NFEXP
S.0105      PAC # FLOATSHPACK
S.0106      NFVROTATINPC<PAC>ANKINPC,KEY<OLDNAT<KEY<&NEWNATINPC
S.0107      4998 CONTINUE
S.0108      UOOTM # RENNAT $1C
S.0109      UOOTM # EMMAT $2C
S.0110      WRITR $1,10CH,UOOTM,UOOTM
S.0111      00 8889 KLJ # 1,4
S.0112      8889 OLDNAT SKLJC # RENNAT SKLJC
S.0113      200 CONTINUE
S.0114      GO TO 1961
S.0115      ENO

```

STORAGE MAP VARIABLES (TAOS: C=COMMON, Z=EQUIVALENCE)

NAME	TAG	REL ADR	NAME	TAG	REL ADR	NAME	TAG	REL ADR	NAME	TAG	REL ADR
X		000158	X		000219	Y		0002P0	C		0002PB
Z		000300	AM		000308	PW		000388	QW		000390
W		000398	MHO		0003A0	ON1		000530	MOM		000536
BETA		000540	BETA		000600	SIGU		000860	TA00		000868
W4W0		000870	W4W0		000878	UOOT		000880	NDOT		000888
RATIO		000940	RATIO		000898	WWON1		0008A0	COSPN		0008A8
SINQ		000980	SINQ		0008B8	SINQN		0008C0	UOOTM		0008C8
ALPHA		000990	ALPHA		000880	BATEA		0008E0	NEWSIO		0008E8
RALPH		0009F0	RALPH		0008FA	OZIPP		000900	RECIPIP		000908
RECIP		000910	RECIP		000918	WBZAM		000920	PERIOD		000928
TESTPR		000930	TESTPR		000938	C/SQARE		000940	RENNAT		000948
I		000968	I		000988	Y		00098C	L		000990
10		000994	10		000A5C	M1		000A60	MK		000A68
KXY		000A68	KXY		000A6C	PAC		000A70	KLJ		000A74
NFAC		000A79	NFAC		000A7C	KWITH		000A80	MIMP1		000A84
LAYERS		000A89	LAYERS		000B50	NCASES		000B54	APASYN		000B58
MODTMP		000B5C	MODTMP		000B60	MODKXY		000B64			

EXTERNAL REFERENCES

NAME	REL ADR	NAME	REL ADR	NAME	REL ADR
	000864	DCOS	00086C	DSIN	000870
	000874			000878	OEZF

CONSTANTS

NAME	REL ADR	NAME	REL ADR	NAME	REL ADR
	000880	00000000	0008B4	00000002	0008B8
	0008C0	00000000	000BC4	416487D51121B7P	000RC8
	0008D8			41100000	00089C

IMPLIED EXTERNAL REFERENCES

INPUT DATA AND FORMAT FOR INTEGRAL

<u>CARD</u>	<u>FORMAT</u>	<u>DATA DESCRIPTION</u>
1	I10	No. of layers in model
	F10.4	Factor for singular matrix criteria in curve fitting subroutine, generally $\approx .99$.
	I10	degree+1 of the polynomial fit to the displacement data
	I10	Read option; 1 if read every set of displacements; 0 if read every other set
2	8F10.6	Layer parameters stored in sequence α, β, ρ, d ; two layers to a card
3	20A4	Text identification ≤ 80 characters
4	I4	Model identification no.
	I4	Mode no.
	I4	No. of layers
	F9.3	Total section thickness
	F9.3	Phase velocity in km/s
	F9.3	Period in sec
5	6E13.6	Displacements stored in pair sequence $v_1, w_1, u_2, w_2 \dots ; 3$ pairs to a card

For computations involving more than one set of displacements corresponding to a (α, T) pair, repeat cards 4 & 5 for each set.

FIGURE : 111766

IBM 03/360 BASIC FORTRAN IV (E) COMPILATION

DATE: 06.11.9

S.00176 DO 231 100START, XTOP
 S.00177 XL = 71
 S.00178 ASKLS = LSF2CZ223X2, NLCSUSSLIC
 S.00179 BNZC = BNZ2CZ223X2, NLCSUSSLIC
 S.00180 210 CONTINUE
 S.00181 220 CONTINUE
 C THE COEFFICIENTS OF DU/DZ DPMC
 C THE COEFFICIENTS OF DU/DZ DPMC
 C N= 1 DEGREE OF "U"
 C U = 1X1C0Z00TH4CA42C02000044-1C6...5A8H1*28A8H81C, SH81C TERMS
 C U=02 = 1X1C0Z00020H4C6C82C03*0020H-1C6...5C82*HHC*EHC82*H81C,
 C 42H81C TRMS.
 S.00182 THOM1 = 82*PMCS1
 S.00183 DO 91 TR = 1,7M0451
 S.00184 BNTRC = 0.0
 S.00185 LTRC = 0.0
 S.00186 IRI = TRA1
 S.00187 DO 90 M = 1,TR
 S.00188 N = TR1 - MN
 S.00189 BNTRC = DTRCABSRPC19HIC
 S.00190 CTRC = CTTRCABSRPC19HIC
 S.00191 90 CONTINUE
 C THE COEFFICIENTS OF DU/DZ UPBIMHC
 C THE COEFFICIENTS OF DU/DZ UPBIMHC
 C N=1 = 1 DEGREE OF DU/DZ
 C M=0 = 1 DEGREE OF DU/DZ 61, FOR INDEXING
 C DU00 = 4PMARIC0Z000044-1C6444-1C042C0200044-2C6...520A844-1C02Z
 C ABP81C TERMS
 C UPBIMHC = SH81-MC0A84C, V81,2,...,HH.HH81 = H81.
 S.00192 DO 18 V81,44
 S.00193 V81 = 1CAT0441-HC
 S.00194 UPBIMHC = V810A8HC
 S.00195 UPBIMHC = X44108HC
 S.00196 91 CONTINUE
 C THE COEFFICIENTS OF DU/DZ UPBIM2
 C THE COEFFICIENTS OF DU/DZ UPBIM2
 C THE COEFFICIENTS OF DU/DZ UPBIM2
 C N=1 = 1 DEGREE OF DU/DZ
 C 2N=1 = 1 DEGREE OF "DU/DZ<002"
 C X1101 = 2584-1601, FOR INDEXING
 C DU00 = UPBIM441C0Z00H-1C0UPBIM42C47884-2C 6 - SUPBIMHC, M8 TRMS
 C DU00 = DU00Z0000 = 2444-1C,61 FOR INDEXING.
 S.00197 THOM1 = 24441
 S.00198 M101 = 24444-1C61
 S.00199 M1 = 44121 = 1
 S.00200 DO 37 M = 1,44
 S.00201 MTRC = 0.0
 S.00202 U237M23TLC = 0.0
 S.00203 U237M23TLC = 0.0
 S.00204 U237M23TLC = 0.0
 S.00205 U237M23TLC = 0.0
 S.00206 IRI = TRA1
 S.00207 DO 97 M = 1,44
 S.00208 N = TR1 - MN
 S.00209 BNTRC = DTRCABSRPC19HIC
 S.00210 CTRC = CTTRCABSRPC19HIC
 S.00211 UPBIM441C = 1CAT0441-HCUPBIM441C
 S.00212 UPBIM441C = 1CAT0441-HCUPBIM441C
 S.00213 92 CONTINUE
 C 1121 = 1121
 C 1122 = 1122
 C 1123 = 1123
 C 1124 = 1124
 C 1125 = 1125
 C 1126 = 1126
 C 1127 = 1127
 C 1128 = 1128
 C 1129 = 1129
 C 1130 = 1130
 C 1131 = 1131
 C 1132 = 1132
 C 1133 = 1133
 C 1134 = 1134
 C 1135 = 1135
 C 1136 = 1136
 C 1137 = 1137
 C 1138 = 1138
 C 1139 = 1139
 C 1140 = 1140
 C 1141 = 1141
 C 1142 = 1142
 C 1143 = 1143
 C 1144 = 1144
 C 1145 = 1145
 C 1146 = 1146
 C 1147 = 1147
 C 1148 = 1148
 C 1149 = 1149
 C 1150 = 1150
 C 1151 = 1151
 C 1152 = 1152
 C 1153 = 1153
 C 1154 = 1154
 C 1155 = 1155
 C 1156 = 1156
 C 1157 = 1157
 C 1158 = 1158
 C 1159 = 1159
 C 1160 = 1160
 C 1161 = 1161
 C 1162 = 1162
 C 1163 = 1163
 C 1164 = 1164
 C 1165 = 1165
 C 1166 = 1166
 C 1167 = 1167
 C 1168 = 1168
 C 1169 = 1169
 C 1170 = 1170
 C 1171 = 1171
 C 1172 = 1172
 C 1173 = 1173
 C 1174 = 1174
 C 1175 = 1175
 C 1176 = 1176
 C 1177 = 1177
 C 1178 = 1178
 C 1179 = 1179
 C 1180 = 1180
 C 1181 = 1181
 C 1182 = 1182
 C 1183 = 1183
 C 1184 = 1184
 C 1185 = 1185
 C 1186 = 1186
 C 1187 = 1187
 C 1188 = 1188
 C 1189 = 1189
 C 1190 = 1190
 C 1191 = 1191
 C 1192 = 1192
 C 1193 = 1193
 C 1194 = 1194
 C 1195 = 1195
 C 1196 = 1196
 C 1197 = 1197
 C 1198 = 1198
 C 1199 = 1199
 C 1200 = 1200
 C 1201 = 1201
 C 1202 = 1202
 C 1203 = 1203
 C 1204 = 1204
 C 1205 = 1205
 C 1206 = 1206
 C 1207 = 1207
 C 1208 = 1208
 C 1209 = 1209
 C 1210 = 1210
 C 1211 = 1211
 C 1212 = 1212
 C 1213 = 1213
 C 1214 = 1214
 C 1215 = 1215
 C 1216 = 1216
 C 1217 = 1217
 C 1218 = 1218
 C 1219 = 1219
 C 1220 = 1220
 C 1221 = 1221
 C 1222 = 1222
 C 1223 = 1223
 C 1224 = 1224
 C 1225 = 1225
 C 1226 = 1226
 C 1227 = 1227
 C 1228 = 1228
 C 1229 = 1229
 C 1230 = 1230
 C 1231 = 1231
 C 1232 = 1232
 C 1233 = 1233
 C 1234 = 1234
 C 1235 = 1235
 C 1236 = 1236
 C 1237 = 1237
 C 1238 = 1238
 C 1239 = 1239
 C 1240 = 1240
 C 1241 = 1241
 C 1242 = 1242
 C 1243 = 1243
 C 1244 = 1244
 C 1245 = 1245
 C 1246 = 1246
 C 1247 = 1247
 C 1248 = 1248
 C 1249 = 1249
 C 1250 = 1250
 C 1251 = 1251
 C 1252 = 1252
 C 1253 = 1253
 C 1254 = 1254
 C 1255 = 1255
 C 1256 = 1256
 C 1257 = 1257
 C 1258 = 1258
 C 1259 = 1259
 C 1260 = 1260
 C 1261 = 1261
 C 1262 = 1262
 C 1263 = 1263
 C 1264 = 1264
 C 1265 = 1265
 C 1266 = 1266
 C 1267 = 1267
 C 1268 = 1268
 C 1269 = 1269
 C 1270 = 1270
 C 1271 = 1271
 C 1272 = 1272
 C 1273 = 1273
 C 1274 = 1274
 C 1275 = 1275
 C 1276 = 1276
 C 1277 = 1277
 C 1278 = 1278
 C 1279 = 1279
 C 1280 = 1280
 C 1281 = 1281
 C 1282 = 1282
 C 1283 = 1283
 C 1284 = 1284
 C 1285 = 1285
 C 1286 = 1286
 C 1287 = 1287
 C 1288 = 1288
 C 1289 = 1289
 C 1290 = 1290
 C 1291 = 1291
 C 1292 = 1292
 C 1293 = 1293
 C 1294 = 1294
 C 1295 = 1295
 C 1296 = 1296
 C 1297 = 1297
 C 1298 = 1298
 C 1299 = 1299
 C 1300 = 1300
 C 1301 = 1301
 C 1302 = 1302
 C 1303 = 1303
 C 1304 = 1304
 C 1305 = 1305
 C 1306 = 1306
 C 1307 = 1307
 C 1308 = 1308
 C 1309 = 1309
 C 1310 = 1310
 C 1311 = 1311
 C 1312 = 1312
 C 1313 = 1313
 C 1314 = 1314
 C 1315 = 1315
 C 1316 = 1316
 C 1317 = 1317
 C 1318 = 1318
 C 1319 = 1319
 C 1320 = 1320
 C 1321 = 1321
 C 1322 = 1322
 C 1323 = 1323
 C 1324 = 1324
 C 1325 = 1325
 C 1326 = 1326
 C 1327 = 1327
 C 1328 = 1328
 C 1329 = 1329
 C 1330 = 1330
 C 1331 = 1331
 C 1332 = 1332
 C 1333 = 1333
 C 1334 = 1334
 C 1335 = 1335
 C 1336 = 1336
 C 1337 = 1337
 C 1338 = 1338
 C 1339 = 1339
 C 1340 = 1340
 C 1341 = 1341
 C 1342 = 1342
 C 1343 = 1343
 C 1344 = 1344
 C 1345 = 1345
 C 1346 = 1346
 C 1347 = 1347
 C 1348 = 1348
 C 1349 = 1349
 C 1350 = 1350
 C 1351 = 1351
 C 1352 = 1352
 C 1353 = 1353
 C 1354 = 1354
 C 1355 = 1355
 C 1356 = 1356
 C 1357 = 1357
 C 1358 = 1358
 C 1359 = 1359
 C 1360 = 1360
 C 1361 = 1361
 C 1362 = 1362
 C 1363 = 1363
 C 1364 = 1364
 C 1365 = 1365
 C 1366 = 1366
 C 1367 = 1367
 C 1368 = 1368
 C 1369 = 1369
 C 1370 = 1370
 C 1371 = 1371
 C 1372 = 1372
 C 1373 = 1373
 C 1374 = 1374
 C 1375 = 1375
 C 1376 = 1376
 C 1377 = 1377
 C 1378 = 1378
 C 1379 = 1379
 C 1380 = 1380
 C 1381 = 1381
 C 1382 = 1382
 C 1383 = 1383
 C 1384 = 1384
 C 1385 = 1385
 C 1386 = 1386
 C 1387 = 1387
 C 1388 = 1388
 C 1389 = 1389
 C 1390 = 1390
 C 1391 = 1391
 C 1392 = 1392
 C 1393 = 1393
 C 1394 = 1394
 C 1395 = 1395
 C 1396 = 1396
 C 1397 = 1397
 C 1398 = 1398
 C 1399 = 1399
 C 1400 = 1400
 C 1401 = 1401
 C 1402 = 1402
 C 1403 = 1403
 C 1404 = 1404
 C 1405 = 1405
 C 1406 = 1406
 C 1407 = 1407
 C 1408 = 1408
 C 1409 = 1409
 C 1410 = 1410
 C 1411 = 1411
 C 1412 = 1412
 C 1413 = 1413
 C 1414 = 1414
 C 1415 = 1415
 C 1416 = 1416
 C 1417 = 1417
 C 1418 = 1418
 C 1419 = 1419
 C 1420 = 1420
 C 1421 = 1421
 C 1422 = 1422
 C 1423 = 1423
 C 1424 = 1424
 C 1425 = 1425
 C 1426 = 1426
 C 1427 = 1427
 C 1428 = 1428
 C 1429 = 1429
 C 1430 = 1430
 C 1431 = 1431
 C 1432 = 1432
 C 1433 = 1433
 C 1434 = 1434
 C 1435 = 1435
 C 1436 = 1436
 C 1437 = 1437
 C 1438 = 1438
 C 1439 = 1439
 C 1440 = 1440
 C 1441 = 1441
 C 1442 = 1442
 C 1443 = 1443
 C 1444 = 1444
 C 1445 = 1445
 C 1446 = 1446
 C 1447 = 1447
 C 1448 = 1448
 C 1449 = 1449
 C 1450 = 1450
 C 1451 = 1451
 C 1452 = 1452
 C 1453 = 1453
 C 1454 = 1454
 C 1455 = 1455
 C 1456 = 1456
 C 1457 = 1457
 C 1458 = 1458
 C 1459 = 1459
 C 1460 = 1460
 C 1461 = 1461
 C 1462 = 1462
 C 1463 = 1463
 C 1464 = 1464
 C 1465 = 1465
 C 1466 = 1466
 C 1467 = 1467
 C 1468 = 1468
 C 1469 = 1469
 C 1470 = 1470
 C 1471 = 1471
 C 1472 = 1472
 C 1473 = 1473
 C 1474 = 1474
 C 1475 = 1475
 C 1476 = 1476
 C 1477 = 1477
 C 1478 = 1478
 C 1479 = 1479
 C 1480 = 1480
 C 1481 = 1481
 C 1482 = 1482
 C 1483 = 1483
 C 1484 = 1484
 C 1485 = 1485
 C 1486 = 1486
 C 1487 = 1487
 C 1488 = 1488
 C 1489 = 1489
 C 1490 = 1490
 C 1491 = 1491
 C 1492 = 1492
 C 1493 = 1493
 C 1494 = 1494
 C 1495 = 1495
 C 1496 = 1496
 C 1497 = 1497
 C 1498 = 1498
 C 1499 = 1499
 C 1500 = 1500
 C 1501 = 1501
 C 1502 = 1502
 C 1503 = 1503
 C 1504 = 1504
 C 1505 = 1505
 C 1506 = 1506
 C 1507 = 1507
 C 1508 = 1508
 C 1509 = 1509
 C 1510 = 1510
 C 1511 = 1511
 C 1512 = 1512
 C 1513 = 1513
 C 1514 = 1514
 C 1515 = 1515
 C 1516 = 1516
 C 1517 = 1517
 C 1518 = 1518
 C 1519 = 1519
 C 1520 = 1520
 C 1521 = 1521
 C 1522 = 1522
 C 1523 = 1523
 C 1524 = 1524
 C 1525 = 1525
 C 1526 = 1526
 C 1527 = 1527
 C 1528 = 1528
 C 1529 = 1529
 C 1530 = 1530
 C 1531 = 1531
 C 1532 = 1532
 C 1533 = 1533
 C 1534 = 1534
 C 1535 = 1535
 C 1536 = 1536
 C 1537 = 1537
 C 1538 = 1538
 C 1539 = 1539
 C 1540 = 1540
 C 1541 = 1541
 C 1542 = 1542
 C 1543 = 1543
 C 1544 = 1544
 C 1545 = 1545
 C 1546 = 1546
 C 1547 = 1547
 C 1548 = 1548
 C 1549 = 1549
 C 1550 = 1550
 C 1551 = 1551
 C 1552 = 1552
 C 1553 = 1553
 C 1554 = 1554
 C 1555 = 1555
 C 1556 = 1556
 C 1557 = 1557
 C 1558 = 1558
 C 1559 = 1559
 C 1560 = 1560
 C 1561 = 1561
 C 1562 = 1562
 C 1563 = 1563
 C 1564 = 1564
 C 1565 = 1565
 C 1566 = 1566
 C 1567 = 1567
 C 1568 = 1568
 C 1569 = 1569
 C 1570 = 1570
 C 1571 = 1571
 C 1572 = 1572
 C 1573 = 1573
 C 1574 = 1574
 C 1575 = 1575
 C 1576 = 1576
 C 1577 = 1577
 C 1578 = 1578
 C 1579 = 1579
 C 1580 = 1580
 C 1581 = 1581
 C 1582 = 1582
 C 1583 = 1583
 C 1584 = 1584
 C 1585 = 1585
 C 1586 = 1586
 C 1587 = 1587
 C 1588 = 1588
 C 1589 = 1589
 C 1590 = 1590
 C 1591 = 1591
 C 1592 = 1592
 C 1593 = 1593
 C 1594 = 1594
 C 1595 = 1595
 C 1596 = 1596
 C 1597 = 1597
 C 1598 = 1598
 C 1599 = 1599
 C 1600 = 1600
 C 1601 = 1601
 C 1602 = 1602
 C 1603 = 1603
 C 1604 = 1604
 C 1605 = 1605
 C 1606 = 1606
 C 1607 = 1607
 C 1608 = 1608
 C 1609 = 1609
 C 1610 = 1610
 C 1611 = 1611
 C 1612 = 1612
 C 1613 = 1613
 C 1614 = 1614
 C 1615 = 1615
 C 1616 = 1616
 C 1617 = 1617
 C 1618 = 1618
 C 1619 = 1619
 C 1620 = 1620
 C 1621 = 1621
 C 1622 = 1622
 C 1623 = 1623
 C 1624 = 1624
 C 1625 = 1625
 C 1626 = 1626
 C 1627 = 1627
 C 1628 = 1628
 C 1629 = 1629
 C 1630 = 1630
 C 1631 = 1631
 C 1632 = 1632
 C 1633 = 1633
 C 1634 = 1634
 C 1635 = 1635
 C 1636 = 1636
 C 1637 = 1637
 C 1638 = 1638
 C 1639 = 1639
 C 1640 = 1640
 C 1641 = 1641
 C 1642 = 1642
 C 1643 = 1643
 C 1644 = 1644
 C 1645 = 1645
 C 1646 = 1646
 C 1647 = 1647
 C 1648 = 1648
 C 1649 = 1649
 C 1650 = 1650
 C 1651 = 1651
 C 1652 = 1652
 C 1653 = 1653
 C 1654 = 1654
 C 1655 = 1655
 C 1656 = 1656
 C 1657 = 1657
 C 1658 = 1658
 C 1659 = 1659
 C 1660 = 1660
 C 1661 = 1661
 C 1662 = 1662
 C 1663 = 1663
 C 1664 = 1664
 C 1665 = 1665
 C 1666 = 1666
 C 1667 = 1667
 C 1668 = 1668
 C 1669 = 1669
 C 1670 = 1670
 C 1671 = 1671
 C 1672 = 1672
 C 1673 = 1673
 C 1674 = 1674
 C 1675 = 1675
 C 1676 = 1676
 C 1677 = 1677
 C 1678 = 1678
 C 1679 = 1679
 C 1680 = 1680
 C 1681 = 1681
 C 1682 = 1682
 C 1683 = 1683
 C 1684 = 1684
 C 1685 = 1685
 C 1686 = 1686
 C 1687 = 1687
 C 1688 = 1688
 C 1689 = 1689
 C 1690 = 1690
 C 1691 = 1691
 C 1692 = 1692
 C 1693 = 1693
 C 1694 = 1694
 C 1695 = 1695
 C 1696 = 1696
 C 1697 = 1697
 C 1698 = 1698
 C 1699 = 1699
 C 1700 = 1700
 C 1701 = 1701
 C 1702 = 1702
 C 1703 = 1703
 C 1704 = 1704
 C 1705 = 1705
 C 1706 = 1706
 C 1707 = 1707
 C 1708 = 1708
 C 1709 = 1709
 C 1710 = 1710
 C 1711 = 1711
 C 1712 = 1712
 C 1713 = 1713
 C 1714 = 1714<br

STORAGE MAP VARTABLES (TAGS: C=COMMON, E=EQUIVALENCE)

NAME	TAG	RFL ADR	NAME	TAG	RFL ADR	NAME	TAG	RFL ADR
W	0000000	0	000293	A	000104	B	000424	
C	0000000	0	000409	Z	000519	E	000650	
S	0000000	X	000504	0	000413	X	000840	
BT	0000000	BT	000608	41	000708	CC	000789	
TT	0000000	TT	000804	RHO	000910	SET	000952	
PP001	0000000	PP001	001408	DIDD	001470	Y441	001514	
PP002	0000000	PP002	001509	SAVE	001540	ALFA	001544	
AL001	0000000	AL001	001600	UPRTR	001700	WPSTR	001420	
AL002	0000000	AL002	001901	DCDII	002040	DENOV	002049	
SP001	0000000	SP001	002004	UPRTW	002170	U237E2	002140	
SP002	0000000	SP002	002200	DRIVOD	002108	SUITIN	002044	
SP003	0000000	SP003	002208	DCDRHO	002290	DELCAP	00248H	
SP004	0000000	SP004	00220E	GRUPVL	002A00	FACTOR	002A00	
SP005	0000000	SP005	002A14	0	002A18	4E	002A1C	
SP006	0000000	SP006	002A24	10	002A28	4G	002A2C	
SP007	0000000	SP007	002A34	L1	002A38	51	002A3C	
SP008	0000000	SP008	002A44	KE	002A48	4X	002A4C	
SP009	0000000	SP009	002A54	41	002A58	42	002A5C	
SP010	0000000	SP010	002A64	85	002A68	86	002A6C	
SP011	0000000	SP011	002A74	RR1	002A78	IR1	002A7C	
SP012	0000000	SP012	002A84	TEXT	002A88	CTOP	002A8C	
SP013	0000000	SP013	002A90	MAMA	002A94	LA1	002A98	
SP014	0000000	SP014	002A96	START	002AA4	DDDM	002AA8	

LEVEL: 1.07166

TRN 05/360 BASIC FORTRAN IV (E) COMPILATION

DATE: 6A.319

```

S.0001      SUBROUTINE GJRT SA,N,EPSC
S.0002      DIMENSION A$10, 2$,P$20C,C$20C,.420C,0$20C
S.0003      DOUBLE PRECISION A,B,C,EPSC,PIVOT,Z
S.0004      INTEGER I,J
S.0005      DO 10 I=1,N
S.0006      DETERMINATOR OF THE PIVOT ELEMENT
S.0007      PIVOT=0.
S.0008      DO 20 J=1,N
S.0009      DO 20 J=1,N
S.0010      TTEMP=ABS(A(J,J))-DABEPPIVOT<<20,20,30
S.0011      10 PIVOT=1/TTEMP
S.0012      PIVOT=1/TTEMP
S.0013      05K8,I
S.0014      10 CONTINUE
S.0015      ITEMP=EPPIVOT-C$20C$0,50,50
S.0016      EXCHANGE OF THE PIVOTAL ROW WITH THE KTH ROW
S.0017      50 TTEMP=K$C60,50,50
S.0018      60 DO 70 J=1,N
S.0019      1024KC
S.0020      2048T,1C
S.0021      4096T,1C
S.0022      8192T,1C
S.0023      16384T,1C
S.0024      32768T,1C
S.0025      65536T,1C
S.0026      131072T,1C
S.0027      262144T,1C
S.0028      524288T,1C
S.0029      1048576T,1C
S.0030      2097152T,1C
S.0031      4194304T,1C
S.0032      8388608T,1C
S.0033      16777216T,1C
S.0034      33554432T,1C
S.0035      67108864T,1C
S.0036      134217728T,1C
S.0037      268435456T,1C
S.0038      516870912T,1C
S.0039      103374184T,1C
S.0040      206748368T,1C
S.0041      413496736T,1C
S.0042      826993472T,1C
S.0043      1653986944T,1C
S.0044      3307973888T,1C
S.0045      6615947776T,1C
S.0046      1323189552T,1C
S.0047      2646378104T,1C
S.0048      5292756208T,1C
S.0049      10585512416T,1C
S.0050      21171024832T,1C
S.0051      42342049664T,1C
S.0052      84684099328T,1C
S.0053      169368198560T,1C
S.0054      338736397120T,1C
S.0055      677472794240T,1C
S.0056      135494548800T,1C
S.0057      270989097600T,1C
S.0058      541978195200T,1C
S.0059      1083956390400T,1C
S.0060      2167912780800T,1C
S.0061      4335825561600T,1C
S.0062      8671651123200T,1C
S.0063      17343202246400T,1C
S.0064      34686404492800T,1C
S.0065      69372808985600T,1C
S.0066      138745617971200T,1C
S.0067      277491235942400T,1C
S.0068      554982471884800T,1C
S.0069      1109964943769600T,1C
S.0070      2219929887539200T,1C
S.0071      4439859775078400T,1C
S.0072      8879719550156800T,1C
S.0073      17759439100313600T,1C
S.0074      35518878200627200T,1C
S.0075      71037756401254400T,1C
S.0076      14207551280250800T,1C
S.0077      28415102560501600T,1C
S.0078      56830205121003200T,1C
S.0079      11366040242006400T,1C
S.0080      227320804840012800T,1C
S.0081      454641609680025600T,1C
S.0082      909283219360051200T,1C
S.0083      1818566438720102400T,1C
S.0084      3637132877440204800T,1C
S.0085      7274265754880409600T,1C
S.0086      14548535109760819200T,1C
S.0087      29097070219521638400T,1C
S.0088      58194140439043276800T,1C
S.0089      116388280878086553600T,1C
S.0090      232776561756173107200T,1C
S.0091      465553123512346214400T,1C
S.0092      931106247024692428800T,1C
S.0093      1862212480483484857600T,1C
S.0094      3724424960966969715200T,1C
S.0095      7448849921933939430400T,1C
S.0096      1489769984386787880800T,1C
S.0097      2979539968773575761600T,1C
S.0098      5959079937547151523200T,1C
S.0099      11918159875094303046400T,1C
S.0100      23836319750478606092800T,1C
S.0101      47672639500957212185600T,1C
S.0102      95345279001914424371200T,1C
S.0103      19069055800382844872400T,1C
S.0104      38138111600765689744800T,1C
S.0105      7627622320015137949600T,1C
S.0106      15255244640030275899200T,1C
S.0107      30510489280060551798400T,1C
S.0108      61020978560121103596800T,1C
S.0109      122041957120242207193600T,1C
S.0110      244083914240484414387200T,1C
S.0111      488167828480968828774400T,1C
S.0112      976335656961937657548800T,1C
S.0113      195267131392387531509600T,1C
S.0114      390534262784775063019200T,1C
S.0115      781068525569550126038400T,1C
S.0116      1562137051139100252076800T,1C
S.0117      3124274102278200504153600T,1C
S.0118      6248548204556400108307200T,1C
S.0119      12497096409112800216614400T,1C
S.0120      24994192818225600433228800T,1C
S.0121      49988385636451200866457600T,1C
S.0122      99976771272902401732915200T,1C
S.0123      19995354254580480346582400T,1C
S.0124      39990708509160960693164800T,1C
S.0125      79981417018321921386329600T,1C
S.0126      15996283403664384277264800T,1C
S.0127      31992566807328768554529600T,1C
S.0128      63985133614657537109059200T,1C
S.0129      127970267229115074218118400T,1C
S.0130      255940534458230148436236800T,1C
S.0131      511881068916460296872473600T,1C
S.0132      102376213783290559374494400T,1C
S.0133      204752427566581118748988800T,1C
S.0134      409504855133162237497977600T,1C
S.0135      819009710266324474995955200T,1C
S.0136      163801942053264854999190400T,1C
S.0137      327603884106529709998380800T,1C
S.0138      655207768213059419996761600T,1C
S.0139      1310415536426188839993523200T,1C
S.0140      2620831072852377679987046400T,1C
S.0141      5241662145704755359974092800T,1C
S.0142      1048332429140951079958157600T,1C
S.0143      2096664858281902159916353200T,1C
S.0144      4193329716563804319832706400T,1C
S.0145      8386659433127608639665412800T,1C
S.0146      16773318866255217279330825600T,1C
S.0147      33546637732510434558661651200T,1C
S.0148      67093275465020869117323202400T,1C
S.0149      13418655093004173823464604800T,1C
S.0150      26837310186008347646929209600T,1C
S.0151      53674620372016695293858419200T,1C
S.0152      107349240744033390587716838400T,1C
S.0153      214698481488066781175433676800T,1C
S.0154      429396962976133562350867353600T,1C
S.0155      858793925952267124701734707200T,1C
S.0156      1717587851904534249403469414400T,1C
S.0157      3435175703809068498806938828800T,1C
S.0158      6870351407618136997613877657600T,1C
S.0159      13740702815236279952337555315200T,1C
S.0160      27481405630472559904675110630400T,1C
S.0161      54962811260945119809350221260800T,1C
S.0162      109925622521882239618704442516800T,1C
S.0163      219851245043764479237408885033600T,1C
S.0164      439702490087528958474817770067200T,1C
S.0165      879404980175057916949635540134400T,1C
S.0166      175880976035011583389927108026800T,1C
S.0167      351761952070023166779854216053600T,1C
S.0168      703523904140046333559708432107200T,1C
S.0169      1407047808280092667119416864214400T,1C
S.0170      2814095616560185334238833728428800T,1C
S.0171      5628191233120370668477667456857600T,1C
S.0172      1125638246640744133695534891315200T,1C
S.0173      2251276493281488267391069782630400T,1C
S.0174      4502552986562976534782139565260800T,1C
S.0175      9005105973125953069564279130521600T,1C
S.0176      18010211946259066139128582261043200T,1C
S.0177      36020423892518132278257164522086400T,1C
S.0178      72040847785036264556514329044172800T,1C
S.0179      144081695570072529113026658088345600T,1C
S.0180      288163391140145058226053316176691200T,1C
S.0181      576326782280290116452106632353382400T,1C
S.0182      1152653564560580232904213265706764800T,1C
S.0183      2305307129121160465808426531413529600T,1C
S.0184      4610614258242320931616853062827059200T,1C
S.0185      9221228516484641863233706125654118400T,1C
S.0186      1844245703296928372646741225310236800T,1C
S.0187      3688491406593856745293482449620473600T,1C
S.0188      7376982813187713490588964899240947200T,1C
S.0189      1475396562637542698117739379848190400T,1C
S.0190      2950793125275085396235478759696380800T,1C
S.0191      5901586250550170792470957519392716800T,1C
S.0192      1180317250100340158494191503878533200T,1C
S.0193      2360634500200680316988383007757066400T,1C
S.0194      4721269000401360633976766015514132800T,1C
S.0195      9442538000802721267953532031028265600T,1C
S.0196      1888507600160544253906766062056531200T,1C
S.0197      3777015200321088507813532124113062400T,1C
S.0198      7554030400642177015627064248226124800T,1C
S.0199      1510806080128355431254412496452249600T,1C
S.0200      302161216025671086258882499290499200T,1C
S.0201      60432243205134217251776499858099200T,1C
S.0202      120864464010268434523532997776198400T,1C
S.0203      241728928020536869047065995552396800T,1C
S.0204      483457856041073738094031991104793600T,1C
S.0205      966915712082147476188063982209587200T,1C
S.0206      193383142401494952377612796441914400T,1C
S.0207      386766284802989904755225592883828800T,1C
S.0208      773532569605979809510451185767657600T,1C
S.0209      154706513921195961902092237153315200T,1C
S.0210      309413027842389923804184474306630400T,1C
S.0211      61882605568477984760836894861320800T,1C
S.0212      12376521113695596952167378932261600T,1C
S.0213      24753042227391193904334757864523200T,1C
S.0214      49506084454782387808669515729046400T,1C
S.0215      99012168909564775617339031458092800T,1C
S.0216      19802437781912955123467806291615600T,1C
S.0217      39604875563825910246935612583231200T,1C
S.0218      79209751127651820493871225166462400T,1C
S.0219      15841950225530364098772445033294800T,1C
S.0220      31683900451060728197544890066589600T,1C
S.0221      63367800902121456395089780133179200T,1C
S.0222      126735601804242912780179560266358400T,1C
S.0223      253471203608485825560359120532716800T,1C
S.0224      506942407216971651120718241065433600T,1C
S.0225      101388814443342310224143648213067200T,1C
S.0226      202777628886684620448287296426134400T,1C
S.0227      405555257773369240896574592845268800T,1C
S.0228      811110515546738481793149185690537600T,1C
S.0229      162222103109347696358638371138075200T,1C
S.0230      324444206218695392717276742276150400T,1C
S.0231      648888412437390785434553484552300800T,1C
S.0232      1297776824874781570869108969104601600T,1C
S.0233      2595553649749563141738217938209203200T,1C
S.0234      5191107299498126283476435876418406400T,1C
S.0235      10382215598996315566932671752836912800T,1C
S.0236      20764431197993131133865343505673825600T,1C
S.0237      41528862395986262267730687011347651200T,1C
S.0238      83057724791972524535461374022695302400T,1C
S.0239      16611544983974504907012274804538604800T,1C
S.0240      33223089967979009814024549609077209600T,1C
S.0241      66446179935958019628049099218154419200T,1C
S.0242      132892359719570039256098198436308398400T,1C
S.0243      265784719439540078512196396872617796800T,1C
S.0244      531569438879520015024392793745355593600T,1C
S.0245      1063138877595100300487855587490711187200T,1C
S.0246      2126277755195006000975711174981422374400T,1C
S.0247      4252555510394900600195355549982844748800T,1C
S.0248      8505111020794800300390711199965689557600T,1C
S.0249      17010222041947006007814223999313779115200T,1C
S.0250      34020444083894001201568447998627558303200T,1C
S.0251      68040888167788002403136885997255116666400T,1C
S.0252      13608176433577004806273771199451023332800T,1C
S.0253      27216352867154009612547542398902046665600T,1C
S.0254      54432705734308001925095084797804093331200T,1C
S.0255      10886541146861003850188016995608086662400T,1C
S.0256      21773082293722007700376033991216173248800T,1C
S.0257      43546164587444001540752067982432346577600T,1C
S.0258      87092329174888003081504135964864681155200T,1C
S.0259      17418465834977006162300827193016936310400T,1C
S.0260      34836931669954001234600414386033872620800T,1C
S.0261      69673863339908002469200828772067745201600T,1C
S.0262      13934772669904004938400457554413549043200T,1C
S.0263      27869545339808009876800911
```

INPUT DATA AND FORMAT FOR TRAVEL

<u>Card</u>	<u>Format</u>	<u>Data Description</u>
1	I4	No. of models for which T-D curves are to be computed
2	20A4	Identification for models \leq 80 characters
3	I4	NLAYER = no. of velocity layers in model
	I4	NR; depths of penetration for which T-D values are to be computed = (NR)*(DELR)
	F8.4	DELR = Interval in (km) for numerical integration
	F8.4	DEPTH = maximum depth (km) of penetration \leq depth of last velocity value
	F8.4	EPSILON = distance (km) from maximum depth to begin using modified trapezoidal rule of integration; usually .3km
	F8.4	DELTA = distance from maximum depth at which integration is stopped; usually .01km
4	10F8.4	Velocities in km/sec
5	10F8.4	Depths (km) from surface of given velocities

```

      DIMENSION T(200),DEL(200),R(200),VEL(200),Z(900),ANGLE(200),V(900)
      D,DT(200),TEXT(20)
      DOUBLE PRECISION T,DEL,R,VEL,Z,V,DZ,DELR,DEPTH,EPS,DELTA,H1,R2,H3,
      TUE,A,B,C,DEPH1,R0,XR,P,P2,SUM,SUM1,SUM2,ETA,FACT,FACT1,FACT2,
      21EST,VV1,00,DL1,DEPTH2,FACT5,FACT6,FACT3,FACT4,TAD,SLOP,SKD,A1,A2
      3,B1,B2,C1,C2
      DOUBLE PRECISION ZMAT(4,4),NDUMMY,VVEC(4),AVEC(4),0
      10 FORMAT(4E25.16)
      HEAD(1,108) NMUN
      DD 300 NRUN = 1, NRUN
      HEAD(1,400) TEXT(1),I=1,20
      HEAD(1,100) NLAYER,NR,DEL4,DEPTH,EPSON,DELTA
      HEAD(1,200) (VEL(I),I=1,NLAYEN)
      HEAD(1,200) (H(I)),I=1,NLAYEN)
      100 FORMAT(214.4F8.4)
      200 FORMAT(10FB.4)
      201 I=1
      202 I=1
      203 I=1
      204 I=1
      205 J=1
      206 K=1
      207 L=1
      208 IJMP=1
      209 J=J+3
      210 NMN=J
      211 CONTINUE
      DD 710 LI=1,4
      NDUMMY = NMN - 4 + LI
      DJMAT = R(NDUMMY)
      WRITE(3,5000) DUMMY
      ZMAT(LI,1) = 1.
      DD 705 LJ=2,4
      ZMAT(LI,LJ) = DUMMY*(LJ-1)
      706 CONTINUE
      710 CONTINUE
      NDUMMY = 4
      EPS = 0.001
      CALL GUR4(ZMAT,NDUMMY,EPS)
      DD 715 LJ=1,4
      NDUMMY = NMN - 4 + LJ
      VVEC(LJ) = VEL(NDUMMY)
      716 CONTINUE
      DD 725 LI=1,4
      DJMAT = 0.
      DD 720 LJ=1,4
      DJMAT = DJMAT + ZMAT(LI,LJ)*VVEC(LJ)
      721 CONTINUE
      AVEC(LI) = DUMMY
      722 CONTINUE
      A = AVEC(1)
      B = AVEC(2)
      C = AVEC(3)
      D = AVEC(4)
      DD TU(31,40),IJMP
      31 V(1) = A + B*Z(1) + C*D(1)*Z(1) + D*D(1)*Z(1)
      I=1
      I=(Z(1))-H(J)) 31,31,30
      32 I=(Z(1))-DEPTH)33,33,34
      33 I=(Z(J+3))-DEPTH) 7,7,32
      32 H(J)=DEPTH
      33 TU 31
      34 DEPTH1=6371.-DEPTH
      I=0
      35 I=1
      Z(1)=6371.-Z(1)
      I=(Z(1))-DEPTH1)36,36,35
      36 I=1
      H=6371.0
      X4=NM
      INC=DEPTH/(XR*DELR)
      INC=INC*NM
      NM=1
      NM1=NM + 1
      INC1 > INC < 1
      NM = 4
      DD 8 J > NM1,INC1,NR
      DEL1=DELH
      IJMP=2
      UZ(V) = 6371.-Z(J)
      X2 = XR*DEL4
      IZ (6371.0-Z(J))-H(NR)) 42,42,45
      45 NM = NM + 3
      DD TU 42
      46 PZ(J)/V(J)
      P2P=2
      IF ((RD/V(1))**2-P2) 4000,405,405
      407 CONTINUE
      SUM=USORT((RD/V(1))**2-P2)
      I=(J-2)11,11,10
      11 >J1=0,
      SUM2=0,
      30 10 12
      10 SUM1=1. / (RD*SUM)
      SUM2=SUM1*(RD/V(1))**2
      K=2
      24 ETA=Z(K)/V(K)
      IF (eTA-P) 4000,240,240
      240 CONTINUE
      FACT=DSORT((ETA-P)*(ETA+P))
      FACT1=1./FACT+Z(K))
      FACT2= FACT1 *(Z(K)/V(K))**2
      SUM1=SUM1*2.*FACT1

```

```

50 JH2=SUM2+2.*FACT2
51 K =K+1
52 IF(Z(K)-Z(J)=EPSLON)22,23,24
22 TEST=Z(J)+EPSLON-.01
53 IF(Z(K)-TEST)12,23,23
23 DEPTH1=Z(J)+EPSLON
DEPTH1 =6371.-DEPTH1
VV1=A*DEPTH1*(B+DEPTH1*(C+DEPTH1*D))
DEPTH1 =6371.-DEPTH1
DD=EPSLON
ETA=DEPTH1/VV1
IF ((ETA-P) 4000,230,230
230 CONTINUE
FACT=DSQRT((ETA-P)*(ETA+P))
FACT1=1./FACT*DEPTH1)
FACT2= FACT1*(DEPTH1/VV1)**2
SUM1 =SUM1+DELH + FACT1*DEL1
SUM2 = SUM2*DELR + FACT2*DEL1
60 TU 21
12 DEL1=Z(J) - EPSLON +Z(K-1)
60 TU 23
21 J=1
WJ=U.
UD =PSLDN
DEPTH2=Z(J)+DD
14 PDW=PDW+1,
IF(I=1)16,15,17
16 DEPTH1=DEPTH2
DEPTH1 =6371.-DEPTH1
VV1=A*B*PDW*(B+DEPTH1*(C+DEPTH1*D))
DEPTH1 =6371.-DEPTH1
ETA=DEPTH1/VV1
IF ((ETA-P) 4000,160,160
160 CONTINUE
FACT=DSQRT((ETA-P)*(ETA+P))
FACT1=1./FACT*DEPTH1)
FACT2=FACT1*(DEPTH1/VV1)**2
I=10
60 TU 18
17 FACT3 = FACT1
FACT4 = FACT2
FACT1=FACT3
FACT2=FACT4
18 DEPTH2=Z(J)+DD/(2.*PDW)
DEPTH2 =6371.-DEPTH2
VV2=A*DEPTH2*(B+DEPTH2*(C+DEPTH2*D))
DEPTH2 =6371.-DEPTH2
ETA=DEPTH2/VV2
IF ((ETA-P) 4000,180,180
180 CONTINUE
FACT=DSQRT((ETA-P)*(ETA+P))
FACT3=1./FACT*DEPTH2)
FACT4=FACT3*(DEPTH2/VV2)**2
SUM1=SUM1+DD*2.*((FACT1*FACT3)/(2.*PDW))
SUM2=SUM2+DD*2.*((FACT2*FACT4)/(2.*PDW))
IF(DU/(2.*PDW)-.03 )15,15,14
15 IF(DU/(2.*PDW)-.03 )15,15,14
16 IF(DU/(2.*PDW)-.03 )60,60,61
61 IAU = DD/(2.*PDW)
DUP = (V(J)-VV2)/TAU
62 FACT5 =FACT1
FAuto = FACT2
FACT1 = FACT3
FACT2 = FACT4
TAO = TAD/Z;
DEPTH1 = Z(J)+TAD
SKD = SLDP*TAD
VV1 = V(J)-SKD
FACT = 2.*P*(V(J)+TAO + Z(J)*SKD) /(V(J)**2-2.*V(J)*SKD)
FACT3 = 1./((DSQRT(FACT)*DEPTH1)
FACT4 = FACT3*(DEPTH1/VV1)**2
SUM1 = SUM1 +TAD*(FACT1 *FACT3)**2,
SUM2 = SUM2 + TAD*(FACT2 *FACT4)**2,
IF ((IAU-DELT)60,60,62
60 A1 =FACT3
A2 =FACT4
B1 = FACT1
B2=FACT2
C1=FACT5
C2=FACT6
E=PDW; TAO=(FACT4+3*A2-5.*B2/2.+5.*C2)/SUM2
WRITE(3,1050) ERDN
SUM1= TAO*(FACT3+3.*A1-5.*B1/2.+5.*C1)+SUM1
SUM2= TAO*(FACT4+3.*A2-5.*B2/2.+5.*C2)+SUM2
DEL(N)=P*SUM1+6371.
I(N)=SUM2
SINU = P*V(1)/RD
COSU= SQRT(1, - SIN(0**2)
ANGLE(N) = ATAN(SIN(0/CDSID)*180./5.1416
N=N+1
60 TU 8
400J CONTINUE
USL(N) = 0.
I(N) = 0.
ANGLE(N) = 0.
N = N + 1
8 CONTINUE
N=N-1
WRITE(3,401) (TEXT(I), I=1,20)
WRITE(3,1000)
1000 P3MMAT ( 5X,10M DEPTH(RM) , 10A,18HV ELD CITY(RM/SEC) )
WRITE(3,1050) (Z(J),V(J),J=1,N)
1050 P3MMAT (2X,E13,6,6X,E13,6)
WRITE(3,401) (TEXT(I), I=1,20)
WRITE(3,2000)
2000 P3MMAT (2X,18M TRAVEL TIME (SEC) ,5X,11H DELTA (KM),5X,21H DEPTH 0
1F PENETRATION ,5X,1VM ANGLE OF INCIDENCE )
WRITE(3,2050) (T(J),DEL(J),DZ(J),ANSLE(J),J=1,N)
2050 P3MMAT ( 5X,F8.2,13X,F8.1,14X,F7.1,16X,F7.2)
401 P3MMAT (141 //,20A,//)
401 P3MMAT (20A4)
300 CONTINUE
STOP
END

```

INPUT DATA AND FORMAT FOR VARGRAV

<u>CARD</u>	<u>FORMAT</u>	<u>DATA DESCRIPTION</u>
1	I3	No. stations
	F10.5	Station spacing in km, Staspa
	F6.1	Depth to mass sheet in km , Depth
	I3	No. of Density layers \leq 50
	I3	No. of Density profiles \leq 100
	F10.5	Minimum ϕ value
	F10.5	Delta z spacing for integration
	F10.5	Subcrustal Density

$$\phi_{\min} \geq \frac{[\exp(\pi \cdot \text{Depth/Staspa}) - 1] * \text{Depth/Staspa}}{\left(\frac{\text{Depth}}{\text{Staspa}}\right)^2 + k^2}$$

$$k = \frac{\text{No. of } \phi \text{'s to be used}}{2}$$

2	10F8.2	Gravity values in milligals
3	40I2	No. of Density profile to be used at each station
4	16F5.2	Density values stored by profile

```

      DIMENSION GRAV(100),DENSTY(50,50),XCURR(100),DEPDIF(100),PHI(50),I
      IPRUF(100)
      READ 100,NOSTA,STASPA,DEPTH,I0ENS,NPRDF,PHIMIN,DELZ ,SUBCRU
  100 FORMAT(13,F10.5,F6.1,2I3,3F10.5)
      READ 200,(GRAV(I),I=1,NOSTA)
  200 FORMAT(10F8.2)
      READ 150,(IPRDF(I),I=1,NOSTA)
  150 FORMAT(4D12)
      READ 300,:(DENSTY(I,J),J=1,I0ENS),I=1,NPRDF)
  300 FORMAT(16F5.2)
      DD 1492 I=1,NPRDF
      DD 1492 J=1, I0ENS
      DENSTY (I,J)= SUBCRU-DENSTY (I,J)
  1492 CONTINUE
      EXPDDO = (-EXP(3.1416* DEPTH/STASPA)-1.)*DEPTH/STASPA
      EXPENV= (EXP(3.1416*DEPTH/STASPA)-1.)*DEPTH/STASPA
      AI=0.
      IZI
      PART =(DEPTH**2)/(STASPA**2)
      6 IF( (I +1)/2 - (I/2)1,1,2
      1 PHI(I)=EXPDDO/(PART+AI**2)
      PRINT 101,PHI(I)
  101 FORMAT (F10.5)
      GO TO 3
      2 PHI(I)=EXPENV/(PART + AI**2)
  102 FORMAT(F10.5)
      3 IF(ABS(PHI(I))-PHIMIN)4,4,5
      > I=I+1
      AI =AI+1.0
      GO TO 6
      4 IX1 = 2*I-1
      IX = I+1
      IX2=
      J=IX
      DD18 I=2,IX2
      PHI(J)=PHI(I)
      J=J+1
  15 CONTINUE
      PHI(IX2 )=PHI(1)
      J=IX1
      IX=IX2-4
      U3 7 I=2,IX2
      PHI(I)=PHI(J)
      J=J+1
  7 CONTINUE
      PRINT 400,DEPTH,STASPA
  400 FORMAT(23H-COMPUTED PHI FACTORS/10M DEPTH(KM),F6.1,2X,20M STATION
      1SPACING(KM),F10.5)
      PRINT 401,(PHI(I),I=1,IX1)
  401 FORMAT(2X,E13.6)
      M=IX1-1
      IX< N=IX+1
      IX2=N-1
      DD 8 I=1,IX2
      XCURR(I)=0.
      DD 9 J=1,IX
      XCURR(I)= GRAV(J)*PHI(K) +XCURR(I)
      K=K+1
      9 CONTINUE
  500 FORMAT(2X,F10.2)
      IX>IX+1
      K= N N-1
      8 CONTINUE
      IX>NOSTA-I+1
      J=IX2+1
      DD 10 I=1,IX3
      XCURR(J)=0.
      K=1
      DD 11 L=1,IX1
      XCURR(J)=GRAV(K)*PHI(L) +XCURR(J)
      K=K+1
  11 CONTINUE
  600 FORMAT(2X,F10.2)
      J=J+1
  12 CONTINUE
      IX>IX3+1
      N=NOSTA-IX2
      DD 12 I=IX3,N
      K=1
      XCURR(J)=0.
      DD 13 L=1,M
      XCURR(J)=GRAV(K)*PHI(L) +XCURR(J)
      K=K+1
  13 CONTINUE
  700 FORMAT(2X,F10.2)
      J=J+1
      M=M+1
  12 CONTINUE
      FACT=2.*(3.1416**2)*6.67
      DD 14 I=1,NOSTA
      XCURR(I)= XCURR(I)/FACT
  14 CONTINUE
      DD 15 J=1,NOSTA
      SJH0,
      AMAX=XCOHR(J)
      IF(AMAX>0.)D>0.51.52
  50 SJH=1.0
      DD TU 53
  52 SJH=1.0
      DD TU 53
  51 DEPDIF(J)=DEPTH
      DD TU 30
  53 I=IPRDF(J)
      DEPDIF(J)= 0.
      K=0

```

```

40 KBR+1
  DENS = DENSTY(I,K)
  DENS1=DENSTY(I,X-1)
  IF (K-IDENS)43,43,44
41 DEPDIF(J)=DEPDIF(J)*DELZ
  SUM=SUM+DENS*DELZ
  F1=ABS(SUM)-ABS(AMAX))40,41,42
42 IF(K=1)54,55-54
53 DENS1=DENS
54 R=ABS(AMAX)-SUM+DENS*DELZ
  DEPDIF(J)=DEPTHN-SGN*(DEPDIF(J)*R/DEVS1-DELZ)
  GO TO 30
41 DEPDIF(J)=DEPTH-SGN* DEPDIF(J)
  GO TO 30
44 DENS = DENSTY(I,K-1)
  DENS1=DENSTY(I,K-1)
  K=K-1
  GO TO 43
30 CONTINUE
  PRINT 2000
2000 FORMAT(1H-,43X,27H THICKNESS OF CRUSTAL LAYER /)
  PRINT 3000
3000 FORMAT(17H DENSITY PROFILES // 2X,10H DEPTH(KM),5X, 9H DENSITY )
  DEPTH=-DELZ
  UJ 3500 I=1, NPROF
  DEPTH=DEPTH + DELZ
  PRINT 3600,(DENSTY (I,J),J=1,1DENS)
3500 CONTINUE
3600 FORMAT (      10F9.3)
  PRINT 1968
1968 FORMAT(8H-STATION,5X,19H GRAVITY(MILLIGALS),2X,10H DEPTH(KM),
14X,21H DENSITY PROFILE USED)
  UJ 1/ I=1,NOSTA
  PRINT 4000,I,GAV(I), DEPDIF(I),IPNDF(I)
4000 FORMAT(2X,13X,FH.2,9X,F8.2,13X,13)
17 CONTINUE
  PAUSE /
  END

```

INPUT DATA AND FORMAT FOR PRESID

<u>CARD</u>	<u>FORMAT</u>	<u>DATA DESCRIPTION</u>
1	I3	No. of stations at which residuals will be computed
2	16F5.1	Jeffreys-Bullen P-travel times in sec
3	20F4.1	Latitude corrections for converting to geocentric coordinates
4	I3	No. of epicenter locations for each station
5	F6.1	Station latitude (geocentric)
	F6.1	Station longitude
6	18F4.1	USGS origin times for earthquakes stored in sequence as HH:MM:SS.S
7	18F4.1	Record arrival times and store in sequence as HH:MM:SS.S
8	16F5.1	USGS focal depths in km
9	12F6.1	USGS latitude and longitude of epicenters stored in pair sequence Lat ₁ , Long ₁ , Lat ₂ , Long ₂ , ... Sign Convention East Long - West Long + North Lat + South Lat -

```

      DIMENSION QUALOC(200),ORTIM(300), DEPTH(100),STATIM(300),RESID(100
1),XITEM(100), DELTA(100),AZIMUT(100), P(14,103),LOCODEL(100),GEOC(9
11),GEQUA(200)
      HEAD 100, LIMSTA
100  FORMAT(13)
      HEAD 150,((P(I,J),I=1,14),J=1,103)
150  FORMAT(10F5.1)
      HEAD 1112,(GEOC(J),J=1,9)
112  FORMAT(20F4.1)
      SET STATION INDEX
      UO 1 I=1,LIMSTA
      HEAD 200, LIMQUA
200  FORMAT(13)
      IX=2*LIMQUA
      HEAD 700,STALAT, STAANG
700  FORMAT(F6.1,F6.1)
      IX2 = 3* LIMQUA
      HEAD 600, (OPTIM(J),J=1,IX2)
300  FORMAT(10F4.1)
      HEAD 400, (STATIM(J),J=1,IX2)
400  FORMAT(10F4.1)
      HEAD 500, (DEPTH(J), J=1,LIMQUA)
500  FORMAT(10F5.1)
      HEAD 300,(QUALOC(J),J=1,IX)
300  FORMAT(12F6.1)
      UO 1111 J=1,IX,2
      Kx2
      ALAT = 1.0
502  IF(QUALOC(J)-ALAT)565,501,501
501  ALAT = A .T +1.0
      KxK+1
      GJ TU 502
      C0M=GEOC(K) -(GEOC(K)-GEOC(K-1))*(ALAT-QUALOC(J))
1111  GEQUA(J) =QUALOC(J) - CORR
      UO 2 J=1,IX,2
      IVUX=J/2+1
      STAANG = STAALAT*3.1416/180,
      UJANG =GEQUA(J)*3.1416/180,
      MJANG = STAANG - QUALOC(J+1)
      IF (MJANG<180.)3,3,4
      4   MJANG= POLANG -360.
      3   MJANG =POLANG*3.1416/180,
      COSDEL=SIN(STAANG)*SIN(UJANG)+COS(AANG)*COS(UJANG)*COS(POLANG)
      SINDEL=SINT(1.,-COSDEL*2)
      DELTA(INDX)=ATAN(SINDEL/COSDEL) *180./3.1415
      DELTA(INDX)= DELTA(INDX)*90. -SIGN(YU..DELTAINDX')
      SINE=DELTA(CJLJANG)*SIN(POLANG)/SINDEL_
      COSDEL=(SIN(UJANG)*CUS(STAANG)-CUS(UJANG)*SIN(STAANG)*COS(POLANG))
      1/SINDEL
      ASIN=ABS(SINDEL)
      BEITA=ATAN(1/SINDEL)*180./3.1416
      BEITA BETTA + 90.-SIGN(90.,BEITA)
      IF(SINDEL < 0.)BEITA,84.83
      54  IF(COSDEL < 0.)BEITA,85.83
      55  BEITA =180.
      56  AZIMUT(INDX)=BEITA
      57  UJ+TINUE
      2   CJ+TINUE
      Kx1
      GJ 12 J=1,LIMQUA
      Kx2
      UEP = 33.0
      IF(DELTAINDX)-102.1 13,13,14
13   IF(DEPTH(J)-DEP)15,15,16
16   UEP = DEP + 63.0
      KxK+1
      GJ TU 13
15   Lx2
      UIST = 1.0
17   IF(DELTAINDX)-DIST)17,17,18
18   DIST=UIST + 1.0
      LxL+1
      GJ TU 19
19   UIF = P(K,L)- (P(K,L) -P(K,L-1))*(UIST-DELTAINDX)
      UIF2 = P(K-1,L)-(P(K-1,L) -P(K-1,L-1))*(DIST -DELTAINDX)
      IF(DEPTH(J)- 1 .0) 90,90,91
90   14e01 = UIF1 -(DIF1-DIF2)*(DEP-DEPTH(J))/33.0
      GJ TU 92
91   14e01 = UIF1 -(DIF1 -DIF2)*(U.P-DEPTH(J))/63.0
92   UTIME=ORTIM(M)*3600.+UMT(MM+1)*60.-ORTIM(M+2)
      UTIME = STATIM(M)*3600. + STATIM(M+1)*60.+STATIM(M+2)
      KxK+3
      IF(UTIME < -65562.6)20,4000,4000
400  IF(UTIME > 85562.6) 21,20,20
21   STIME = UTIME + 86400.
20   RESIDU(J)= STIME -UTIME -THEUTH
      GJ TU 12
C   MAX BRANCH OF RESIDUAL TIME
14   RESIDU(J)=0.
      Kx1+3
12   CONTINUE
C   UTIME EPICENTERS &4 DISTANCE
      XITEM(1)=DELTAINDX
      XITEM(2)=DELTAINDX
      LOCODEL(1)=1
      LOCODEL(2)=2
      UO 86 K=3, LIMQUA
      P=1
      Lx1
      GJ 22
50   IF(DELTAINDX-XITEM(L))22,22,23

```

```

23 L=L+1
24 IF (L-K)24,25,25
25 M=M+1
26 GO TO 30
27 XITEM(L)=DELTA(K)
28 LOCDEL(M+1)=K
29 GO TO 80
30 IX1=L
31 XITEM(IX1)= XITEM(IX1-1)
32 LOCDEL(IX1)=LOCDEL(IX1-1)
33 IX1=IX1-1
34 IF((I1-M)27,27,51
35 XITEM(IX1)=DELTA(K)
36 LOCDEL(IX1)=K
37 GO TO 80
38 CONTINUE
39 PRINT 800
40 FORMAT(25H-RECORDING STATION COORD /26X,9H LATITUDE,4X,10M LONGI
21JUE)
41 PRINT 900, STALAT,STALNG
42 FORMAT(27X,F6.1,9X,F6.1)
43 PRINT 1000
44 FORMAT(188H EPICENTER PARAMETERS ORDERED BY DISTANCE -AZIMUTH MEAS
188D COUNTER-CLOCKWISE FROM NORTH //)
45 PRINT 2000
46 FORMAT(3X,9H DISTANCE,3X,9H LATITUDE,3X,10H LONGITUDE,3X,6H DEPTH,
13X,8H AZIMUTH,3X,33H P-RESIDUAL(OBSERVED-THEORETICAL))
47 UJ 60 K=1,IX,2
48 IX1=IX/2+1
49 L=LOCDEL(IX1)
50 M=2*L-1
51 PRINT 3000,XITEM(IX1),QUALOC(M),QUA_UC(M+1),DEPTH(M),AZIMUT(L),RES
110(L)
52 3000 FORMAT(5X,F7.2,5X,F6.1,7X,F6.1,7X,F6.1,7X,F6.1,12X,F/.1)
53 CONTINUE
54 URDEN EPICENTERS BY AZIMUTH
55 XITEM(1)=AZIMUT(1)
56 XITEM(2)= AZIMUT(2)
57 LOCDEL(1)=1
58 LOCDEL(2)=2
59 UJ 93 K=3,LIMQUA
60 M=1
61 L=1
62 IF(AZIMUT(K)=XITEM(L)) 101,101,102
63 L=L+1
64 I=(L-K) 103,104,104
65 M=M+1
66 GO TO 105
67 104 XITEM (L)=AZIMUT(K)
68 LOCDEL(M+1)=K
69 GO TO 93
70 IX1=L
71 XITEM(IX1)=XITEM(IX1-1)
72 LOCDEL(IX1)=LOCDEL(IX1-1)
73 IX1=IX1-1
74 IF((I1-M)108,108,107
75 XITEM(IX1)=AZIMUT( )
76 LOCDEL(IX1)=K
77 GO TO 93
78 CONTINUE
79 PRINT 5000
80 5000 FORMAT ( 25H-RECORDING STATION COORD, /32X,9H LATITUDE,9X,10H LONGI
101JUE)
81 PRINT 5001,STALAT,STALNG
82 5001 FORMAT(36X,F6.1,23X,F6.1)
83 PRINT 5002
84 5002 F MMAT(187H ERICENTER PARAMETERS ORDERED BY AZIMUTH-AZIMUTH MEASUR
188 COUNTED-CLOCKWISE FROM NORTH //)
85 PRINT 5003
86 5003 FORMAT(/3X,8H AZIMUTH,3Y,9H LATITUDE,3X,10H LONGITUDE,7X,6H DEPTH
13X,18M DISTANCE(DEGREES) ,12X,33M P-RESIDUAL(OBSERVED-THEORETICAL
1J )
87 UJ 139 K=1,IX,2
88 IX1=IX/2+1
89 L=LOCDEL(IX1)
90 M=2*L-1
91 PRINT 5004,XITEM(IX1),QUALOC(M),QUA_UC(M+1),DEPTH(L),DELTA(L),
1MEASIVL)
92 5004 FORMAT(5X,F6.1,5X,F6.1,7X,F6.1,7X,F6.1,11X,F6.1,27X,F7.1)
93 CONTINUE
94 XITEM (1)=DEPTH(1)
95 XITEM(2)= DEPTH(2)
96 LOCDEL(1)=1
97 LOCDEL(2)=2
98 UJ 207 K=3,LIMQUA
99 M=1
100 L=1
101 IF (DEPTH(K)=XITEM(L)) 203,203,204
102 L=L+1
103 IF(L-K)205,206,206
104 M=M+1
105 GO TO 202
106 XITEM(L)= DEPTH(K)
107 LOCDEL(M+1)=K
108 GO TO 207
109 IX1=L
110 XITEM(IX1)=XITEM(IX1-1)
111 LOCDEL(IX1)=LOCDEL(IX1-1)
112 IX1=IX1-1
113 IF((I1-M) 209,209,208
114 XITEM(IX1)=DEPTH(K)
115 LOCDEL(IX1)=K
116 GO TO 207
117 CONTINUE
118 PRINT 501
119 501 FORMAT (25 H-RECORDING STATION COORD, /26X,9H LATITUDE,4X,10M LONG
11TITUDE)
120 PRINT 802,STALAT,STALNG

```

```
802 FORMAT (27X,F6.1,9X,F6.1)
PRINI 803
803 FORMAT (/85H EPICENTER PARAMETERS ORDERED BY DEPTH-AZIMUTH MEASUR
1ED COUNTER-CLOCKWISE FROM NORTH //)
PRINI 804
804 FORMAT(3X,6H DEPTH,3X,9H DISTANCE,3X,9H LATITUDE,3X,10H LONGITUDE,
13X,3H AZIMUTH,3X,33H P-RESIDUAL (OBSERVED-THEORETICAL)
DD 805 K=1,1X,2
IX1=L/2+1
L=LLOCDEL(IX1)
M=L-L+1
PRINI 806,XITEM(IX1),DL,TX(L),QVALOC(M),QVALOC(M+1),AZIMUT(L),
1MRESID(L)
806 FORMAT (5X,F6.1,5X,F6.1,7X,F6.1,7X,F6.1,7X,F6.1,27X,F7.1)
805 CONTINUE
1 CONTINUE
PAUSE 7
END
```

APPENDIX IV

CURVES OF PARTICLE DISPLACEMENT

**CURVES OF PARTIAL DERIVATIVES OF PHASE VELOCITY WITH RESPECT
TO LAYER PARAMETERS**

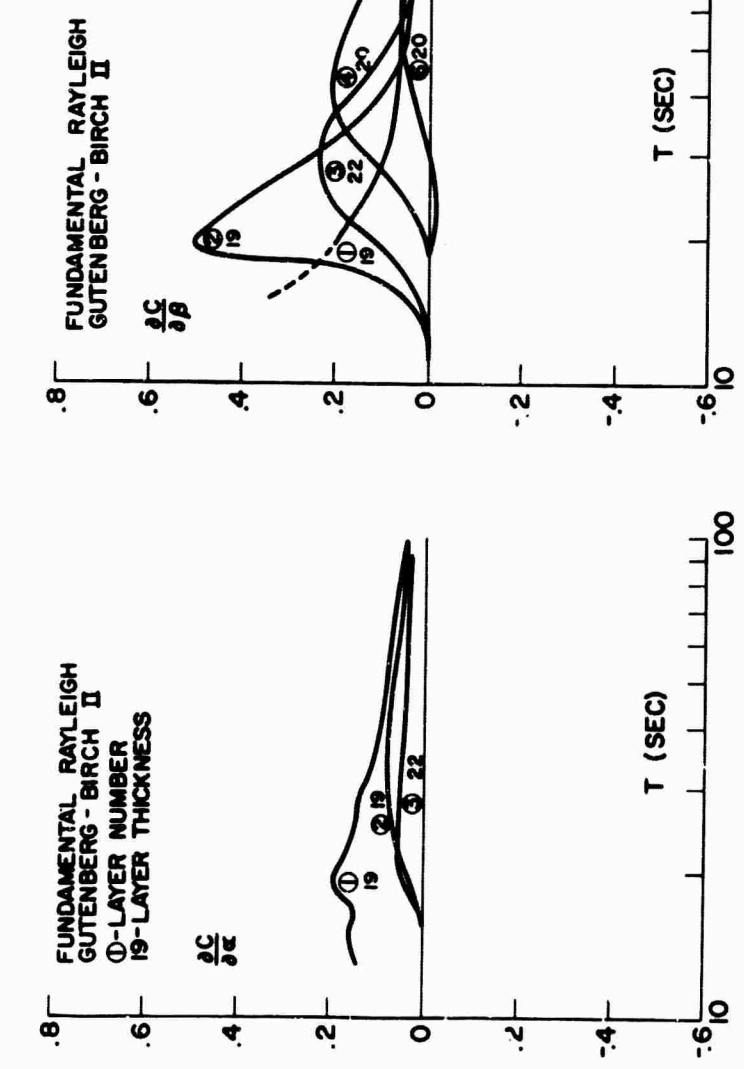
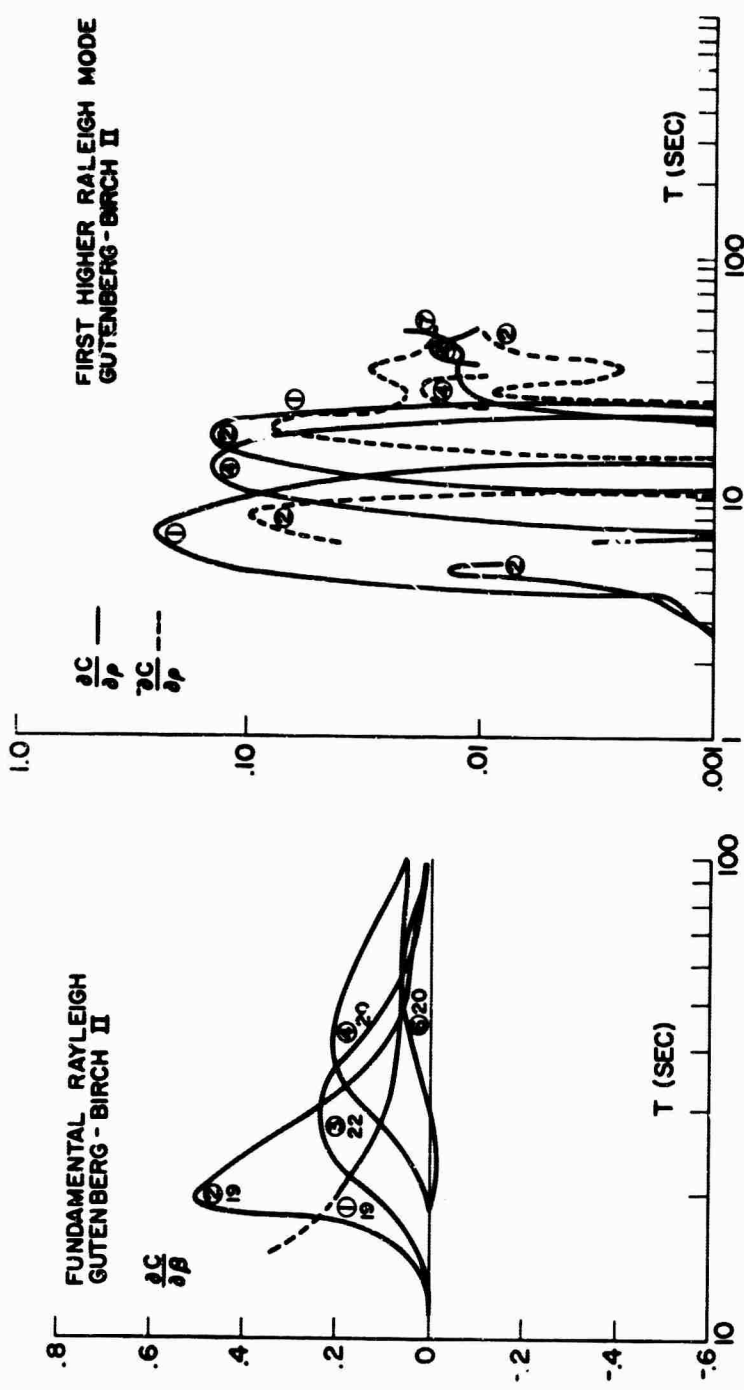
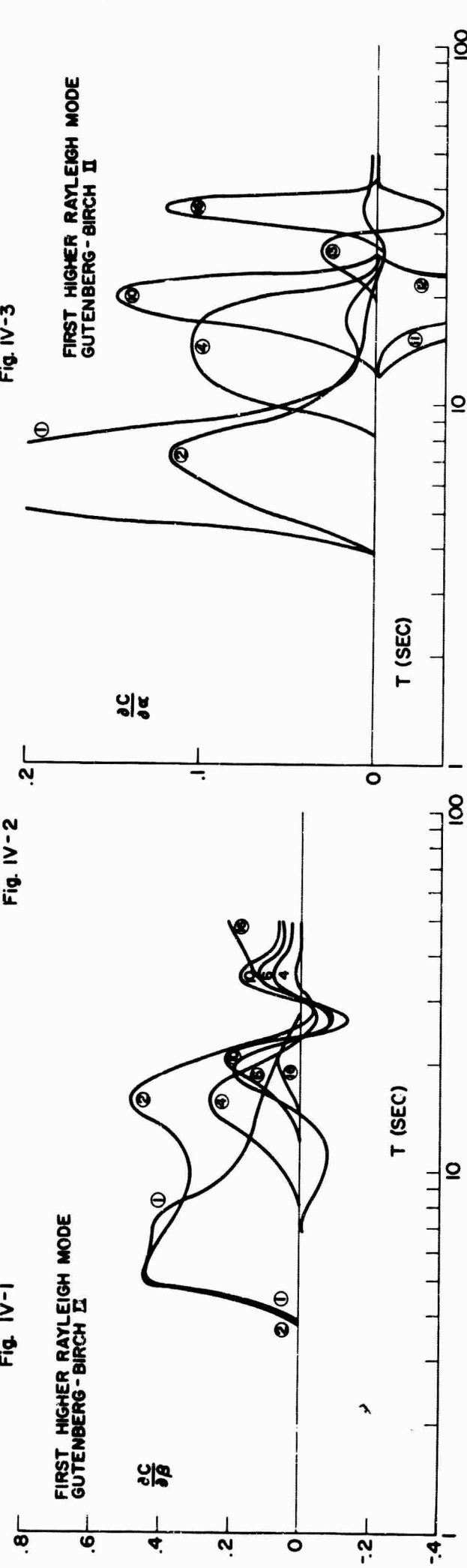


Fig IV-1



VARIATION OF PHASE VELOCITY WITH SHEAR WAVE VELOCITY.



VARIATION OF PHASE VELOCITY WITH DENSITY

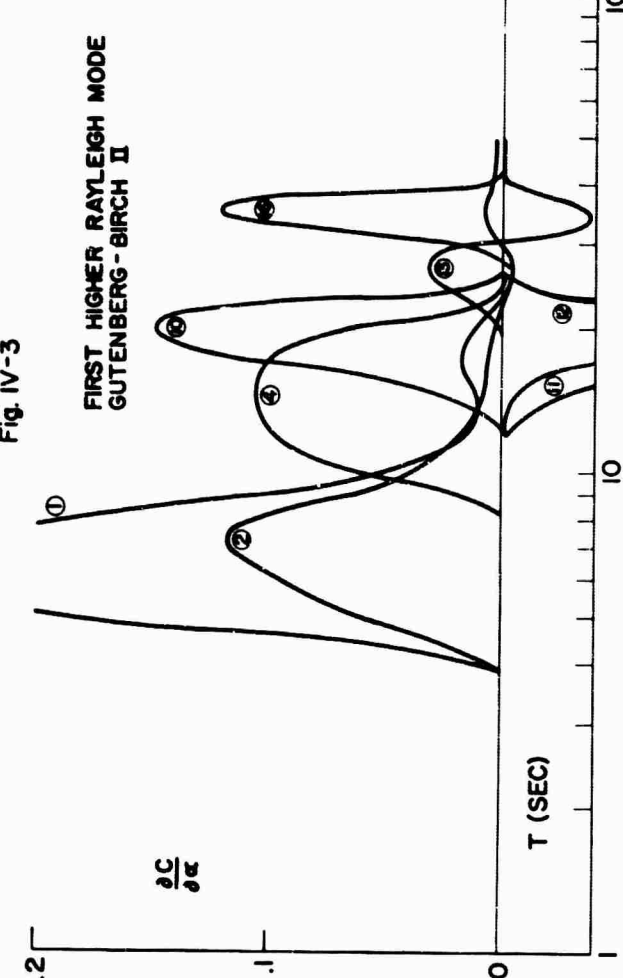
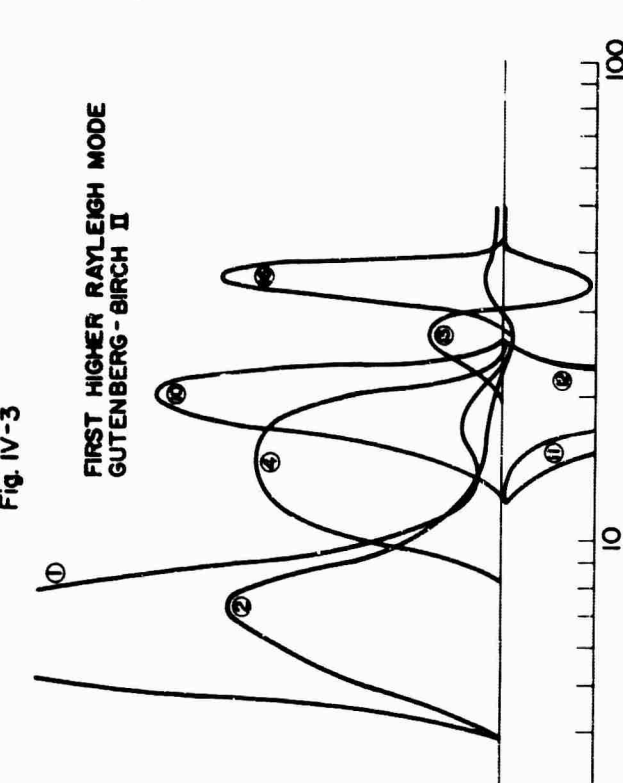
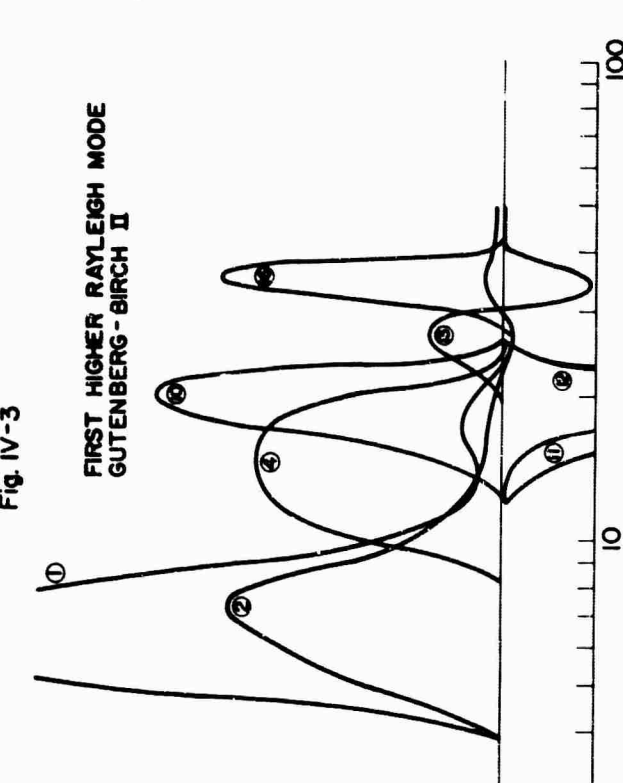


Fig. IV-3



**FIRST HIGHER RAYLEIGH MODE
GUTENBERG-BIRCH II**



VARIATION OF PHASE VELOCITY WITH COMPRESSIVE WAVE VELOCITY.



W 1

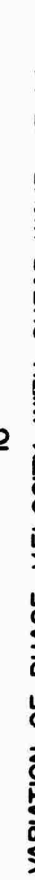
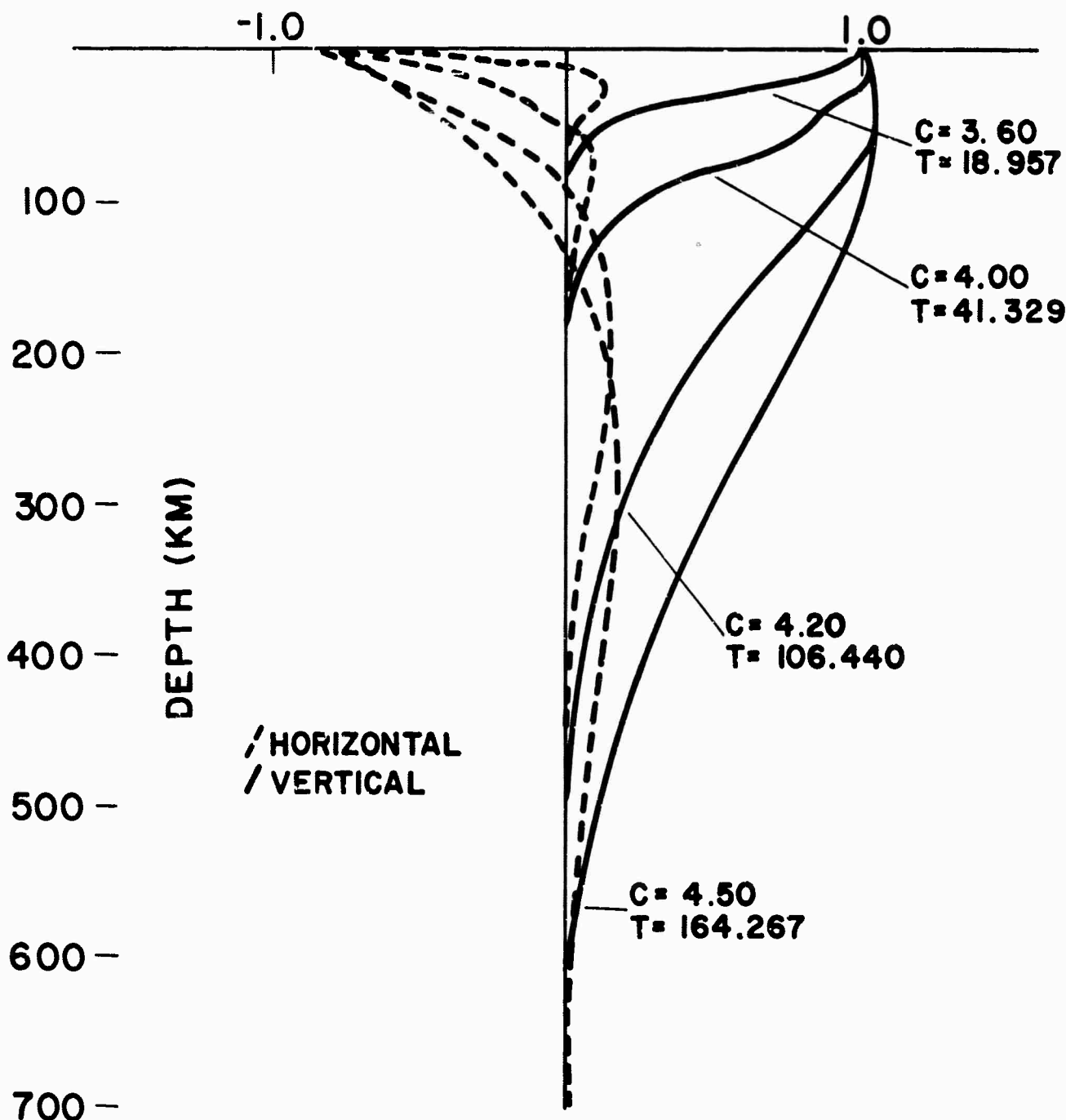
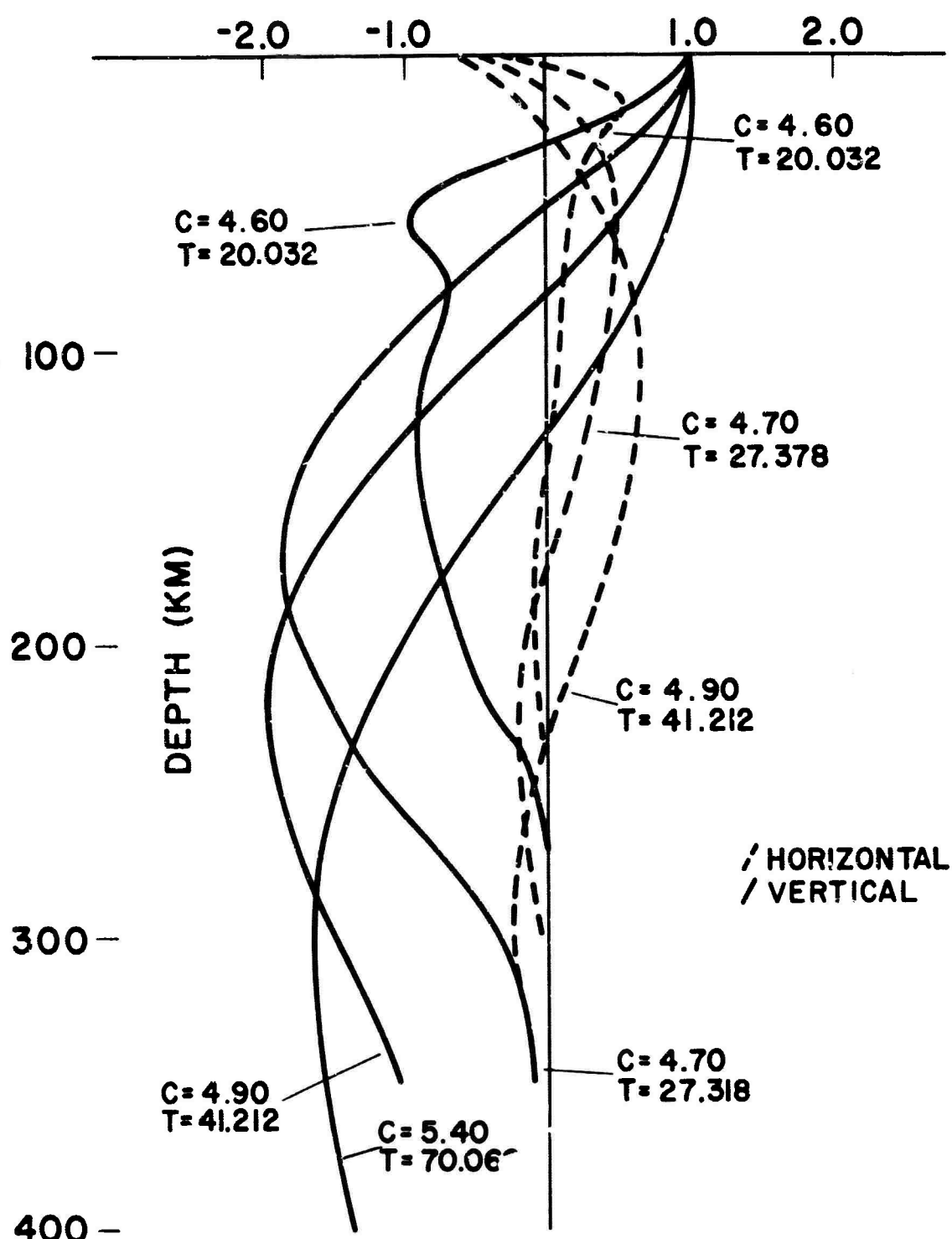


Fig 1V-4



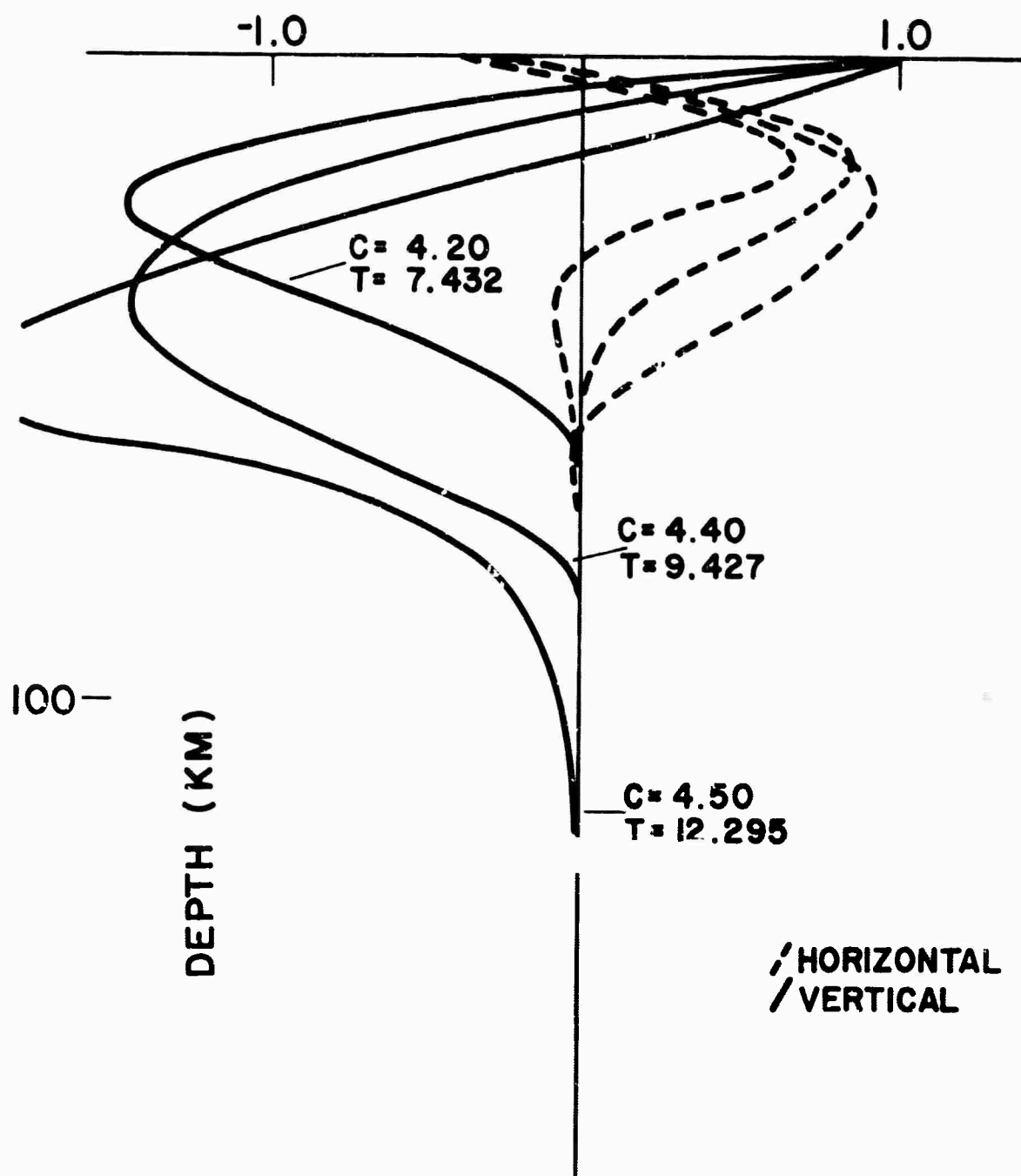
HORIZONTAL AND VERTICAL PARTICLE AMPLITUDES
NORMALIZED TO THE VERTICAL AMPLITUDE AT THE
SURFACE FOR FUNDAMENTAL RAYLEIGH MODE,
GUTENBERG - BIRCH II MODEL.

Fig. IV - 6



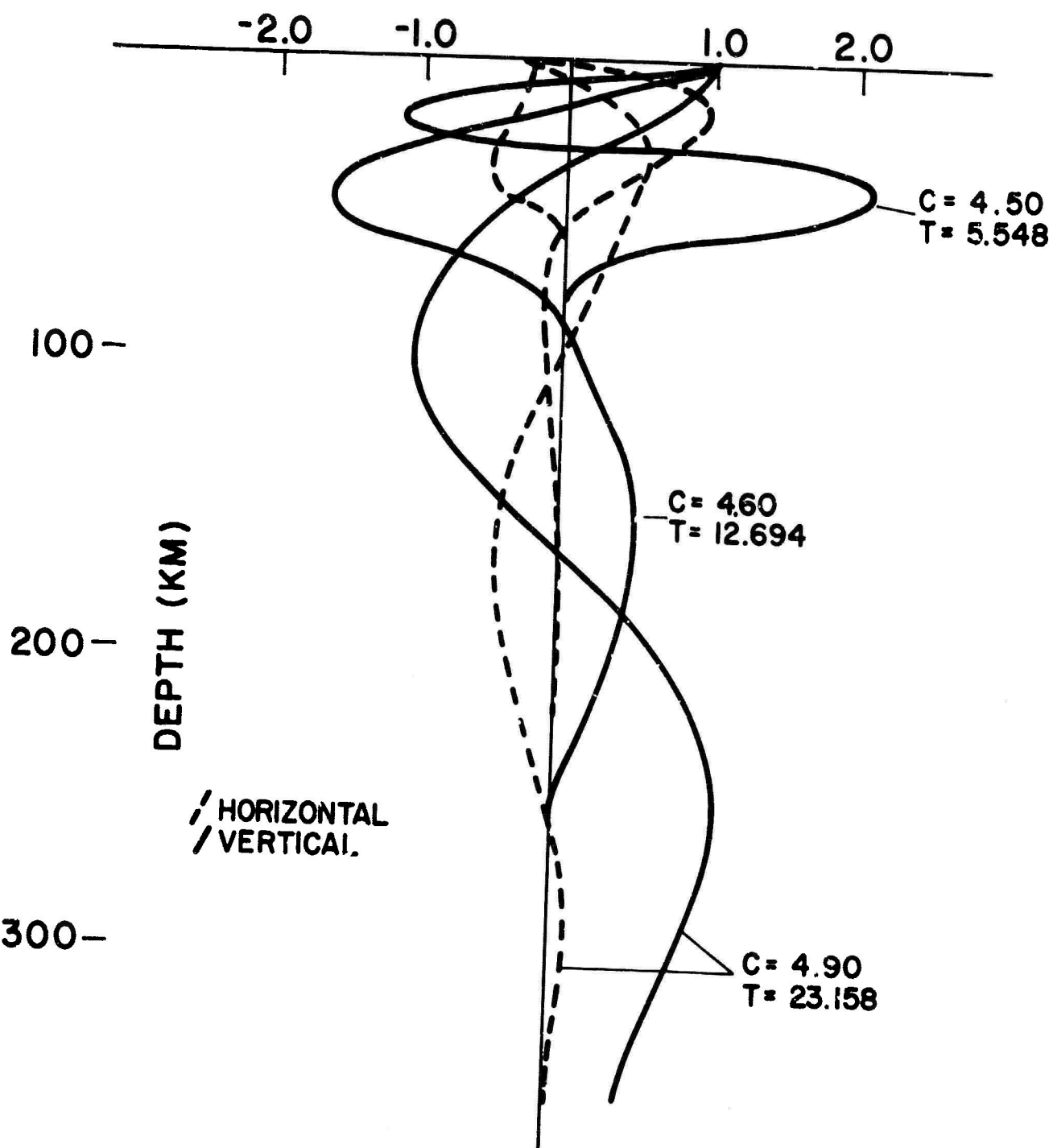
FIRST HIGHER RAYLEIGH MODE PARTICLE AMPLITUDES
NORMALIZED TO THE VERTICLE AMPLITUDE AT THE
SURFACE FOR THE GUTENBERG-BIRCH II MODEL.

Fig. IV-7



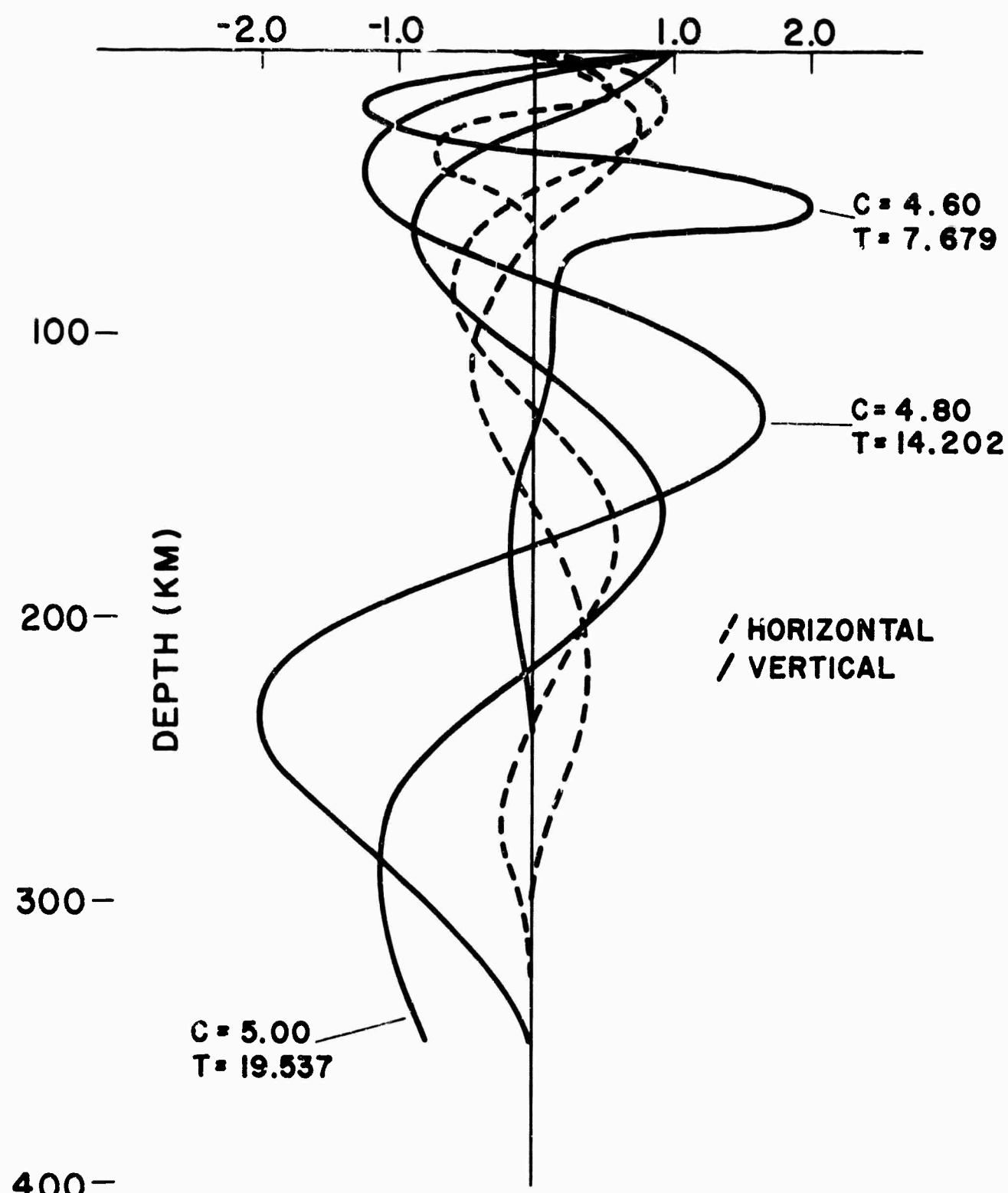
FIRST HIGHER RAYLEIGH MODE PARTICLE AMPLITUDES
NORMALIZED TO THE VERTICAL AMPLITUDE AT THE
SURFACE FOR THE GUTENBERG - BIRCH II MODEL.

Fig. IV - 8



SECOND HIGHER RAYLEIGH MODE PARTICLE AMPLITUDES
NORMALIZED TO THE VERTICLE DISPLACEMENT AT THE
SURFACE FOR THE GUTENBERG-BIRCH II MODEL.

Fig. IV-9



THIRD HIGHER RAYLEIGH MODE NORMALIZED TO THE
VERTICAL AMPLITUDE AT THE SURFACE FOR
THE GUTENBERG - BIRCH II MODEL.

Fig. IV - 10